DET NORSKE VERITAS™

REPORT

FATIGUE CALCULATIONS FOR EXISTING GULF OF MEXICO FIXED STRUCTURES

FOR

BUREAU OF OCEAN ENERGY MANAGEMENT, REGULATION, AND ENFORCEMENT
TA&R NO. 675

This study was funded by the Bureau of Ocean Energy Management, Regulation, and Enforcement, U.S. Department of the Interior, Washington, D.C., under Contract Number M10PC00109.

REPORT NO. EP034372-2011-01
REV. 1 2012-02-16

Disclaimer

This report has been reviewed by the BOEMRE and approved for publication. Approval does not signify that the contents necessarily reflect the views and policies of the Service, nor does mention of the trade names or commercial products constitute endorsement or recommendation for use.

MANAGING RISK

Fatigue Calculations for Existing Gulf of Mexico Fixed Structures

For:
Bureau of Ocean Energy Management, Regulation, and Enforcement
BOEMRE TA&R No. 675

Account Ref.:
Timothy J Steffek, COR, Lisa A. Algarin, CO

Det Norske Veritas (USA) Inc
1400 Ravello Dr
77449 Katy, United States
Tel: (281) 396-1000
Fax: (281) 396-1900
http://www.dnv.com

Date of Current Issue:	2012-02-16	Project No.:	EP034372
Revision No.: 1 No. of Pages: 105		Organisation Unit: ANMUS475	Regional Approval and Technology Center North America Maritime
DNV Reg. No.:	EP034372-2011-01	Report No.:	EP034372-2011-01

Summary:

This project utilized information from BOEMRE platform database to categorize existing platforms according to their age, water depth, size, and average age at removal time. Current Fatigue Design Methods were discussed and the effect of high stress and low cycle fatigue was evaluated. Fatigue of existing cracks in welds in tubular joints was investigated. Connections were evaluated and procedures for calculation of remaining fatigue life or fracture during a high stress event were proposed and applied in case studies. The following conclusions are drawn from the work carried out in this project:

1. Experience indicates that fatigue of welded tubular joints in fixed offshore platforms in the Gulf of Mexico may not be a significant issue. However extensive corrosion or damage due to collisions or dropped objects can be of greater significance. Redundancy, when present, can be effective in reducing the consequence of fatigue failure or redistributing the stresses in neighbouring joints and members.
2. The estimation of reduced strength due to damage caused by local thinning resulting from corrosion or deformation due to impact or collision is possible by applying a methodology that accounts for these effects on raising the stress range. Estimating the remaining number of stress cycles (fatigue life) may then be calculated from relevant S-N curves.
3. The use of risk based inspection (RBI) techniques may be considered to be more comprehensive than deterministic fatigue or fracture assessment since RBI normally addresses the failure consequences issue and quantifies the uncertainties involved.
4. The calculation of fatigue life of a welded joint in the presence of a flaw is possible through application of a fracture mechanics procedure that was derived based on the BS-7910:2005 standard. A viable preliminary tool has been proposed herein for specific application of this procedure.
5. The proposed fracture mechanics approach was applied to an example jacket platform under GOM environment. Results indicate that the presence of a crack in a connection can significantly reduce the connection strength in a storm condition. However the ultimate strength of the structure may not be greatly affected due to; e.g., redundancy if present.
6. A method for calculating fatigue damage due to low cycle high stress environmental conditions due to storms or hurricanes is also proposed based on NORSOK N-006.

Prepared by:	*Name and Position* Liqun Yang, Michal Moczulski, Senior Engineers	*Signature*
Verified by:	*Name and Position* G. Abdel Ghoneim, Inge Lotsberg, Hans Bratfos Sr. Principal Engineers	*Signature*
Approved by:	*Name and Position* Santhosh Kumar Mony, Head of Department	*Signature*

- ☒ Unrestricted distribution (internal and external)
- ☐ Unrestricted distribution within DNV
- ☐ Limited distribution within DNV after 3 years
- ☐ No distribution (confidential)

Keywords
Fatigue, Tubular joints, Deformed/corroded/cracked welds, Offshore fixed jacket platforms, Fracture Mechanics

Rev. No.	Date	Reason for Issue	Prepared by	Supervised by	Approved by
0	2011-12-21	Client Review	LIQUN, MIMOC	GHO	KKMS
1	2012-02-16	Final	GHO	JLU	KKMS

Reference to part of this report which may lead to misinterpretation is not permissible.

Table of Contents *Page*

1 EXECUTIVE SUMMARY 1

2 INTRODUCTION 2
2.1 Background 2
2.2 Objective 3
2.3 Scope of Work 3
2.4 Relevant Codes and Standards 4
2.5 Report Organization 4

3 GULF OF MEXICO STRUCTURES OVERVIEW 5
3.1 Gulf of Mexico Inspection Reports 5

4 PLATFORM VINTAGE AND CONDITION ASSESSMENT 10
4.1 Introduction 10
4.2 Platform Condition Assessment 10
4.2.1 Information Required for Platform Condition Assessment 10
4.2.2 GOM Platform Database 11
4.2.3 Inspection Methods 16
4.3 General Issues Related to Extended Life 16
4.4 Challenges of Ageing and Life Extension 16
4.5 Current Design Codes Related to Assessment of Existing Structures 19

5 CURRENT FATIGUE DESIGN METHODS 23
5.1 General 23
5.2 Fatigue Assessment Using S-N data 23
5.2.1 Fatigue Parameter 23
5.2.2 Simplified Fatigue 25
5.2.3 Detailed Fatigue 25
5.3 Fatigue Assessment Using Fracture Mechanics 26
5.4 Fatigue Assessment by Other Methods 27

6 LOW CYCLE FATIGUE 36
6.1 General 36
6.2 Storm Load History 36
6.3 Tubular Joint Low Cycle Fatigue 37

7 FATIGUE OF FLAWED WELDS 40
7.1 General 40
7.2 Fatigue Capacity 40
7.3 Fatigue Parameters 41

7.4 Fatigue of Deformed/Corroded Welds 41
7.5 Fracture Mechanics Assessment 42
7.5.1 Fatigue Assessment 43
7.5.2 Fracture Assessment 53
7.5.3 Corrosion Assessment 61

8 CASE STUDY 62
8.1 Introduction 62
8.2 Deterministic Fatigue Analysis 63
8.2.1 General Information and Methodology 63
8.2.2 Loads 65
8.2.3 Results 67
8.3 Fracture Mechanics Calculations 68
8.3.1 Introduction and Methodology 68
8.3.2 Loads 70
8.3.3 Analysis Input 73
8.3.4 Results 75

9 CONCLUSIONS AND RECOMMENDATIONS 78

10 REFERENCES 80

APPENDIX A MATHCAD WORKSHEETS 83
Appendix A.1 Crack Growth of Surface Flaw in Tubular Joint 84
Appendix A.2 Parametric Formulae of the Degree of Bending 94

APPENDIX B CASE SUDY DETAILS 99
Appendix B.1 Deterministic Fatigue (S-N) 100
Appendix B.2 Fracture mechanics Results Comparison 103

List of Figures

Figure 3-1 Hurricane Damage 6
Figure 3-2 Overload Damage 7
Figure 3-3 Buckling Damage 7
Figure 3-4 Holes 8
Figure 3-5 Linear Indications/Cracks 8
Figure 3-6 Corrosion 9
Figure 3-7 Welding Corrosion 9
Figure 3-8 Minor Pitting 9
Figure 4-1 NOAA map of the 3858 oil and gas platforms extant in the Gulf of Mexico in 2006 12
Figure 4-2 GOM Platform Activity (Source: MMS, B.J. Kruse, III) /14/ 12
Figure 4-6 Assessment procedure in ISO 19902 (2007) 21
Figure 6-1 S-N Curve for LCF for Tubular Joint in Seawater with CP 37
Figure 7-1 BS-7910 Annex B Assessment Methodology Flowchart 44
Figure 7-2 Crack and welded joint geometries 50
Figure 7-3 BS-7910 Fracture Assessment Methodology 54
Figure 7-4 Level 2A FAD 55
Figure 7-5 Surface Flaw Parameters 57
Figure 8-2 Default hotspot location for fatigue calculations (Framework) 63
Figure 8-3 Deterministic Fatigue Analysis Procedure (Norsok N-004) 64
Figure 8-4 Wave Exceedance Diagram (identical for each direction) 66
Figure 8-5 Default hotspot location for fatigue calculations (Framework) 68
Figure 8-6 Analyzed Hotspot Location (GeniE) 69
Figure 8-7 Example of Hotspot Stress Level for Analyzed Hotspot (Dir 315°, Wave 1) 70

List of Tables

Table 2-1 Main Design Codes 4
Table 4-1 GOM Installation by Type 13
Table 4-2 Comparison of Traditional Vs. RBI Approaches 16
Table 4-3 Assessment criteria for existing platform (ISO 19902:2007) 18
Table 4-4 Assessment Criteria Proposed in API RP 2A WSD (2007) 22
Table 5-1 NORSOK N-004 Design Fatigue Factors 25
Table 5-2 Simplified Fatigue 29
Table 5-3 Detailed Fatigue 31
Table 6-1 S-N data for low cycle fatigue analysis of tubular joints 37
Table 7-1 Values of ν and w for axial and bending loading 50
Table 7-2 Constants for A and m in air 51
Table 7-3 Constants for A and m in a marine environment 52

Table 8-1 Spectral Scatter Diagram for the GoM (ISO 19901-1) 65
Table 8-2 Single Wave Exceedance Used in Analysis 66
Table 8-3 Comparison of Calculated Fatigue Damage 67
Table 8-4Crack Growth Analysis Stress Input (for Dir 0° through 135°) 71
Table 8-5 Crack Growth Analysis Stress Input (for Dir 180° through 315°) 72
Table 8-6 Material Properties and Input Parameters 73
Table 8-7 Stress Intensity Magnification Factors M_k(for L/B = 2) 74
Table 8-8 Analysis Results – Fatigue 76
Table 8-9 Analysis Results – Fatigue and Fracture 77

Nomenclature

A: constant in fatigue crack growth relationship
a: flaw height for surface flaw, half flaw length for through-thickness flaw, or half height for embedded flaw (mm)
Δa increment in a
da/dN: crack growth per cycle
B: the section thickness of plate in mm
c: half flaw length for surface or embedded flaws (mm)
Δc increment in c
C_v: Charpy impact energy in Joules,
d: external diameter of brace
D: external diameter of chord
E: Young's modulus of steel
IPB, OPB:
refer to In-Plane or Out-of-Plane Bending
K: Stress Intensity Factor in MPa√m
ΔK: $K_{max} - K_{min}$=stress intensity factor (SIF) range
ΔK_o: Threshold Stress Intensity Factor Range
K_{mat}: material toughness measured by stress intensity factor, in MPa√m.
k_m: stress magnification factor due to misalignment
k_t: stress concentration factor
k_{tb}: bending stress concentration factor
k_{tm}: membrane stress concentration factor
$k_{t.HS}$: hot spot stress concentration factor in tubular joint
$k_{t.IPB}$, $k_{t.OPB}$:
in plane and out of plane stress concentration factors in tubular joints
L: chord length (attachment length in BS7910)
L_r: collapse parameter; ratio of applied load to yield load
$L_{r,max}$: permitted limit of L_r
m: exponent in flaw growth law
M: bulging correction factor
M_m and M_b, M_{km}, M_{kb}:
stress intensity magnification factors which is a function of crack size, geometry and loading
M_{ci} and M_{co}
plastic collapse loads in the cracked condition for axial loading, in-plane bending and out-of-plane bending respectively
N = Number of cycles of the SIF range
P_m and P_b:
the linearized primary membrane and bending not including stress concentration due to weld geometry (with no k_t applied)
P_c: plastic collapse loads in the cracked condition for axial loading
Q: secondary stress
Q_b: secondary bending stress

Q_m: secondary membrane stress

R-ratio:
Minimum Stress / Maximum Stress

SCF: the stress concentration factor from linear elastic analysis (the same as used for high cycle fatigue)

t: brace wall thickness

T: chord wall thickness

Y_m, Y_b:
stress intensity correction factors for membrane and bending stress

α: geometry ratio (2L/D)

β: geometry ratio (d/D)

γ: geometry ratio (D/2T)

τ: geometry ratio (t/T)

θ: brace angle (in radians)

δ_m: CTOD at first attainment of maximum force plateau

δ_{mat}: material toughness measured by CTOD method

Ω_{Tot}, Ω_{Ax},Ω_{IPB}, Ω_{OPB}:
total, axial, in plane and out of plane degrees of bending in tubular joints

$\sigma_{n:}$ the nominal stress

$\sigma_{actual\ HSS}$:
the actual stress at the considered hot spot from a non-linear finite analysis using a cyclic stress-strain curve

$\Delta\sigma_{m,}$ $\Delta\sigma_b$:
membrane and bending component of stress range

$\Delta\sigma_{HS.Ax}$, $\Delta\sigma_{HS.IPB}$, $\Delta\sigma_{HS.OPB}$:
axial, in and out of plane hot spot stress ranges in tubular joint

$\Delta\sigma_{n.Ax}$, $\Delta\sigma_{n.IPB}$, $\Delta\sigma_{n.OPB}$:
nominal axial, in and out of plane stress ranges in tubular joint

$\Delta\sigma_{HS.Tot}$:
total hot spot stress range in tubular joint

1 EXECUTIVE SUMMARY

This project utilized information from BOEMRE platform database to categorize existing platforms according to their age, water depth, size, and average age at removal time. Current Fatigue Design Methods were discussed and the effect of high stress and low cycle fatigue was evaluated. Fatigue of existing cracks in welds in tubular joints was investigated. Connections were evaluated and procedures for calculation of remaining fatigue life or fracture during a high stress event were proposed and applied in case studies.

The following conclusions are drawn from the work carried out in this project:

1. Experience indicates that fatigue of welded tubular joints in fixed offshore platforms in the Gulf of Mexico may not be a significant issue. However extensive corrosion or damage due to collisions or dropped objects can be of greater significance. Redundancy, when present, can be effective in reducing the consequence of fatigue failure or redistributing the stresses in neighbouring joints and members.
2. The estimation of reduced strength due to damage caused by local thinning resulting from corrosion or deformation due to impact or collision is possible by applying a methodology that accounts for these effects on increased stress range. Estimating the remaining number of stress cycles (fatigue life) may then be calculated from relevant S-N curves.
3. The use of risk based inspection (RBI) techniques may be considered to be more comprehensive than deterministic fatigue or fracture assessment since RBI normally addresses the failure consequences issue and quantifies the uncertainties involved.
4. The calculation of fatigue life of a welded joint in the presence of a flaw is possible through application of a fracture mechanics procedure that was derived based on the BS-7910:2005 standard. A viable preliminary tool has been proposed herein for specific application of this procedure.
5. The proposed fracture mechanics approach was applied to an example jacket platform under GOM environment. Results indicate that the presence of a crack in a connection can significantly reduce the connection strength in a storm condition. However the ultimate strength of the structure may not be greatly affected due to; e.g., redundancy if present.
6. A method for calculating fatigue damage due to low cycle high stress environmental conditions due to storms or hurricanes is also proposed based on NORSOK N-006.

Research work is needed for further verification of the fracture parameters employed in fracture and fatigue calculation. The effect of combined membrane and bending loadings in calculating the surface and part-thickness crack growth requires further investigation. Further case studies for actual scenarios of damaged or cracked welds covering both surface and through thickness flaws and complex tubular joint geometries would be valuable to further the understanding of the fracture behaviour of cracked welded joints with cracks in brace or chord. Further development of the MathCAD sheets to include more scenarios and scope and to perform verification work to turn it into a tool that can be applied by interested parties is also recommended.

2 INTRODUCTION

2.1 Background

This work is based on DNV White Paper entitled "Fatigue Calculations for Existing Gulf of Mexico Fixed Structures", submitted in response to the U.S. Department of the Interior, Minerals Management Service (MMS), Ref: Board Agency Announcement (BAA) Number M10PS00185, "Proposed Research on Safety of Oil and Gas Operations in the US Outer Continental Shelf" dated 17 March 2010, and the request for proposal (RFP) from the MMS, dated May 26, 2010. The proposal covered only Topic 3 of the BAA. The MMS was renamed as Bureau of Ocean Energy management, Regulation, and enforcement (BOEMRE) in 2010 and is now (as of October 2011) Bureau of Safety and Environmental Enforcement (BSEE) which is one of two branches of the original BOEMRE, the other being the Bureau of Energy Management (BOEM).

The need for this work is evident from the literature review carried out as part of this study. There has been little work carried out on tubular joint behavior when defects are present in the welds of the joint. A lot of research work was carried out since the late 1970's until early 2000's on the effect of such defects on the ultimate strength of such joints but does not at all address their effect on the fatigue strength /25/, /26/, /35/ and /40/. The API RP 2A 21st Edition /4/ states:

> "In the U.S. Gulf of Mexico, cracking due to fatigue is not generally experienced; if cracks occur, they are most likely found at joints in the first horizontal conductor framing below water, normally resulting from fatigue degradation; or cracks may also occur at the main brace to leg joints in the vertical framing at the first bay above mudline, normally due to environmental overload (for example, low cycle fatigue), or at the perimeter members in the vertical framing at the first bay below water level, normally as a result of boat impact." and
>
> "If crack indications are reported, they should be assessed by a qualified engineer familiar with the structural integrity aspects of the platform."

With regards to application of fracture mechanics API RP 2A states:

> "Fracture mechanics methods may be employed to quantify fatigue design lives of welded details or structural components in situations where the normal S-N fatigue assessment procedures are inappropriate. Some typical applications are to assess the fitness-for-purpose and inspection requirements of a joint with and without known defects, or to assess the structural integrity of castings", and
>
> "It is important that the fracture mechanics formulation that is used should be shown to predict, with acceptable accuracy, either the fatigue performance of a joint class with a detail similar to that under consideration, or test data for joints that are similar to those requiring assessment."

This is useful guidance but does not give any specific procedures for such evaluations.

The only relevant documents that touched on the issue are the NORSOK N-006 /12/ and the BS-7910 /2/. This project uses both as the basis for the procedures proposed for calculating the fatigue strength of tubular joints experiencing cracking or defects.

2.2 Objective

As stated in the BOEMRE Contract No. M109C00109 documentation and the DNV proposal NO 1-2Q1N5t-02, the objective is to perform a state-of-art review of the current fatigue design methods for deformed or corroded welds on existing OCS structures operating close to or beyond their original design life. The results of this TAR project may be employed in the assessment of the US Gulf of Mexico (GOM) and the West Coast fixed offshore structures.

2.3 Scope of Work

The original scope of work as specified in BOEMRE Contract No. M109C00109 and DNV proposal NO 1-2Q1N5t-02 entailed the following six tasks:

1. GOM Structures Overview: Utilize information from previous BOEMRE TAR program to categorize existing platforms according to their condition with regards to remaining fatigue life.
2. Platform Vintage and Condition: Assessing the conditions of the primary structural joints and numbers of a platform will be specified and applied to the main types of GOM platforms.
3. Current Fatigue Design Methods: A critical review of existing fatigue design methods will be carried out in this task.
4. High Stress Low Cycle Fatigue: Develop a procedure for the evaluation of cyclic high stress on fatigue of critical connection on GOM OCS structures.
5. Fatigue of Deformed/Corroded Welds: Corroded/deformed connections will be evaluated and methodologies for their quantification will be developed.
6. Validation: Actual fatigue tests performed at the DNV laboratory, or fatigue performance from existing platform connections will be employed to compare with calculated results.

In addition, project management, coordination and reporting tasks were also detailed in the contract documents.

However, during execution of the work, it was recognized that the development of new fatigue calculation method for corroded/deformed tubular joint welds would require extensive testing in order to establish the relevant S-N curves. The scope of such an effort would substantially exceed the available resources for this project. Review of limited number of inspection reports for platforms in the GOM indicates that fatigue of corroded/deformed joints may not be a major damage scenario. However with the ageing structures in the GOM fatigue could prove to be important. Therefore, it was decided that the scope of work be revised to allow the application of existing fracture mechanics and fatigue calculation methods to evaluate the viability of tubular joints with existing defects either due to initial fabrication or due to in-service fatigue.

Therefore Tasks 5 and 6 were replaced by:

5. Fatigue of existing cracks in welds in tubular joints: connections will be evaluated and procedures for calculation of remaining fatigue life will be proposed.
6. Case studies: proposed joint fatigue strength calculation procedures will be applied to a

jacket structure and the results verified against existing experience/technology.

Although probabilistic methods are normally applied in association with RBI (Risk Based Inspection) and fracture mechanics evaluations, the present work is limited to the deterministic approach as requested by BOEMRE in the project terms of reference.

2.4 Relevant Codes and Standards

Table 2-1 lists salient current standards considered to be of direct use/benefit to the subject matter of this study. These standards are also included as references in Section 9.

A detailed review and comparison of the fatigue strength requirements in these design codes is given in a recent DNV study performed for BOEMRE under TA&R No. 677 /39/.

Table 2-1 Main Design Codes

Number	Revision	Title
API RP 2A (WSD)	21st Edition October 2007	Recommended Practice for Planning, Designing and Constructing Fixed Offshore Platforms – Working Stress Design
ISO 19900	1st Edition December 2002	General Requirements for Offshore Structures
ISO 19902	1st Edition December 2007	Fixed Steel Offshore Structures
NORSOK Standard N-001	7th Edition June 2010	Integrity of Offshore Structures
NORSOK Standard N-004	2nd Edition October 2004	Design of Steel Structures
NORSOK Standard N-006	1st Edition March 2009	Assessment of Structure Integrity for Existing Offshore Load-bearing Structures
British Standard BS-7910	2005	Guide to Methods of Assessing the Acceptability of Flaws in Metallic Structures

2.5 Report Organization

This report is organized in six main sections (Sec. 3 to Sec. 8); in addition to this introductory section, addressing the main six tasks of the project as discussed above. Conclusions and recommendations are given in Section 9 and the references are listed in Section 10. In addition Appendices A and B give supporting documentation related to the developed application software and case studies performed.

3 GULF OF MEXICO STRUCTURES OVERVIEW

Considerable work has been carried out under the current BOEMRE TA&R program and significant database already exists that includes invaluable information which may be utilized to categorize existing platforms according to their condition with regards to remaining life. The work will avoid duplication with previous TA&R projects and will focus on structures with existing defects, corrosion or deformed weldments. The database was searched and a few representative corroded/deformed joints were selected for in depth evaluation.

3.1 Gulf of Mexico Inspection Reports

DNV has reviewed a small number of inspection reports received from BOEMRE and the following observations were made:

- There are several reasons for the inspection findings other than fatigue. For example, majority of cases relate to mechanical damages. There are damages caused by overload
- Fatigue is not the dominant source for reported anomalies in the received inspection reports
- Few findings exist where corrosion is the primary anomaly
- There are several cases of mechanical damages
- There are damages caused by overload

Typical types of damages from inspection reports received from BOEMRE and TA&R reports on the BOEMRE website are summarized as follows:

- Hurricane/Overload
- Buckling
- Holes
- Missing Members
- Dents/bowed members
- Linear Indications/Cracks
- Corrosion

Figure 3-1 to Figure 3-8 show example anomalies in experienced by GOM platforms during hurricanes or due to in service incidents or wear and tear.

Figure 3-1 is taken from Ghoneim presentation at the SNAME Houston Section meeting in December, 2005 following the most severe hurricane season in history with Katrina and Rita Category 3 at land fall. As many as 113 offshore GOM production platforms were destroyed due to these two hurricanes. In addition, the Typhoon sea star mini TLP was toppled and significant topsides damage occurred. In addition, many Mobile offshore units were adrift due to anchor and mooring failures causing significant damage to pipelines. Such hurricanes and extreme storms cause very high stresses that exceed the material yield strength at local and even global locations in some cases. More details refer to /15/, /16/, /17/, /18/, /19/, /20/ and /21/. Should existing damage, corrosion, or flaws be present in structures exposed to such extreme storms, the potential for platform loss increases due to low cycle fatigue, fracture, and buckling of structural elements and connections.

Figure 3-1 Hurricane Damage

Examples of overload damage in the form of tearing, punching shear, bursting due to external compression are shown in Figure 3-2. Member global and local buckling are demonstrated in Figure 3-3. In some incidents holes were discovered as shown in Figure 3-4. It appears that the

diagonal bracing was detached and discovered at a later date as evidenced by the amount of marine growth shown.

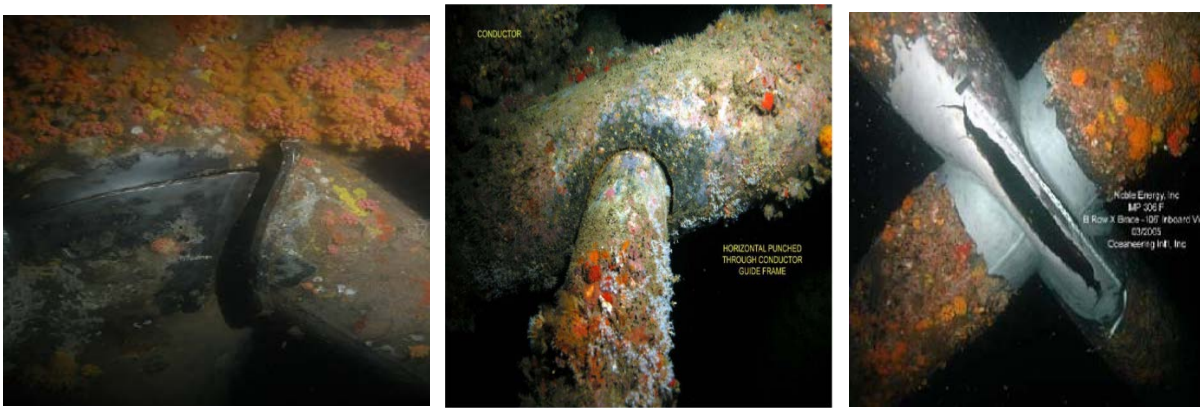

Figure 3-2 Overload Damage

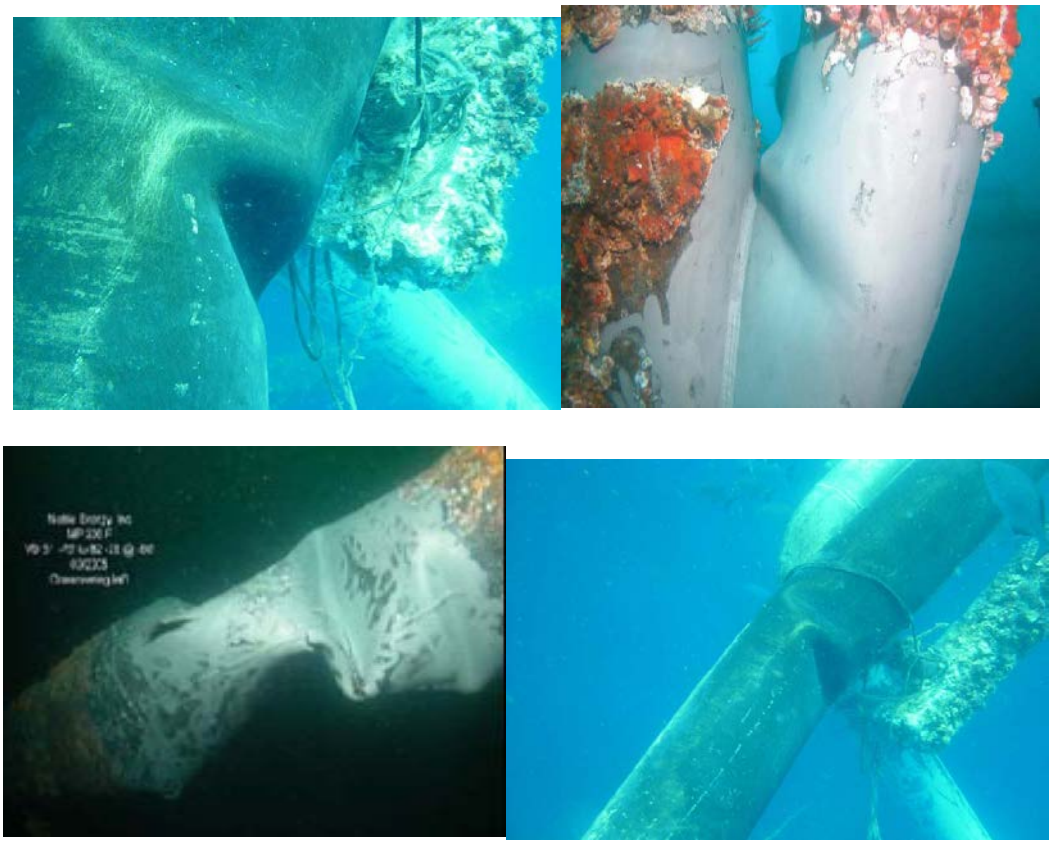

Figure 3-3 Buckling Damage

Figure 3-4 Holes

Linear indications in the form of cracks are noted in base material and welds at joints as shown in Figure 3-5.

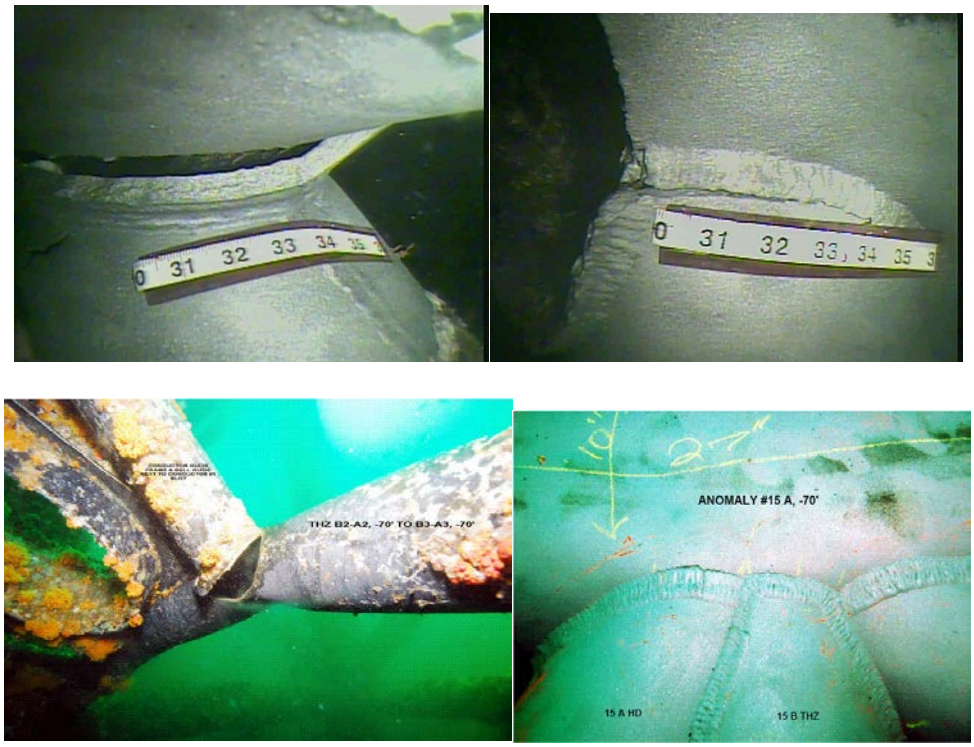

Figure 3-5 Linear Indications/Cracks

Corrosion of members and welds at tubular joins is shown in Figure 3-6, Figure 3-7, and Figure 3-8.

Figure 3-6 Corrosion

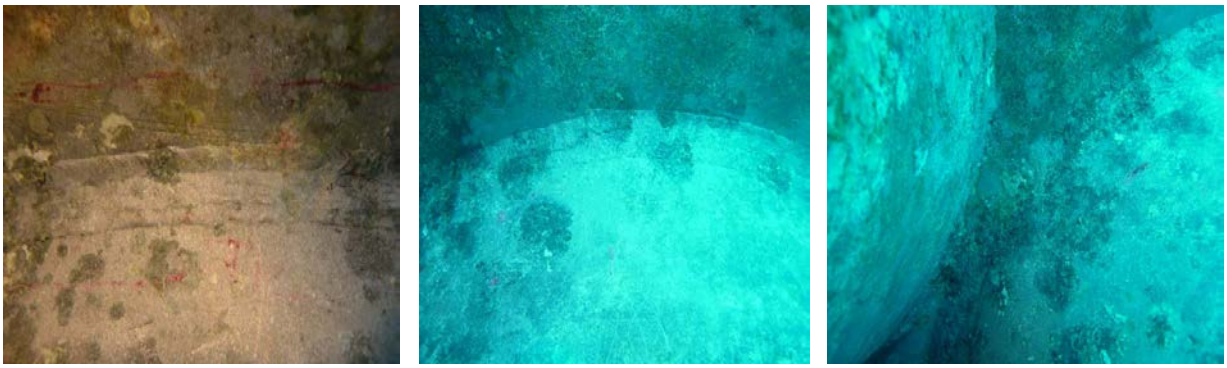

Figure 3-7 Welding Corrosion

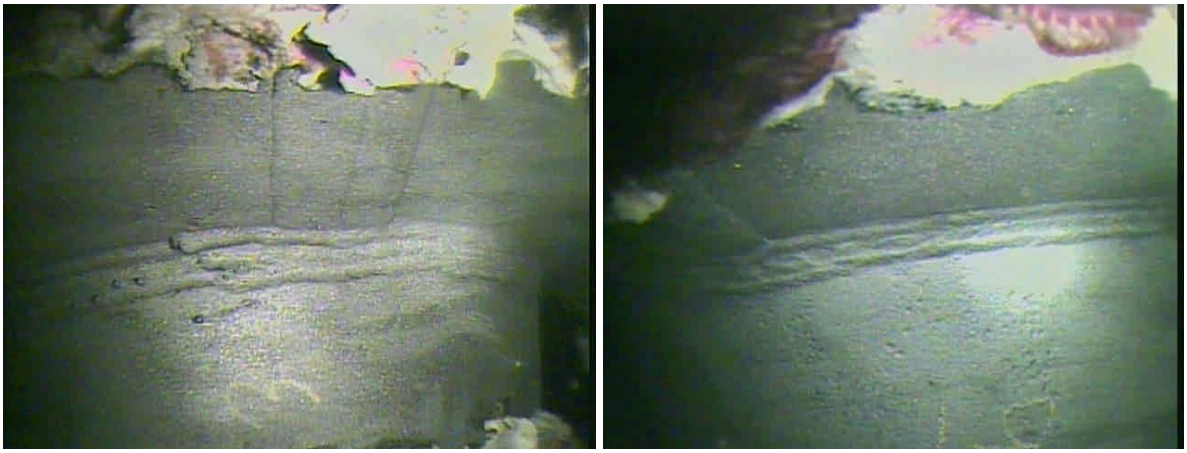

Figure 3-8 Minor Pitting

4 PLATFORM VINTAGE AND CONDITION ASSESSMENT

4.1 Introduction

Although important, the age of the platform is not directly related to its condition. A consistent methodology for defining platform condition is needed. The existing BOEMRE database suffers from inconsistencies due to the lack or misinterpretation of such definitions of, e.g., damage, failure, and corrosion. The existing standards do not adequately address such issues. The important factors that must be incorporated in assessing the condition of the primary structural joints and members of a platform are corrosion extent, degree of pitting, general or local corrosion, defects or flaws in deformed or corroded welds.

4.2 Platform Condition Assessment

4.2.1 Information Required for Platform Condition Assessment

Platform condition assessment should rely on sufficient information collected to allow an engineering assessment. The following is a summary of data that may be required (see e.g.; API RP 2A-WSD, Sec. C17.4.1):

1. General information:
   a) Original and current owner.
   b) Original and current platform use and definition
   c) Location, water depth and orientation
   d) Platform type – caisson, tripod, 4/6/8-leg, etc.
   e) Number of wells, risers and production rate.
   f) Other site-specific information, manning level, etc.
   g) Performance during past environmental events.
2. Original design:
   a) Design contractor and date of design.
   b) Design drawings and material specifications.
   c) Design code.
   d) Environmental criteria – wind, wave, current, seismic, ice, etc.
   e) Deck clearance elevation (underside of cellar deck steel).
   f) Operational criteria – deck loading and equipment arrangement.
   g) Soil data.
   h) Number, size, and design penetration of piles and conductors.
   i) Appurtenances – list and location as designed.
3. Construction:

a) Fabrication and installation contractors and date of installation.
b) "As-built" drawings.
c) Fabrication, welding, and construction specifications.
d) Material traceability records.
e) Pile and conductor driving records.
f) Pile grouting records, (if applicable).

4. Platform history:
   a) Environmental loading history – hurricanes, earthquakes, etc.
   b) Operational loading history – collision and accidental loads.
   c) Survey and maintenance records.
   d) Repairs – descriptions, analyses, drawings and dates.
   e) Modifications – descriptions, analyses, drawings, and dates.
5. Present condition:
   a) All decks – actual size, location and elevation.
   b) All decks – existing loading and equipment arrangement.
   c) Field measured deck clearance elevation (bottom of steel).
   d) Production and storage inventory.
   e) Appurtenances – current list, sizes and locations.
   f) Wells – number, size, and location of existing conductors.
   g) Recent above-water survey (Level I).
   h) Recent underwater platform survey (Level II minimum).

If original design data or as-built drawings are not available, assessment data may be obtained by field measurements. The thickness of tubular members can be determined by ultrasonic procedures, both above and below water, for all members except the piles. When the wall thickness and penetration of the piles cannot be determined and the foundation is considered to be the critical element in the structural adequacy, it may not be possible to perform an assessment. In this case, it may be necessary to downgrade the use of the platform to a lower assessment category by the reducing the risk or to demonstrate adequacy by prior exposure.

4.2.2 GOM Platform Database

Figure 4-1 through Figure 4-5 show the platform activity in the US GOM as of 2006, 2009 (see Ghoneim /42/), and 2011. Figure 4-2 shows the platforms by water depth as of the end of 2009 as reported by the MMS/14/. Figure 4-3 categorizes the GOM installations by type as noted in Table 4-1 being caisson, fixed, well protector, or floater type platform.

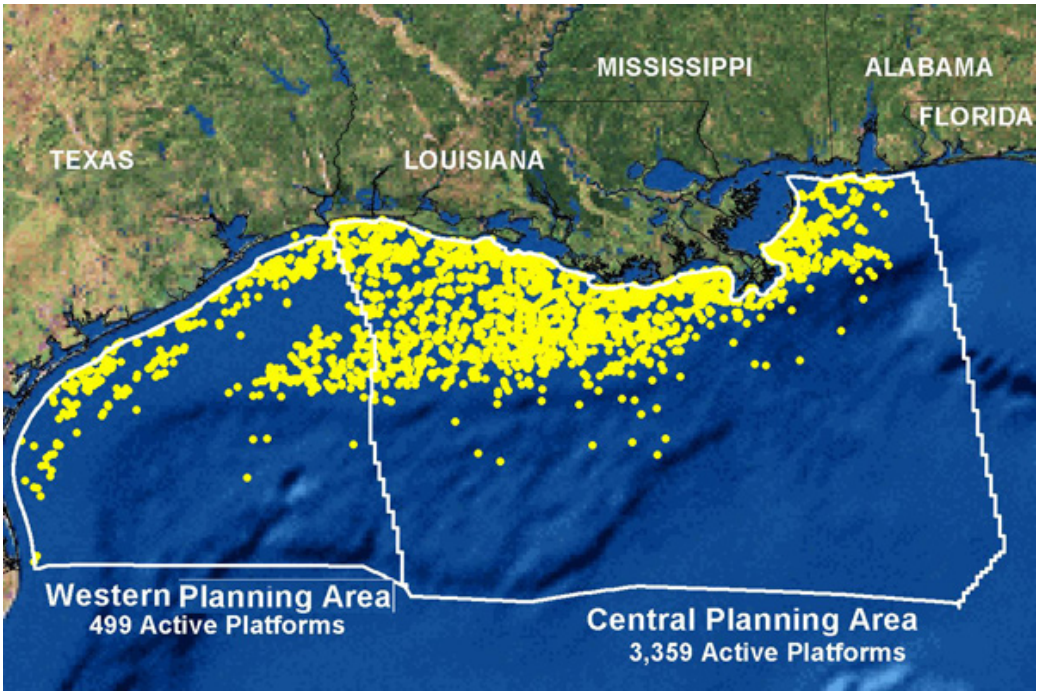

Figure 4-1 NOAA map of the 3858 oil and gas platforms extant in the Gulf of Mexico in 2006

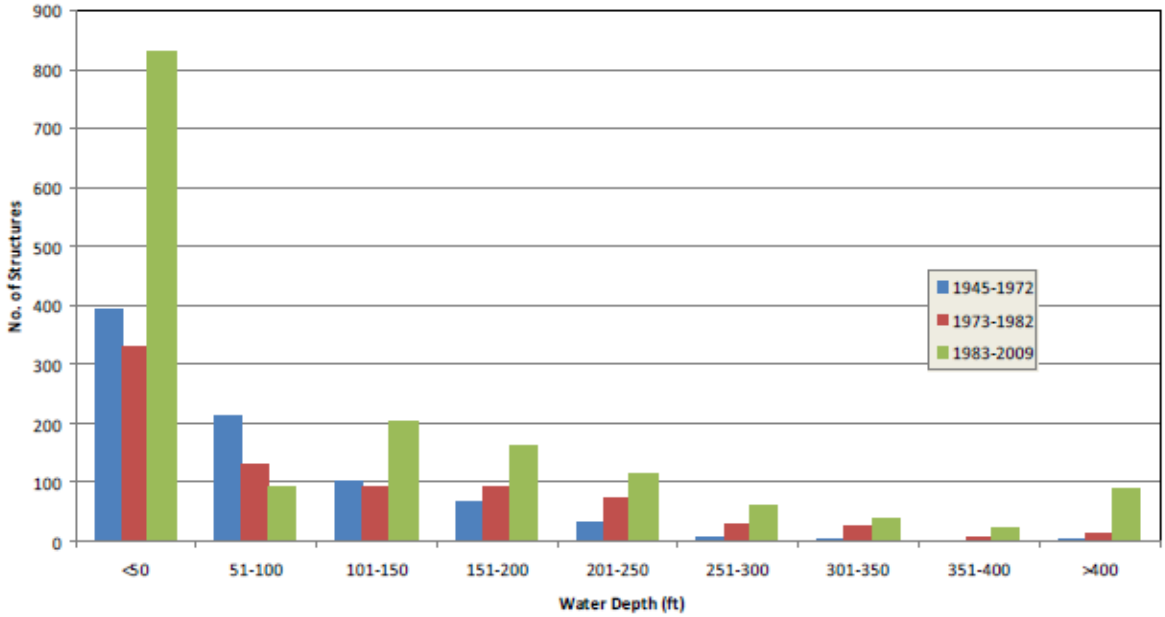

Figure 4-2 GOM Platform Activity (Source: MMS, B.J. Kruse, III) /14/

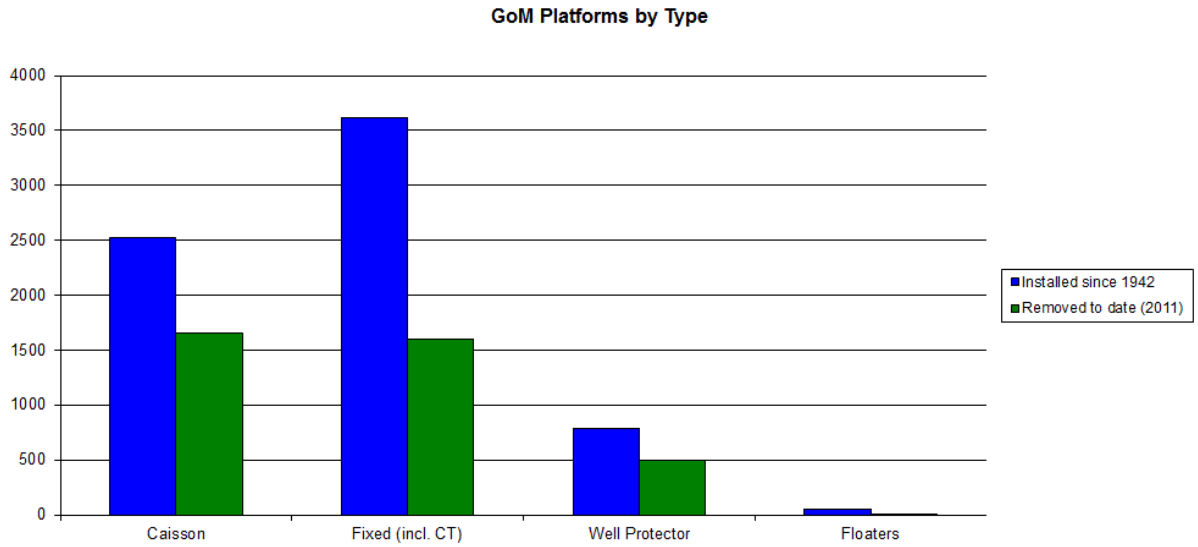

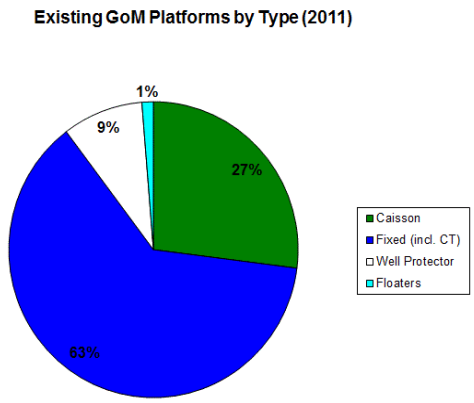

Figure 4-3 Existing GOM Platforms Categorized by Type (2011)

Table 4-1 GOM Installation by Type

	Installed	Removed	Existing
Caisson	2528	1660	868
Fixed (incl. CT)	3616	1600	2016
Well Protector	784	494	290
Floaters	46	5	41
TOTAL	6974	3759	3215

Existing fixed platforms range in age from new to as high as 60 years old as shown in the vintage bar and pie charts in Figure 4-4. It is interesting that about 9% of the platforms is more than 50 years old. Approximately 50% of all platforms (48%) are 30 years or older. Most of these platforms were designed for life of 20 years in accordance with the earlier API RP 2A requirements.

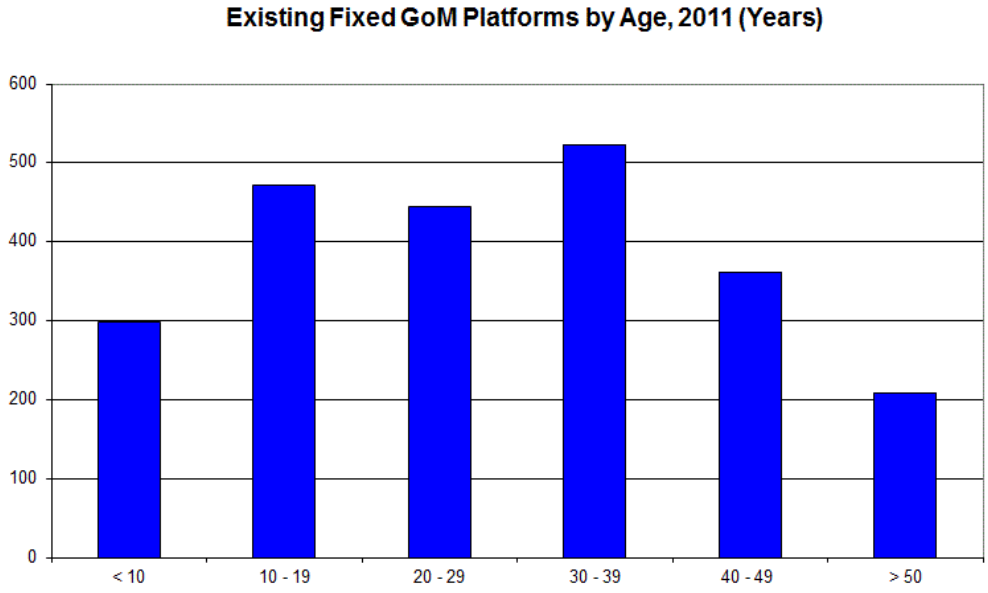

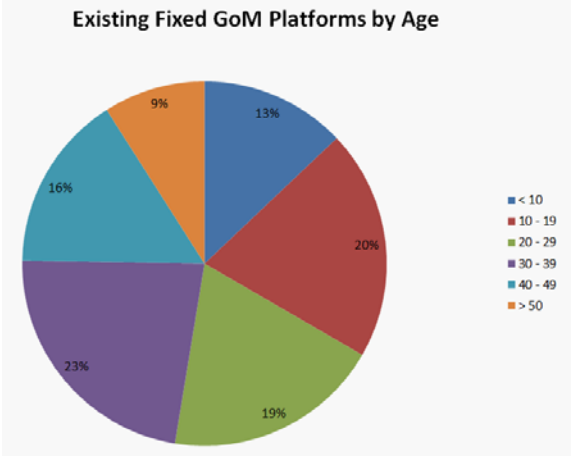

Figure 4-4 Existing GOM Platforms Vintage (2011)

Figure 4-5 indicates that the number of platform installations peaked in 1980 at 120 platforms whereas platform removals peaked at about 140 platforms in 2010 when only about 15 platforms were installed. Hurricanes are probably responsible for removal of many platforms.

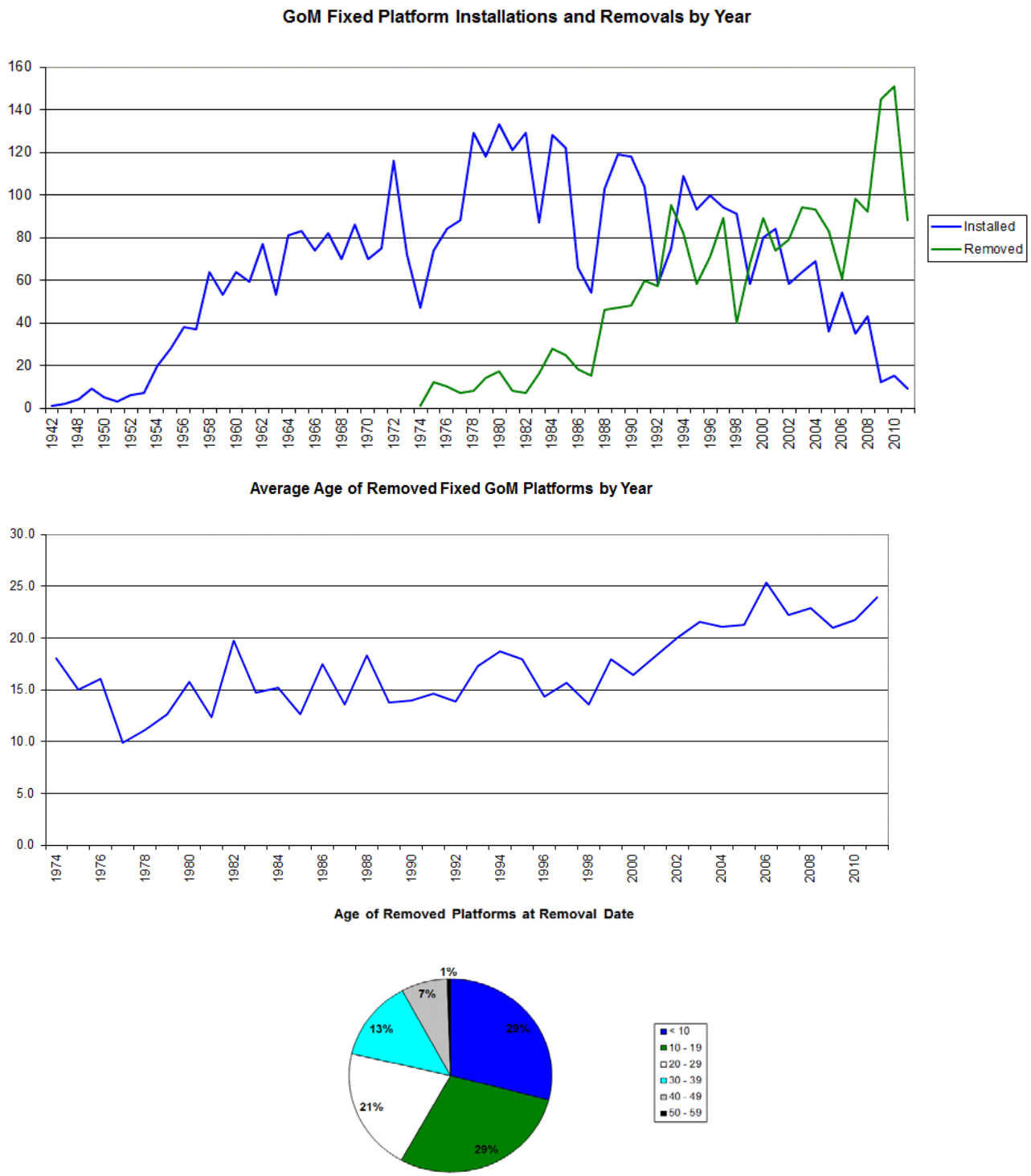

Figure 4-5 GOM Platform Removals (2011)

4.2.3 Inspection Methods

Table 4-2 shows that the RBI methodology entails a risk screening process employed to identify critical areas and specify the associated failure modes. The consequences of possible failures and repair strategy are established in close co-operation with the operator. The costs of inspection and repair of failures are established. Probabilistic progressive collapse analyses are performed for a number of representative mechanisms in the structures. A cost optimal inspection strategy is established.

Table 4-2 Comparison of Traditional Vs. RBI Approaches

Traditional Inspection Planning	RBI Planning
Inspection based on experience (usually by previous failures/breakdowns)	Inspection based on experience and systematic (risk) review
Inspection effort driven by “likelihood of failure”	Inspection effort driven by “risk”, i.e. likelihood of failure and consequences of failure
Reactive “firefighting”, running behind the ball	Pro-active planning and execution of inspections
Use of appropriate/Inappropriate NDT techniques	Systematic identification of appropriate NDT techniques

4.3 General Issues Related to Extended Life

Structural integrity can be maintained for aging platforms by inspection and repair/maintenance strategies (Stacey /32/). From experience it is found that if the platform has a functioning corrosion protection system the structure may serve adequately as long as the CP system is maintained. The fatigue life can be extended considerably beyond a theoretical design life if the structure is inspected according to a relevant inspection plan. Inspection findings are a valuable source for evaluation of the structural reliability of an existing structure.

Recognizing the above, the current project scope of work is focused on discussion of procedures/methodologies for fatigue life prediction of damaged/corroded joints on GOM fixed offshore platforms and will therefore be limited to this objective.

4.4 Challenges of Ageing and Life Extension

“Asset Integrity can be defined as the ability of an asset to perform its required function effectively and efficiently whilst protecting *health, safety and the environment*.” (see Ersdal 2005, /2/)

For existing structures at the end of their calculated design life, the main concern will be if the safety established in the design is still valid.

The following possible hazards have been identified using methods such as HAZID/HAZOP, (see Ersdal 2005, /2/) for the life extension of aging structures:

1. Fatigue: multiple fatigue cracks reducing the structures capacity within an inspection period, leading to unacceptable high probability of failure.
2. Fatigue crack continues to develop at same spot and has been repaired several times. This will give insufficient material quality in the area if welding is used for repair.
3. Widespread fatigue is relevant for life extension, but is normally not evaluated for structures in their design life.
4. Accelerated fatigue in surrounding joints after a fatigue failure of a component.
5. Micro-cracks in material that develop into fatigue failure of a component, especially in ageing structures.
6. Corrosion protection stops working: leading to damages not experienced within the calculated design of the structure.
7. Hydrogen penetration in steel due to corrosion leads to hardening of material
8. Insufficient inspection and maintenance.
9. Marine growth increases resulting in additional loading to the structure.
10. Structure is designed according to old outdated standards for strength, or to outdated environmental criteria.
11. Insufficient strength in damaged condition after component failure. A component failure will be more likely in a life extension. Damage tolerance for a single failure is an important counteracting measure to ensure the safety of the installation if such a failure should occur.
12. Subsidence: results in a decreased safety margin towards wave in deck loading, being the worst hazard for many of the offshore structures of jacket type.
13. Worsening of wave climate: resulting in overloading of jacket structure.

There are also some challenges for life extension of aging structures:

- History of incidents
- Lack of relevant Documentation
- Procedures lost and forgotten
- Possible changes to design basis and environmental conditions
- Integrity of non-accessible areas

ISO Assessment criteria for existing platforms are given in Table 4-3.

Table 4-3 Assessment criteria for existing platform (ISO 19902:2007)

	Assessment criteria
Environment	As criteria for "new" platform, with inclusion of recent data collection and use of: - current state of the art review - experience from adjacent fields - additional data from actual field sea-states
Loading	Conservative evaluation from as-built records and use of recent survey info on: - marine growth - appurtenances - removals/additions/modifications - topsides weight control - wind areas
Foundation	As criteria for "new" platform with inclusion of: - subsidence information - current state-of-the-art review - experience from adjacent fields - post-drive foundation analyses - scour survey and maintenance
Structural model	The structure dimensions are fixed and known: In-service inspection may be applied. Actual characteristics strength of steel based on actual material certificates may be used. Structural performance may have been measured and used to update structural analysis.
Stress analysis	The quality of the analysis is critical. Sufficient time for model tests, removing of conservatism where possible, redundancy studies to determine ultimate strength of structure and foundation, and sensitivity studies on various parameters to improve confidence levels.
Results	Structure has some stresses up to yield stress, but some assessment standards allow for some yielding if the structure has proven strength and redundancy.

4.5 Current Design Codes Related to Assessment of Existing Structures

ISO 19900 (2002) /8/ gives general design rules for assessment of existing structures. It refers to ISO 19902 (2004) /9/ for detailed assessment procedures for existing structures. API-RP2A-WSD (2007) /4/ and NORSOK N-006 (2009) /12/also include detailed procedures for assessment of existing structures. The upcoming API RP 2SIM /5/ will replace Section 17 in 2A 21st Ed. and is expected to be published soon (2012).

Based on screening these standards, the existing assessment procedures consist of the following steps:

- Consideration of initiators.
- Information review (design, fabrication, installation and operation history).
- Structure condition assessment (major damage, corrosion, history of incidents, environmental changes etc.).
- Analysis of the structure (ultimate strength analysis, fatigue analysis etc.).
- Decision making (fit-for-purpose, mitigation).

Both ISO and NORSOK /10/, /11/ and /12/ state that an existing platform should be assessed to demonstrate its fitness for purpose if one or more of the following conditions exist:

1) Changes from the original design or from previous assessment basis, including
   a) Addition of personnel or facilities such that the platform exposure level is changed to a more onerous level.
   b) Modification to the facilities such that the magnitude or dispositions of the permanent, variable or environmental actions on a structure are more onerous.
   c) More onerous environmental conditions and/or criteria.
   d) More onerous component or foundation resistance data and/or criteria.
   e) Physical changes to the structure's design basis, e.g. excessive scour or subsidence, and
   f) Inadequate deck height, such that waves associated with previous or new criteria will impact the deck, and provided such action was not previously considered.
2) Damage or deterioration of a primary structural component: minor structural damage can be assessed by appropriate local analysis without performing a full assessment; cumulative effects of multiple damage shall be documented and included in a full assessment, where appropriate.
3) Exceedance of design service life, if either
   a) The fatigue life (including safety factors) is less than the required extended service life, or
   b) Degradation of the structure due to corrosion is present, or is likely to occur, within the required extended service life.

API RP 2A gives similar initiators as ISO and NORSOK:

2) Addition of personnel: if the life safety level, the platform must be assessed.
3) Additional of facilities: if the original operational loads on a structure or the level deemed acceptable by the most recent assessment are significantly exceeded by the addition of facilities or the consequence of failure level change, the platform must be assessed.

4) Increased loading on structure: if the structure is altered such that the new combined environmental/operational loading is significantly increased beyond the combined loadings of the original design criteria or the level deemed accepted by the most recent assessment, the structure must be assessed.
5) Inadequate deck height: if the platform has an inadequate deck height for its exposure category and the platform was not designed for the impact of wave loading on the deck, the platform must be assessed.
6) Damage found during inspections: Minor structural damage may be justified by appropriate structural analysis without performing a detailed assessment. However, the cumulative effects of damage must be documented and, if not justified as insignificant, be accounted for in the detailed assessment.

ISO 19902 states that the assessment procedures of existing structures are to demonstrate their fitness-for-purpose for the given site and operating conditions. The fit-for-purpose is defined such that the risk of structural failure leading to unacceptable consequences is sufficiently low. The acceptable level of risk depends on regulatory requirements supplemented by regional or industry standards and practice. The design philosophy for existing structures in ISO allows for accepting limited damage to individual component, provided that both the reserve strength against overall system failure and associated deformations remain acceptable. This standard is applicable to both existing jacket structures and topside structures. Its procedure includes two limit state checks: ultimate limit state and fatigue limit state.
Figure 4-6 charts the steps of the ISO 19902:2007 assessment procedure.

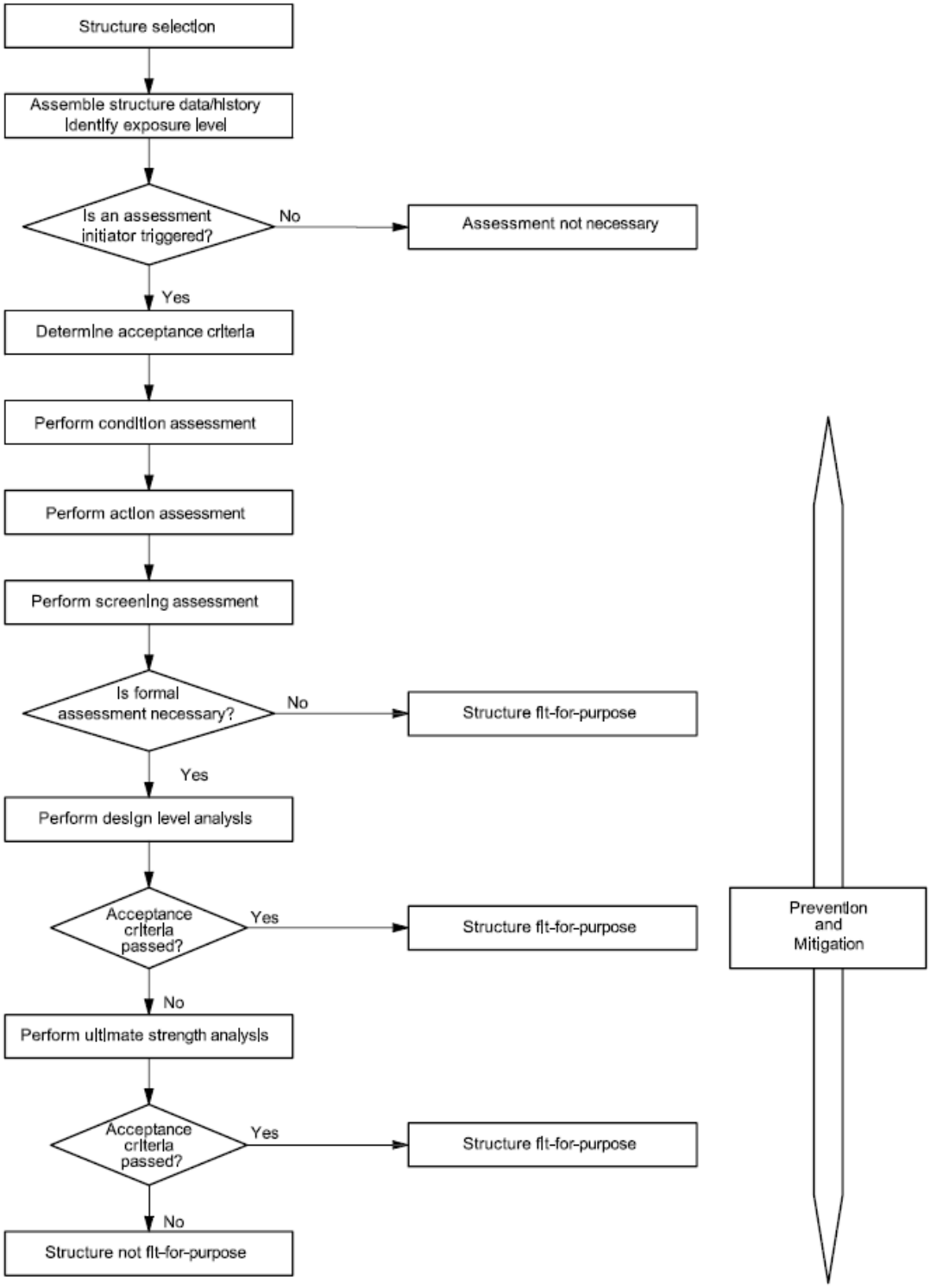

Figure 4-6 Assessment procedure in ISO 19902 (2007)

API RP 2A Section 17 is dedicated to the assessment of existing structures with specific detailed procedures. The section states that the assessment process is applicable only for the assessment of platforms which were designed in accordance with the 20th or earlier editions and prior to the first edition of API RP 2A. The reduced environmental criteria specified in Section 17 are stated not to be used to justify modifications or additions to a platform that will result in an increased loading on the structure for platforms that have been in service less than five years. For the structures designed according to the 21st or later Editions, assessment is to be in accordance with the criteria originally used for the design of the platform, unless a special study can justify a reduction in Exposure Category as defined in Section 1 of API RP 2A.

There are two potential sequential analysis checks mentioned in API RP 2A-WSD, a design level analysis and an ultimate strength analysis. Design level analysis is a simple and conservative check and ultimate strength check is more complex and less conservative. Table 4-4 gives the assessment criteria in the Gulf of Mexico. There is no RSR defined for platform assessment in GOM. Instead, the design level and ultimate strength Metocean criteria are provided in API in the format of wave height versus water depth curves. The ultimate strength wave height is shown to be higher than the design wave height by about 30%. Section 17 of API RP 2A allows reduced design criteria for assessment of existing structures compared with the criteria for new design (see also /39/) with the limitations as stated above.

Table 4-4 Assessment Criteria Proposed in API RP 2A WSD (2007)

Table 17.5.2a–ASSESSMENT CRITERIA–U.S. GULF OF MEXICO

(see Table 17.6.2-1)

Assessment Category	Exposure Category		Design Level Analysis (see Notes 1 and 2)	Ultimate Strength Analysis
	Consequence of Failure	Life Safety		
A-1	High	Manned-Non-Evacuated, Manned-Evacuated or Unmanned	High Consequence design level analysis loading (see Figure 17.6.2-2a)	High Consequence ultimate strength analysis loading (see Figure 17.6.2-2a)
A-2	Medium	Manned-Evacuated or Unmanned	Sudden hurricane design level analysis loading (see Figure 17.6.2-3a)	Sudden hurricane ultimate strength analysis loading (see Figure 17.6.2-3a)
A-3	Low	Unmanned	Minimum consequence design level analysis loading (see Figure 17.6.2-5a)	Minimum consequence ultimate strength analysis loading (see Figure 17.6.2-5a)

Notes 1. Design level analysis is not applicable for platforms with inadequate deck height.
2. One-third increase in allowable stress is permitted for design level analysis (all categories).

NORSOK N-006 provides similar assessment procedures for existing platform assessment with three limit state checks required: Fatigue limit state, Ultimate limit state and Accidental limit state.

API RP 2SIM /5/ describes the reliability approach (similar to RBI) proposed for assessing existing platforms employing all the original procedures of Section 17 of API RP 2A 21st Ed. in a probabilistic format.

5 CURRENT FATIGUE DESIGN METHODS

5.1 General

There are several fatigue design methods used in the industry and the fatigue requirements for each method are summarized here. Both simplified and detailed fatigue methodologies and associated fatigue criteria are addressed. The ISO does not give requirements for simplified fatigue because it mandates detailed fatigue for all structures.

The detailed fatigue requirements in API, ISO, and NORSOK are summarized in

Table 5-3 taken from DNV Code comparison study/39/. The table shows the procedure as recommended in the codes for performing fatigue assessments.

NORSOK refers to DNV fatigue codes directly. Experience gained by DNV over more than 60 years of offshore operation assessing the performance of existing structures with respect to fatigue susceptibility has been incorporated in its most recent recommended practice RP-C203 (October 2010) /1/ (see also Lotsberg/28/). Another DNV recommended practice; RP-C206 (April 2007) /3/ gives guidance on "Fatigue Methodology of Offshore Ships" applicable to ship-shaped offshore units. A critical review of existing fatigue design methods is carried out in these RP's and reported briefly in this section. The sources of variability in the fatigue life calculation methods include the difficulty in arriving at the correct SCF, the definition of the principal stress magnitude and direction relative to that employed in deriving the S-N curve, and the detail complex geometry. These issues are discussed with emphasis on application to typical GOM structures.

5.2 Fatigue Assessment Using S-N data

5.2.1 Fatigue Parameter

5.2.1.1 Loading

API RP 2A /4/ recommends that wave steepness between 1:20 to 1:25 is generally used for the Gulf of Mexico and a minimum height equal one foot and a maximum height equal to the design wave height should be used.

ISO recommends that steepness between 1:20 to 1:25 is used and a wave height equal to the one year return period wave height used as a maximum.

Hot spot stress formula for tubular joints in API and ISO are identical. For other than tubular joints, API RP 2A refers to ANSI/AWS D.1.1 for details.

5.2.1.2 Stress Concentration Factor

The Efthymiou's equations are used in design codes. The same SCF formulas for T/Y joints are adopted at crown positions for long chord members. DNV-RP-C203 /1/ offers recommendations for improvement on such formulas (see Ref. /30/).

The design codes utilize the same SCF formulas for X joints under the conditions of balanced axial load, in-plane bending and balanced out-of plane bending.

For K-joints and KT-joints, design codes also provide same formulas for the conditions of balanced axial load, unbalanced in-plane bending and unbalanced out-of-plane bending.

Fatigue analysis may be based on different methodologies depending on what is found most efficient for the considered structural detail. It is important that stresses are calculated in agreement with the definition of the stresses to be used together with a particular S-N curve. DNV-RP-C203 /1/ gives the three different concepts of S-N curves:

1. Nominal stress S-N curve: Normal stress is a stress in a component that can be derived by classical theory such as beam theory. In a simple plate specimen with an attachment, the nominal stress is simply the membrane stress that is used for plotting of the S-N data from the fatigue testing.
2. Hot spot stress S-N curve for plated structures and tubular joints: Hot spot stress is the geometric stress created by the considered detail.
3. Notch stress S-N curve: It can be used together with finite element analysis where local notch is modeled by an equivalent radius. This approach can be used only in special cases where it is found difficult to reliably assess the fatigue life using other methods.

API RP 2A only gives two S-N curves for two joint classes (WJ for tubular joints and CJ for cast joints) and does not address plated structures. ISO provides additional eight S-N curves for the other connection details based on the nominal stress approach.

In DNV-RP-C203 /1/, all tubular joints are assumed to be class T. Other types of joint, including tube to plate, fall in one of 14 classes depending on:

- The geometrical arrangement of the detail
- The directional of the fluctuating stress relative to the detail
- The method of fabrication and inspection of the detail

DNV-RP-C203 also gives some guidance on assessment of a design S-N curve based on limited test data (see also /29/). Finite element analysis and hot spot stress methodology is important for plated structures. Only DNV-RP-C203 provides guidance for the calculation of hot spot stresses by finite element analysis.

5.2.1.3 Design Fatigue Factor

As shown in Table 5-1, NORSOK recommends design fatigue factors (DFF's) varying from 1, 2, 3, and 10 whereas API DFF's are 2, 5, and 10. NORSOK has DFF ranges for below and above splash zone while API does not make this distinction. NORSOK considers all structural joints deeper than 150m to be inaccessible for inspection. ISO used the same factors as API (2, 5, and 10) for fixed platforms and 1, 2, 5 and 10 for floaters (see

Table 5-3).

Table 5-1 NORSOK N-004 Design Fatigue Factors

Table 8-1 Design fatigue factors

Classification of structural components based on damage consequence	Access for inspection and repair		
	No access or in the splash zone	Accessible	
		Below splash zone	Above splash zone
Substantial consequences	10	3	2
Without substantial consequences	3	2	1

"Substantial consequences" in this context means that failure of the joint will entail
danger of loss of human life;
significant pollution;
major financial consequences.

Design codes suggest that the fatigue life may be calculated based on S-N fatigue approach under the assumption of linear cumulative damage (Palmgren-Miner rule). Even though the cumulative fatigue damage passing criteria looks different, but the basic principle is all the same. Only difference is that where the design safety factor (DFF) is introduced.

5.2.2 Simplified Fatigue

API allows simplified fatigue calculations only for Category L-3 template type platforms that are constructed of notch-tough ductile steels, have redundant inspectable structure, and have natural period of less than 3s or for preliminary design of all structure categories in water depth up to 400 ft (122m). As shown in Table 5-2 API RP 2A WSD defines in Section 5.1 and its commentary the fatigue design wave and allowable peak hot spot stresses. Simple tubular joints SCF formulas are also presented in addition to recommended DFF (Design Fatigue Factor) depending on criticality of the fatigue failure and accessibility for inspection see Table 5-2.

NORSOK refers to DNV-RP-C203, Section 5 for the details of the methodology and the allowable stress range as function of the Weibull shape parameter and the applicable fatigue curve (depending on the joint detail and stress field configuration; i.e., the fatigue curve) for 20 years' service life (10^8 cycles).

The simplified fatigue methodology given in DNV-RP-C203 is applicable to mass dominated structures such as Semisubmersible, ships, FPSOs and TLPs in conceptual design phase. It is less appropriate for drag dominated structures such as jackets and truss towers with slender tubular members.

5.2.3 Detailed Fatigue

The comparison in

Table 5-3 covers the assumptions, loading definitions, hot spot stress range calculation, stress concentration factor formulas, S-N curves for tubular joints, and DFF required values. In addition,

details of the spectral analysis, utilization of fracture mechanics, and fatigue life improvement techniques are also compared in

Table 5-3. As noted detailed fatigue analysis involves the following main steps:

- Loading definition
- Stress range calculation
- Stress Concentration factor determination
- S-N curves definition for tubular joints
- Fatigue damage design factor
- Fatigue damage accumulation

The use of spectral analysis, fracture mechanics, and weld improvement techniques are also noted in the table.

5.3 Fatigue Assessment Using Fracture Mechanics

Fracture mechanics may be used for fatigue analyses as supplement to S-N curve.

Fracture mechanics is recommended for use in assessment of acceptable defects, evaluation of approach criteria for fabrication and for planning in-service inspection.

The purpose of analysis is to document, by means of calculations, that fatigue cracks, which might occur during service life, will not exceed the crack size corresponding to unstable fracture. The calculation should be performed such that the structural reliability by use of fracture mechanics will be not less than that achieved by use of S-N curve data. To achieve this, the following procedure may be followed:

Crack growth parameter C determined as mean plus 2 standard deviations. A careful evaluation of initial defects that might be present in the structure when taking into account the actual NDE inspection method used to detect cracks during fabrication. Use of geometry functions that are on the safe side. Use of utilization factors similar to those used when the fatigue analysis is based on S-N data.

As crack initiation is not included in the fracture mechanics approach, shorter fatigue life is normally derived from fracture mechanics than S-N curve.

There are several fatigue crack growth equations that have been used in API 579-2/ASME FFS-2 (2009) /7/ and summarized in API 579-1/ASME FFS-1 (2007) /6/, Annex F.5.2. The Paris' equation is the simplest of the fatigue crack growth models which is mentioned in DNV-RP-C203 /1/, ISO 19902 /9/, and BS-7910 /2/.

$$da/dN = C(\Delta K)^m \qquad (5.1)$$

where

$\Delta K = K_{max} - K_{min}$=stress intensity factor (SIF) range

N = Number of cycles of the SIF range

a = crack depth. It is here assumed that the crack depth/length ratio is low (less than 1:5)

C, m = material parameters, see BS 7910
The stress intensity factor K may be expressed as:

$$K = \sigma \cdot g \cdot \sqrt{\pi a} \tag{5.2}$$

where
σ = nominal stress in the member normal to the crack
g = factor depending on the geometry of the member and the crack
Further guidance related to fatigue assessment based on fracture mechanics is given in BS-7910.

5.4 Fatigue Assessment by Other Methods

Probabilistic fatigue methods have been used in Risk Based Inspection (RBI) planning programs with regard to fatigue for many years. The probabilistic S-N Fatigue model used to determine the acceptable reliability level is outlined in the following:

The limit state function applied in the reliability analysis is expressed as:

$$g(D, \Delta) = \Delta - D \tag{5.3}$$

The random variable Δ describes general uncertainty associated with the fatigue capacity and D is the accumulated fatigue damage.

Defining the mean number of stress cycle per time unit to be ν_0, the total accumulated fatigue damage in a service period T can be expressed as:

$$D = T\, \nu_0\, D_{cycle} \tag{5.4}$$

D_{cycle} is the expected damage per stress cycle, which depends on the distribution of the local stress range response process and the associated S-N curve. For a Weibull long-term stress range distribution, the expected damage per stress cycle is calculated as:

$$D_{cycle} = \frac{1}{a_2} q^{m_2} \gamma\left(1 + \frac{m_2}{h}; \left(\frac{S_0}{q}\right)^h\right) + \frac{1}{a} q^m \Gamma\left(1 + \frac{m}{h}; \left(\frac{S_0}{q}\right)^h\right) \tag{5.5}$$

S_0 is the stress range level for which change in slope occurs for the bilinear SN-curve, a, a_2, m and m_2 are the parameters defining the S-N curve, γ(;) and Γ(;) are the Incomplete and Complementary Incomplete Gamma functions, and q and h are Weibull distribution parameters:

$$F_S(s) = 1 - \exp[(-s/q)^h] \qquad (5.6)$$

The applied procedure for calculating the target reliability level may be outlined as:

- Define the structure detail
- Select the SN curve to be applied to the detail
- Derive the shape parameter, h, in the long-term stress range distribution
- Define the design life for the structural detail (assumed equal to 20 years in some cases)
- Define the fatigue life design fatigue factor (DFF) to be applied (depends on the consequence of failure and inspectability) with values ranging from 1 to 10 are assigned.
- Calculate the highest allowable scale parameter, q, in the long-term stress range, for the design life and the design fatigue factor.
- Calculate the failure probability at the end of the design life.

Table 5-2 Simplified Fatigue

Table - Simplified Fatigue

	API RP 2A - WSD	NORSOK N-001, N003/DNV-RP-C203
Simplified fatigue analysis (section 5.1 and C 5.1)		DNV-RP-C203 5. Simplified fatigue analysis
Limitations	- Have been calibrated for the design wave climate - May be applied to tubular joints in Category L-3 template type platforms as defined in Section 1.7 1. Are constructed of notch-tough ductile steels 2. Have redundant, inspectable strutcural framing 3. Have natural periods less than 3 seconds - Particularly useful for preliminary design of all structure categories and types, in water depths up to 400 feet (122 m)	These design charts have been derived based on an assumption of an allowable fatigue damage e=1.0 during 10^8 cycles (20 years service life which corresponds to an average period 6.3 sec).
Evironmental Data	Fatigue design wave: - Fatigue design wave is the reference level -wave for the platform water depth as defined in Figure 2.3.4-3. 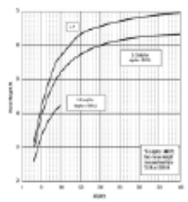 - Wave Foces - Follow the procedures in Section 2.3.1 except that the omni-directional wave should be applied in all directions with wave kinematics factor equal to 0.88. - Wave should be applied to the structure without wind, current and gravity load effects. - In general, four wave approach directions (end-on, broadside and two diagonal) and sufficient wave positions relative to the platform should be considered to identify the peak hot stress at each member end for the fatigue design wave.	
	Tide as defined in Figure 2.3.4-7 should be included. 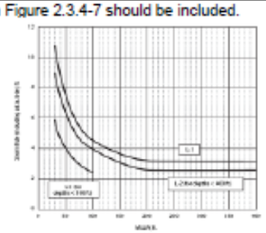	
Allowable Peak Hot Spot Stresses	The allowable peak hot spot stress, Sp, is determined from Figure C5.1-1 or C5.1-2. 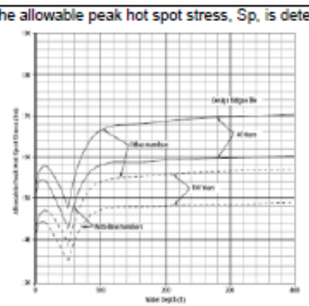 Figure C5.1-1—Allowable Peak Hot Spot Stress, S_p (AWS Level I) 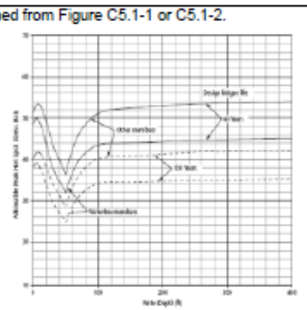 Figure C5.1-2—Allowable Peak Hot Spot Stress, S_p (AWS Level II)	-Design charts for steel components in air and in seawater with cathodic protection are given. 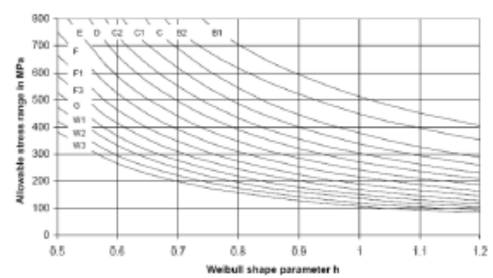 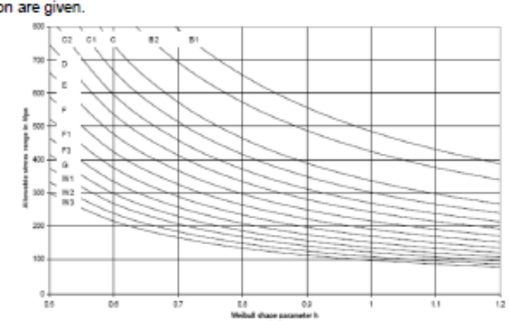

Peak Hot Spot Stress for the Fatigue Design Wave

The peak hot spot stress at a joint should be taken as the maximum value of the following expression calculated at both the chord and brace sides of the tubular joint:

$$|SCF_{ax} f_{ax}| + \sqrt{[(SCF_{ipb} f_{ipb})^2 + (SCF_{opb} f_{opb})^2]} \quad (C5.5\text{-}1)$$

where f_{ax}, f_{ipb} and f_{opb} are the nominal member end axial, in-plane bending and out-of-plane bending stresses; SCF_{ax}, SCF_{ipb} and SCF_{opb} are the corresponding stress concentrations factor for axial, in-plane bending and out-of-plane bending stresses for the chord or the brace side.

Table C5.1-1 includes SCF's developed from the referenced examples, to be used with equation (C5.1-1) for simple joints.

DFF

Table 5.2.5-1 Fatigue Life Safety Factors

Failure critical	Inspectable	Not Inspectable
No	2	5
Yes	5	10

- Table above is for assessment of Category L-1 structures;
- A reduced safety factor is recommended for Category L-2 and L-3 conventional steel jacket structures on the basis of in-service performance data: SF=1.0 for redundant diver or ROV inspectable framing, with safety factors for other cases being half those in the table;

Design fatigue factor in DNV-RP-C203 refers to DNV-OS-C101 Section 6, Table A1, which is valid for units with low consequence of failure and where it can be demonstrated that the structure satisifes the requirement to damaged condition according to the ALS with failure in the actual element as the defined damage.

Table A1 Design fatigue factors (DFF)

DFF	*Structural element*
1	Internal structure, accessible and not welded directly to the submerged part.
1	External structure, accessible for regular inspection and repair in dry and clean conditions.
2	Internal structure, accessible and welded directly to the submerged part.
2	External structure not accessible for inspection and repair in dry and clean conditions.
3	Non-accessible areas, areas not planned to be accessible for inspection and repair during operation.

NORSOK N-004, Tables 8-1 and K.4-1 also give the DFFs and are included in Detailed Fatigue comparison table.

SCF

Table C5.1-1 - Selected SCF Formulas for Simple Joints

	Joint Type	α	Axial Load	In-Plane Bending	Out-of-Plane Bending
Chord SCF	K	1.0	αA	2/3A	3/2A
	T & Y	1.7			
	X $\beta < 0.98$	2.4			
	X $\beta \geq 0.98$	1.7			
Brace SCF's			$1.0+0.375\,[1+(\tau/\beta)^{0.5}\,SCF_{chord}] \geq 1.8$		

Where $A = 1.8\,\gamma^{0.5}\,\tau \sin(\theta)$, $\beta = d/D$, $\gamma = D/(2T)$, $\tau = t/T$
d = Brace outside diameter, in. (mm)
D = Chord outside diameter, in. (mm)
t = Brace wall thickness at intersection, in. (mm)
T = Chord wall thickness at intersection, in. (mm)

SCF Formulas for tubular joints are given in DNV-RP-C203 Appendix B "SCF's for Tubular Joints"; SCF's for Penetrations with Reinforcements are given in Appendix C;

Table 5-3 Detailed Fatigue

Table - Detailed Fatigue

	API RP 2A - WSD	ISO 19902/19904	Norsok N-004/DNV RP-C203
Validity	The fatigue assessment of welded joints is based on the assumption that the connection has full-penetration single or double sided welding.	- The requirements in this ISO are applicable to the fatigue design of new structures as well as the fatigue assessment of existing structures. However, they only relate to fatigue evaluations of "uncracked" locations; therefore, in the case of exisitng structures, the proviso is that there be no crack already present. -The fatigue assessment of welded joints is based on the assumption that the connection has full-penetration single or double sided welding, unless otherwise stated.	- In this standard, the requirements in relation to fatigue analyses are based on fatigue tests and fracture mechanics. -Reference is made to DNV-RP-C203 for more details with respect to fatigue design. - DNV RP-C203 1) It is valid for steel materials in air with yield strength less than 960 MPa. For steel materials in seawater with cathodic protection or steel with free corrosion the RP is valid up to 550 MPa. It may be used for stainless steel. 2) This RP is valid for material temperatures of up to 100°C. For higher temperatures the fatigue resistance data may be modified with a reduction factor.
Loading	The wave force calculations should follow the procedures described in Section 2.3.1 with the following exceptions: - Current - may be neglected and considerations for apparent wave period and current blockage are not required; - For the Gulf of Mexico a steepness between 1:20 and 1:25 is generally used. A minimum height equal one foot and a maximum height equal to the design wave height should be used. - Wave kinematics factor = 1.0 - Conductor shieding factor = 1.0 - For small waves (1.0 < K < 6.0 for platform legs at mean water level), values of C_m = 2.0, C_d = 0.8 for rough members and C_d = 0.5 for smooth members - Use 60 to 150 sea states each with its wave energy spectrum	- In determining stress variations for a fatigue analysis the partial action factors shall be taken as 1.0. - The partial resistance factor on the fatigue assessment shall also be taken as 1.0.	- In determining stress variations for a fatigue analysis the partial action factors shall be taken as 1.0. - The partial resistance factor on the fatigue assessment shall also be taken as 1.0. - Fatigue analysis can normally be counducted with no current. - Wave kinematics factor = 1.0 - Conductor shielding factor = 1.0 - For small waves with KC referred to the mean water level in the range 1.0<KC<6, the hydrodynamic coefficients can be taken to be: C_d = 0.65 and C_m = 2.0 (smooth member); C_d = 0.80 and C_m = 2.0 (rough members) - In lack of site specific data, the wave periods shall be determined based on a wave steepness of 1/20. - For a stochastic fatigue analysis, it is important to select periods such that response amplifications and cancellations are included. Also selection of wav periods in relation to the platform fundamental period of vibration is important. The number of periods inlcuded in the analysis should not be less than 30, and be in the range from T = 2 s to at least T = 20 s.
Stress Range	**hot spot stress and hot spot stress range (HSSR)** - A minimal of eight stress range locations need to be considered around each chord-brace intersection in order to adequately cover all relevant locations. These are: chord crowns (2), chord saddles (2), brace crowns (2) and brace saddles(2). - HSS for saddle and crown are given by: $HSS_{sa} = SCF_{axsa} f_{ax}$ +/- $SCF_{opb} f_{opb}$ $HSS_{cr} = SCF_{axcr} f_{ax}$ +/- $SCF_{ipb} f_{ipb}$ +CE where f = nominal stress sa = saddle cr = crown ax = axial ipb = in-plane bending opb = out-of-plane bending CE = the effect of nominal cyclic stress in the chord **- Other than tubular joints** Where variations of stress are applied to conventional weld details, idetified in the ANSI/AWS D1.1 - 2002 Table 2.4, the associated S-N curves provided in Figure 2.11 should be used, dependent on degree of redundancy.	**geometric stress (GS) and geometric stress range (GSC)** **-Tubular Joints** - A minimum of eight stress range locations need to be considered around each chord/brace intersection weld in order to adequately cover all relevant locations. These are: the chord sides at two crown positions, the brace sides at two crown positions, the chord sides at two saddle posotions and the brace sides at two saddle positions. - The GSRs for the chord and the brace side of the weld are determined: $\sigma_{GS,s}(t) = C_{ax,s}\sigma_{ax}(t)$ +/- $C_{opb,s}\,\sigma_{opb}(t)$ $\sigma_{GS,c}(t) = C_{ax,c}\sigma_{ax}(t)$ +/- $C_{ipb,c}\,\sigma_{ipb}(t) + \sigma_{C,c}(t)$ where σ_{Gs} = the geometric stress on the chord or the brace side of the weld between chord and brace σ_{ax} = the nominal axial stress in the brace (or stub) σ_{ipb} = the nominal in-plane bending stress in the brace (or stub) σ_{opb} = the nominal out-of-plane bending stress in the brace (or stub) $\sigma_{C,c}$ = the nominal stress in the chord (or chord can) at the crown position C_{ax} = the stress concentration factor for axial brace stress C_{ipb} = the stress concentration factor for in-plane bending stresses in the brace C_{opb} = the stress concentration factor for out-of-plane bending stresses in the brace t = time s = the subscript denoting the saddle position c = the subscript denoting the crown position - The effect of nominal variable stresses in the chord member can be covered by including the stress due to axial force in the chord can member, combined with an axial SCF of 1.25, i.e. $\sigma_{C,c}(t) = 1.25\,\sigma_{ax,c}(t)$ **- Other than tubular joints** - The stree range indicated in Tables A.16.10-7 to A.16.10-11 and used as the GSR is the maximum principle stress range adjacent to the detail under consideration, except for the throat of load carrying fillet or partial penetration welds, for which it is the shear stress range calculated on the minimum throat area. - For details that are not expressly classified, the following minimum classification class should be used, unless a higher class can be justified from published experimental work, or by specific tests: - W_1 for load carrying fillet or partial penetration weld metal; - F_2 for other cases	**hot spot stress and hot spot stress range** **- Tubular Joints and Members** The stresses are calculated at the crown and the saddle ponits. $\sigma_1 = SCF_{AC}\,\sigma_x + SCF_{MIP}\,\sigma_{ay}$ $\sigma_2 = \frac{1}{2}(SCF_{AC} + SCF_{AS})\,\sigma_x + \frac{1}{2}\sqrt{2}\,SCF_{MIP}\,\sigma_{ay} - \frac{1}{2}\sqrt{2}\,SCF_{MOP}\,\sigma_{az}$ $\sigma_3 = SCF_{AS}\,\sigma_x - SCF_{MOP}\,\sigma_{az}$ $\sigma_4 = \frac{1}{2}(SCF_{AC} + SCF_{AS})\,\sigma_x - \frac{1}{2}\sqrt{2}\,SCF_{MIP}\,\sigma_{ay} - \frac{1}{2}\sqrt{2}\,SCF_{MOP}\,\sigma_{az}$ $\sigma_5 = SCF_{AC}\,\sigma_x - SCF_{MIP}\,\sigma_{ay}$ (3.3.1) $\sigma_6 = \frac{1}{2}(SCF_{AC} + SCF_{AS})\,\sigma_x - \frac{1}{2}\sqrt{2}\,SCF_{MIP}\,\sigma_{ay} + \frac{1}{2}\sqrt{2}\,SCF_{MOP}\,\sigma_{az}$ $\sigma_7 = SCF_{AS}\,\sigma_x + SCF_{MOP}\,\sigma_{az}$ $\sigma_8 = \frac{1}{2}(SCF_{AC} + SCF_{AS})\,\sigma_x + \frac{1}{2}\sqrt{2}\,SCF_{MIP}\,\sigma_{ay} + \frac{1}{2}\sqrt{2}\,SCF_{MOP}\,\sigma_{az}$ 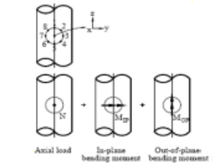 Figure 3-7 Superposition of stresses **- Welded connections other than tubular joints** In plates structures, three types of hot spots at weld toes can be identified: a) at the weld toe on the plates surface at ending attachment b) at the weld toe around the plate edege of an ending attachment c) along the weld of an attached plate (weld toes on both the plate and attachment surface) 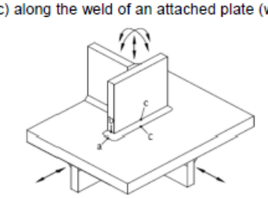 Figure 4-3 Different hot spot positions

Stress Concentration Factor (SCF)

SCF = HSSR at location (excluding notch effect) / Norminal Brace Stress Range;

1. The SCF should include all stress raising effects associated with the joint geometry and type of loading, except the local (microscopic) weld notch effect, which is included in the S-N curve.
2. The geometric stress or strain is defined as the total range that would be measured by a strain guage adjacent to the toe of the weld and oriented perpendicular to the weld so as to reflect the stress which will be amplified by the weld toe discontinuities. Typical geometric strain gauges are centred within 6 mm to $0.1(rt)^{0.5}$ from the weld toes with a guage length of 3 mm. r and t refer to the outside radius and thickness of the member instrumented, whether chord or brace.
3. The Efthymiou equations (in Tables C5.3.2-1 to C5.3.2-4) are recommended because this set of equations is considered to offer the best option for all joint types and load types and is the only widely vetted set that covers overlapped K and KT joints.

The validity ranges for the Efthymiou parametric SCF equations are as follows:

β = d/D from 0.2 to 1.0
τ = t/T from 0.2 to 1.0
γ = g/2T from 8 to 32
α = L/2D (length) from 4 to 40
θ from 20 to 90 degresss
ξ = g/D (gap) from -0.6β/sin(θ) to 1.0

4. For all welded tubular joints under all three types of loading, a minimum SCF of 1.5 should be used.
5. SCFs for internally ring-stiffened joints can be determined by applying the Lloyds reduction factors to the SCFs for the equivalent unstiffened joint. For ring-stiffened joints analyzed by such means, the minimum SCF for the brace side under axial or OPB loading should be taken as 2.0. A minimum value of 1.5 is recommended for all other locations.

SCF = the range of the GS at a particular location of the intersection weld (excluding notch effect) / the range of the nominal brace stress

1. The recommeded S-N curves and SCF equations used is ISO are based on European definition and are consistent.
2 The **Efthymiou equations** are recommended because this set of equations is considered to offer either the best option or a very good option for all joint types and types of brace forces and is the only set which covers overlapped K- and KT-joints.
3. The validity ranges for the Efthymiou parametric SCF equations are as follows:

β = d/D from 0.2 to 1.0
τ = t/T from 0.2 to 1.0
γ = g/2T from 8 to 32
α = L/2D (length) from 4 to 40
θ from 20 to 90 degresss
ξ = g/D (gap) from -0.6b/sin(θ) to 1.0

4. Increasing the chord wall thickness is an effective way of reducing stress concentrations. For T/Y- and X-joints, a doubling of the chord wall thickness reduces the saddle SCFs by a factor of 4; crown SCFs are also reduced considerably.
5. SCF Equations for tubulars are given in ISO 19902 Table A.16.10-2 "Equations for SCFs in T/Y joints" and Table A.16.10-4 "Equations for SCFs in gap/overlap K-joints".

SCF = hot spot stress range/nominal stress range

- The local weld notch effect is excluded by using stress values just outside the weld notch region and extrapolating these (linearly) to the weld toe. The European definition is based on maximum principal stress, i.e. the stress components are extrapolated to the weld toes and then used in Mohr's Circle to establish the maximum principal stress at the toe.The stress normal to the weld toe, used in the US definition, is somewhat lower than this, but for the all-important saddle location the two are virtually identical.
- SCF Formulas for tubular joints are given in DNV-RP-C203 Appendix B "SCF's for Tubular Joints", Table B1 - B5; SCF's for Penetrations with Reinforcements are given in Appendix C;
- The validity range for the equations in Table B-1 to Table B-5 is as follows:

β = d/D from 0.2 to 1.0
τ = t/T from 0.2 to 1.0
γ = g/2T from 8 to 32
α = L/2D (length) from 4 to 40
θ from 20 to 90 degresss
ξ = g/D (gap) from -0.6b/sin(q) to 1.0

or Tubular Connections

The basic **tubular joint** S-N curve has been derived from an analysis of data on tubular joints manufaured using welds conforming to a standard flat profile given in AWS.
The basic design S-N curve is of the form:

$Log_{10}(N) = Log_{10}(k1) - mLog_{10}(S)$ (5.4.1-1)

where N = the predicted number of cycles to failure under stress range S,
k1 = a constant,
m = the inverse slope of the S-N curve

Table 5.5.1-1 - Basic Design S-N Curves

Curve	$\log_{10}$ (k1) S in ksi	$\log_{10}$ (k1) S in MPa	m
Welded Joints (WJ)	9.95 11.92	12.48 16.13	3 for N < 10^7 5 for N > 10^7
Cast Joints (CJ)	11.80 13.00	15.17 17.21	4 for N < 10^7 5 for N > 10^7

- The basic design S-N curves given in Table 5.5.1-1 are applicable for joints in air and submerged coated joints.
- These S-N curves are based on steels with yield strength less than 72 ksi (500 MPa)
- The WJ curve is based on 5/8-in (16mm) reference thickness. For material thickness above the reference thickness, the following thickness effect should be applied for as-welded joints:

$S = S_o (t_{ref}/t)^{0.25}$

where: tref = the reference thickness, 5/8-inch (16 mm),
S = allowable stress range
So = the allowable stress range from the S-N curve
t = member thickness for which the fatigue life is predicted

- The material thickness effect for castings is given by:

$S = So (t_{ref}/t)^{0.15}$

where the reference thickness t_{ref} is 1.5 in (38 mm)

- For Welded Joints in seawater with adequate cathodic protection, the m = 3 branch of the S-N curve should be reduced by a factor of 2.0 on life, with the m = 5 branch remaining unchanged and the position of the slope change adjusted accordingly.

The basic design S-N curve is of the form:

$\log_{10}(N) = \log_{10}(k1) - m\log_{10}(S)$ (16.11-1)

where N = the predicted number of cycles to failure under constant amplitude stress range S,
k1 = a constant, (k1 = N for S=1)
m = the inverse slope of the S-N curve
S = the constant amplitude stress range, which is the geometrical stress range

Table 16.11-1 - Basic representative S-N curves for air and sea water

Curve	Air		Sea water with adequate corrosion protection	
	$\log_{10}$ (k1) S in MPa	m	$\log_{10}$ (k1) S in MPa	m
Welded Joints (WJ)	12.48 16.13	3.0 for N≤10^7 5.0 for N>10^7	12.18 16.13	3.0 for N≤ 1.8 x 10^6 5.0 for N>1.8 x 0^6
Cast Joints (CJ)	15.17	4		
Other joints (OJ)				
B	15.01 17.01	4.0 for N≤10^7 5.0 for N>10^7	14.61 17.01	4.0 for N≤10^5 5.0 for N>10^5
C	13.63 16.47	3.5 for N≤10^7 5.0 for N>10^7	13.23 16.47	3.5 for N≤4.68 x 10^5 5.0 for N>4.68 x 10^5
D	12.18 15.63	3.0 for N≤10^7 5.0 for N>10^7	11.78 15.63	3.0 for N≤10^6 5.0 for N>10^6
E	12.02 15.37	3.0 for N≤10^7 5.0 for N>10^7	11.62 15.37	3.0 for N≤10^6 5.0 for N>10^6
F	11.80 15.00	3.0 for N≤10^7 5.0 for N>10^7	11.40 15.00	3.0 for N≤10^6 5.0 for N>10^6
F_2	11.63 14.71	3.0 for N≤10^7 5.0 for N>10^7	11.23 14.71	3.0 for N≤10^6 5.0 for N>10^6

The basic design S-N curve is of the form:

$\log_{10}(N) = \log(\bar{a}) - m\log_{10}(\Delta\sigma)$ (2.4.1 DNV RP-C203)

where N = the predicted number of cycles to failure under constant amplitude stress range $\Delta\sigma$,
m = negative inverse slope of the S-N curve
$\Delta\sigma$ = stress range
log $\bar{a}$ = log a -2s intercept of log N-axis by S-N curve
a = constant relating to mean S-N curve
s = standard deviation of log N

Table 2-1 S-N Curve in Air and Table 2-2 S-N curve in seawater with cathodic protection

S-N Curve	Air		Sea water with adequate cathodic protection	
	log $\bar{a}_1$ S in MPa	m	$\log_{10}$ (k1) S in MPa	m
T	12.164 15.606	3.0 for N≤10^7 5.0 for N>10^7	11.764 15.606	3.0 for N≤ 10^5 5.0 for N>10^6
C	12.592 16.320	3.0 for N≤10^7 5.0 for N>10^7	12.192 16.320	3.0 for N≤ 10^6 5.0 for N>10^6
Other joints (OJ)				
B1	15.117 17.146	4.0 for N≤10^7 5.0 for N>10^7	14.971 17.146	4.0 for N≤ 10^5 5.0 for N>10^6
B2	14.885 16.858	4.0 for N≤10^7 5.0 for N>10^7	14.685 16.856	4.0 for N≤ 10^5 5.0 for N>10^6
C1	12.449 16.081	3.0 for N≤10^7 5.0 for N>10^7	12.049 16.081	3.0 for N≤10^6 5.0 for N>10^6
C2	12.301 15.835	3.0 for N≤10^7 5.0 for N>10^7	11.901 15.835	3.0 for N≤10^6 5.0 for N>10^6
D	12.164 15.606	3.0 for N≤10^7 5.0 for N>10^7	11.764 15.606	3.0 for N≤10^6 5.0 for N>10^6
E	12.010 15.350	3.0 for N≤10^7 5.0 for N>10^7	11.610 15.350	3.0 for N≤10^6 5.0 for N>10^6

S-N Curves fc

- The curve for cast joints is only applicable to castings having an adequate fabrication inspection plan.

G	11.40 14.33	3.0 for N≤10^7 5.0 for N>10^7	11.00 14.33	3.0 for N≤10^6 5.0 for N>10^6
W_1	10.97 13.62	3.0 for N≤10^7 5.0 for N>10^7	10.57 13.62	3.0 for N≤10^6 5.0 for N>10^6

- The basic design S-N curves given in Table 16.11-1 are applicable for joints in air and seawater with adequate corrosion protection.
- These S-N curves are based on steels with yield strength less than 500 MPa.
- The WJ curve is based on 16mm) material thickness. For material thickness above 16 mm, the following thickness effect should be applied for as-welded joints:

$S = S_o\,(16/t)^{0.25}$

where: S = the stress range of S-N curve, when adjusted for thickness effects
So = the stress range from the S-N curve in Table 16.11-1
t = member thickness in mm for which the fatigue life is predicted

- The material thickness effect for castings is given by:

$S = So\,(38/t)^{0.15}$

- The curve for cast joints is only applicable to castings having an adequate fabrication inspection plan.

F	11.855 15.091	3.0 for N≤10^7 5.0 for N>10^7	11.455 15.091	3.0 for N≤10^6 5.0 for N>10^6
F1	11.699 14.832	3.0 for N≤10^7 5.0 for N>10^7	11.299 14.832	3.0 for N≤10^6 5.0 for N>10^6
F3	11.546 14.576	3.0 for N≤10^7 5.0 for N>10^7	11.146 14.576	3.0 for N≤10^6 5.0 for N>10^6
G	11.398 14.330	3.0 for N≤10^7 5.0 for N>10^7	10.998 14.330	3.0 for N≤10^6 5.0 for N>10^6
W1	11.261 14.101	3.0 for N≤10^7 5.0 for N>10^7	10.861 14.101	3.0 for N≤10^6 5.0 for N>10^6
W2	11.107 13.845	3.0 for N≤10^7 5.0 for N>10^7	10.707 13.845	3.0 for N≤10^6 5.0 for N>10^6
W3	10.970 13.617	3.0 for N≤10^7 5.0 for N>10^7	10.570 13.617	3.0 for N≤10^6 5.0 for N>10^6

- S-N curves are obtained from fatigue tests. The design S-N curves which follows are based on the mean-minus-two-standard-deviation curves for relevant experimental data. The S-N curves are associated with 97.6% probability of survival.
- The thickness effect is accounted for by a modification on stress such that the design S-N curve for thickness larger than the reference thickness reads:

$\log_{10}(N) = \log(\bar{a}) - m\log_{10}(\Delta\sigma(t/t_{ref})^k)$ (2.4.3 DNV RP-C203)

where t_{ref} = reference thickness equal 25 mm for welded connections other than tubular joints. For tubular joints the reference thickness is 32 mm. For bolts t_{ref} = 25 mm
k = thickness exponent on fatigue strength as given in Tables 2-1, 2-2 and 2-3
k = 0.10 for tubular butt welds made from one side
k = 0.25 for threaded bolts subjected to stress variation in the axial direction
- It is recommended to use the C curve for cast nodes. t_{ref} = 38 mm may be used.
- For forged nodes the B1 curve may be used for nodes designed with a Design Fatigue Factor equal to 10. For designs with DFF less than 10 it is recommended to use the C-curve to allow for wled repair if fatigue cracks should occur during service life.

Fatigue damage design factors

Table 5.2.5-1 Fatigue Life Safety Factors

Failure critical	Inspectable	Not Inspectable
No	2	5
Yes	5	10

- Table above is for assessment of Category L-1 structures;
- A reduced safety factor is recommended for Category L-2 and L-3 conventional steel jacket structures on the basis of in-service performance data: SF=1.0 for redundant diver or ROV inspectable framing, with safety factors for other cases being half those in the table;

ISO 19902 - Table A.16.12.-1 - Fatigue damage design factors, γ_{FD}

Failure critical component	Inspectable	Not Inspectable
No	2	5
Yes	5	10

- The factors given in Table A.16.12-1 should be considered to relate to exposure Level L1, but should also be used for exposure levels L2 and L3. There is currently insufficient background to establish different factors for lower exposure levels.

ISO 19904 Table 6- Fatigue damage design safety factors

Consequence of fauilure	Degree of accessibility for inpsection and repair		
	Not accessible	Underwater access	Dry access
Substantial	10	5	2
Non-substantial	5	2	1

Table 8-1 Design Fatigue Factors (DFF's)

Classification of structural components based on damage consequence	Access for inspection and repair	
	No access or in the splash zone	Accessibility Below splash zone
Substantial consequences	10	3
Without substantial consequences	3	2

"Subtantial consequences" in this context means that failure of the joint will entail danger of loss of human life; significant pollution; major financial consequences
"Without substantial consequences" is understood failure where it can be demonstrated that the structure satisfy the requirement to damaged condition according to the ALSs with failure in the actual joint as the defined damage

Table K.4-1 Fatigue design factors in jackets

Classification of structural components based on damage consequence	Access for inspection and repair	
	No access or in the splash zone	Accessibility Below splash zone
- Brace/stub to chord welds in main loadtransferring joints in vertical plans - chord/cone to leg welds, between leg connections - Brace to stub and Brace to Brace welds in main loadtransferring members in vertical plans - Shear plates and yoke plates incl. stiffening - Piles and bucket foundation plates incl. stiffening	10	3
- Brace/stub to chord welds in joints in horizontal plans - chord/cone to leg welds, between leg connections - Chord/cone to brace welds and welds between sections in horizontal plans - Appurtenance supports - Anodes, doubler plates - Outfitting steel	3	2

The cumulative fatigue damage ratio, D,

$D = \sum (n/N)$ (5.2.4-1)

A linear accumulation of fatigue damage under constant amplitude stress ranges, according to the Palmgren-Miner rule:

- Under the assumption of linear cumulative damage (Palmgren-Miner rule)

Fatigue damage accumulation	where n = number of cycles applied at a given stress range N = number of cycles for which the given stress range would be allowed by appropriate S-N curve When faigue damage can occur due to other cyclic loadings, such as tansportation, the following equations should be satisfied: $\sum_j SF_j D_j < 1.0$ (5.2.5-1) where Dj = the fatigue damage ratio for each type of loading SFj = the associated safety factor	$D = k_{LE} \cdot \gamma_{FD} \cdot \sum_i \frac{n_i}{N_i}$ (16.12-1) where D is a non-dimensional number, the Palmgren-Miner sum or damage ratio for a time T; k_{LE} is a local experience factor, see 16.12.3; γ_{FD} is a fatigue damage design factor, see 16.12.2; n_i is the number of cycles of stress range, S_i, occurring during time period, T; N_i is the number of cycles to failure under constant amplitude stress range, S_i, taken from the relevant S–N curve.	$D = \sum_{i=1}^{k} \frac{n_i}{N_i} = \frac{1}{\bar{a}} \sum_{i=1}^{k} n_i \cdot (\Delta\sigma_i)^m \le \eta$ (2.2.1) where D = accumulated fatigue damage $\bar{a}$ = intercept of the design S-N curve with the log N axis m = negative inverse slope of the S-N curve k = number of stress blocks n_i = number of stress cycles in stress block i N_i = number of cycles to failure at constant stress range $\Delta\sigma_i$ η = usage factor = 1 / Design Fatigue Factor from OS-C101 Section 6 Fatigue Limit States.
Spectral Analysis Technique	**1. Transfer functions developed using regular waves in the time domain** - Charaterize the wave climate using either the two, three, four and eight parameter format - Select a sufficient number of frequencies to define all the peaks and valleys inherent in the jacket response transfer functions - Select a wave height corresponding to each frequency; 1) For GoM, a steepness between 1:20 and 1:25 is generally used. 2) A minimum height of one foot and a maximum height equal to the design wave height should be used. 3) Compute a stress range transfer function at each point where fatigue damage is to be accumulated for a minimum of four platform directions (end-on, broadside and two diagonals). More directions may be required for jackets with unusual geometry or where wave directionality or spreading or current is considered 4) A minimum of four hot spot locations at both the brace and chord side of the connection should be considered. 5) Compute the stress response spectra. **2. Transfer functions developed using regular waves in the frequency domain** - This approach is similar to method (1) except that the analysis is linearized prior to the calculation of structural response. **3. Transfer functions developed using random waves in the time domain**: Nonliearities arising from wave-structure interaction can be taken into account and difficulties in selecting wave heights and frequencies for transfer function generation can be avoided. - Characterize the wave climate in terms of sea state scatter diagram - Simulate random wave time histories of finite length for a few selected reference sea states - Computer response stress time histories at each point of a structure where fatigue life is to be determined and transform the response stress time histories into response stress spectra - Generate "exact" transfer functions from wave and response stress spectra - Calculate pseudo transfer functions for all the remaining sea states in the scatter diagram using the few " exact" transfer functions - Calculate pesudo response stress spectra as described in Section C5.2.2-1	- A pratical method that is best able to represent the random nature of the wave environment - only applicable to linear system as it is based on superimposition of many individual frequency components; this formal constraint can be overcome by suitable linearization of non-linear elements. - **Stress transfer functions** 1) to be determined by performing global stress analyses directly in the frequency domain; If this method is chosen, the global analyses shall be performed using linear wave theory and the drag term in Morison's equation shall be linearized. The calculated stresses are linearly dependent on the wave height and non-linear wave height influences are not included. 2) to be determined by performing global stress analyses in the time domain by stepping a full wave cycle past the structure. Various wave theories can be used and linear drag term can be allowed. - **Selection of wave frequencies** Select a sufficient number of frequencies to define all the peaks and valleys - **Selection of wave heights** Typical wave steepness values are in the range of 1:15 to 1:20. A wave height equal to the wave height with a one year return period should normally be used as a maximum. Typically, a broadside, an end-on and a diagonal wave direction are considered as a minimum. - **Short-term stress range statistics** - **Long-term stress range statistics**	Refer to DNV Classification Notes 30.7 - Fatigue Assessment of Ship Structures
chanics	The details refer to ISO 19902 Clause A.16.15	- Typical applications: 1) to assess the fitness-for-purpose of a component with or without known defects 2) to assess the inspection requirements for a component with or without known defects 3) to assess the inspection requirements for components which may not be subjected to PWHT 4) to assess the structural integrity of castings - The principal modes of failure in offshore structures: 1) crack growth driven by fatigue followed by the onset of fracture due to exceedance of the fracture toughness at a critical crack size (not necessarily through-thickness) 2) the occurrence of plastic collapse - Fatigue crack growth law	- This method is recommeded for use in assessment of acceptable defects, evaluation of acceptance criteria for fabrication and for planning in-service inspection. - This can be achieved by performing the analysis according to the following procedures: 1) crack growth parameter C determined as mean plus 2 standard deviation 2) a careful evaluation of initial defects that might be present in the structure when taking into account the actual NDE inspection method used to detect cracks during fabrication 3) use of geometry functions that are on the safe side 4) use of utilization factors similar to those used when the fatigue analysis is based on S-N data The Paris' equation may be used to predict the crack propagation or the fatigue life:

Fracture Mec

whe $da/dN = C\,(\Delta K)^m$

N = the number of cycles to failure

ΔK = the stress intensity factor range

C and m = parameters of the crack growth rate

whe $\Delta K = Y(\Delta\sigma)\sqrt{\pi a}$ stress intensity factor

Δσ = the stress range

$$\frac{da}{dN} = C(\Delta K)^m$$

where $\Delta K = K_{max} - K_{min}$

N = Number of cycles to failure

a = crack depth. It is assumed that the crack depth/length ratio is low (less than 1:5)

C, m = materail parameters, see BS 7910

$$K = \sigma g \sqrt{\pi a}$$

s = nominal stress in the member normal to the crack

g = factor depending on the geometry of the member and the crack

- See BS 7910 for more detailed guidelines related to fatigue assessment

Weld Improvement Techniques

- **Welding profiling**
- **Weld Toe Grinding**

Experimental data indicate that this technique can lead to an increase in the fatigue performance by a factor of 2.

The grinding procedure should ensure that all defects in the weld toe region have been removed by grinding to a depth not less than 0.5mm below the bottom of any visible undercut or defect. The maximum depth of local grinding should not exceed 2 mm or 5% of the plate thickness, whichever is less.

NDE of the joint is required after grinding to verify that no significant defects remain, for fillet-welded connections, it is important that the required throat size is maintained.

- **Full Profile Grinding, e.g., Butt Welds**

For welded tubular nodes, full grinding of the surface profile to a radius of not less than 0.5t qualified for both the life improvement factor of 2 on curve WJ, and the 0.15 size effect exponent applicable to geometrically similar notch-free scale-ups

- **Hammer Peening** - The objective is to obtain a smooth groove at the weld toe.

The groove depth should be at least 0.3mm, but should not exceed 0.5 mm.

The recommended fatigue performance improvement factor is 4.

The benefits of hammer peening on fatigue performance can only be realized through adoption of adequate quality control procedures.

Peened weld toes should be inspected directly after peening and any burr grinding with MPI

- **Post-Weld Heat Treatment**

Table 5.5.3-1—Factors on Fatigue Life for Weld Improvement Techniques

Weld Improvement Technique	Improvement Factor on S	Improvement Factor on N
Profile per 11.1.3d	[a] $\tau^{-0.1}$	varies
Weld toe burr grind	1.25	2
Hammer peening	1.56	4
[a] Chord side only.		

- **Post-weld heat treatment (PWHT)** - have a beneficial effect on the fatigue behaviour of welded joints; the knowledge of the residual stress distribution including the contribution of long-range fit-up stresses is required.
- **Welding profiling** - no clear evidence that weld profiling leads to improved fatigue performance
- **Weld toe grinding of tubular joint welds** - especially beneficial at low stress ranges;

Experimental data indicate that this technique can lead to an increase in the fatigue performance by a factor of 2.

- **Grinding of butt welds** - to improve the joint classifications
- **Hammer peening** - The objective is to obtain a smooth groove at the weld toe.

The groove depth should be at least 0.3mm, but should not exceed 0.5 mm.

The recommended fatigue performance improvement factor is 4.

The benefits of hammer peening on fatigue performance can only be realized through adoption of adequate quality control procedures.

Table 16.16-1 — Achievable improvement factors on fatigue performance for weld improvement techniques

Weld improvement technique	Improvement factor
Weld toe burr grinding	2
Hammer peening	4

- **Welding profiling by machining and grinding**

The maximum improvement factor from the grinding only should be limited to a factor 2 on fatigue life

- **Weld toe grinding**

Where local grinding of the weld toes below any visible undercuts is performed the fatigue life may be increased by a factor given in Table 7-1.

The thickness effect may be reduced to an exponent k =0.20

- **TIG dressing**
- **Hammer peening with the following limitations:**

1) only be used on members where failure will be without substantial consequences

2) overload in compression must be avoided

3) It is recommended to grind a steering groove by means of a rotary burr of a diameter suitable for the hammer head to be used for the peening. The peening tip must be small enough to reach weld toe.

Table 7-1 Improvement on fatigue life by different methods

Improvement method	*Minimum specified yield strength*	*Increase in fatigue life (factor on life)* [1]
Grinding	Less than 350 MPa	$0.01f_y$
	Higher than 350 MPa	3.5
TIG dressing	Less than 350 MPa	$0.01f_y$
	Higher than 350 MPa	3.5
Hammer peening [3]	Less than 350 MPa	$0.011f_y$
	Higher than 350 MPa	4.0

1) The maximum S-N class that can be claimed by weld improvement is C1 or C depending on NDE and quality assurance for execution see Table A-5 in Appendix A.

2) f_y = characteristic yield strength for the actual material.

3) The improvement effect is dependent on tool used and workmanship. Therefore, if the fabricator is without experience with respect to hammer peening, it is recommended to perform fatigue testing of relevant detail (with and without hammer peening) before a factor on improvement is decided.

6 LOW CYCLE FATIGUE

6.1 General

Fatigue strength of offshore structures is normally associated with the capacity against high cycle fatigue loading. High cycle loading normally corresponds to number of cycles of more than 10,000. However, low cycle fatigue (high stress ranges) may be of interest in specific cases, such as fatigue damage accumulation derived from a storm. A fatigue assessment of response that is associated with number of cycles leading to failure for less than 10^4 cycles is considered as low cycle fatigue.

Recent experience gained following the assessment of structural performance of floaters and fixed structures during recent hurricanes in the GOM indicates that during hurricanes, a substantial portion of the design fatigue life can be expended. This is due to the large stress ranges and not the cycles less than 10^4. NORSOK N-006 /12/ is the only standard which gives the design guidelines for low cycle fatigue. No design methods exist at present in other codes to evaluate the effect of cyclic high stresses on fatigue of critical connections. The procedure is also applicable for the evaluation of this effect on GOM OCS structures as discussed herein.

Typical S-N test data are derived for number of cycles between 10^4 and $5x10^6$ cycles. High cycle fatigue analysis is based on calculation of elastic stresses that are used in the assessment.

The acceptance criterion for low cycle fatigue is given as

$$D_{LCF} \leq 1 - D_{HCF} \tag{6.1}$$

where D is the cumulative fatigue damage and the suffixes LCF and HCF refer to low and high cycle fatigue, respectively.

6.2 Storm Load History

The following analysis procedure for low cycle fatigue during a severe storm requires that the values of action effects related to number of wave cycles are established. It is usually site-specific data.

An empirically based short term wave height distribution is the Weibull distribution defined as:

$$F_H(h) = 1 - \exp\left\{ -\left(\frac{h}{\alpha_H \cdot H_s} \right)^{\beta_H} \right\} \tag{6.2}$$

The scale and shape parameters values are to be determined from data. The parameter values $\alpha_H = 0.681$ and $\beta_H = 2.126$ of the Forristall wave height distribution /43/ are originally based on buoy data from the Mexican Gulf, but have been found to have a more general applicability.

6.3 Tubular Joint Low Cycle Fatigue

Low cycle fatigue (LCF) checks for tubular joints encountered during a storm can be assessed by carrying out a fatigue check based on the S-N-curve defined by the following equation. The low cycle fatigue check may be made similar to ordinary fatigue checks as given in DNV-RP-C203 with use of linear elastic analyses.

$$\log N = \log \bar{a} - m \log \Delta\sigma \tag{6.3}$$

Values for log ā and m is given in Table 6-1.

Table 6-1 S-N data for low cycle fatigue analysis of tubular joints

Environment	m	log ā
Air	5,834	19,405
Seawater with cathodic protection	4,927	16,084

The low cycle S-N-curve is valid up to 10^5 cycles where it coincides with the ordinary high cycle S-N curve. This is shown in Figure 6-1 /12/ for tubular joints in seawater with cathodic protection (CP).

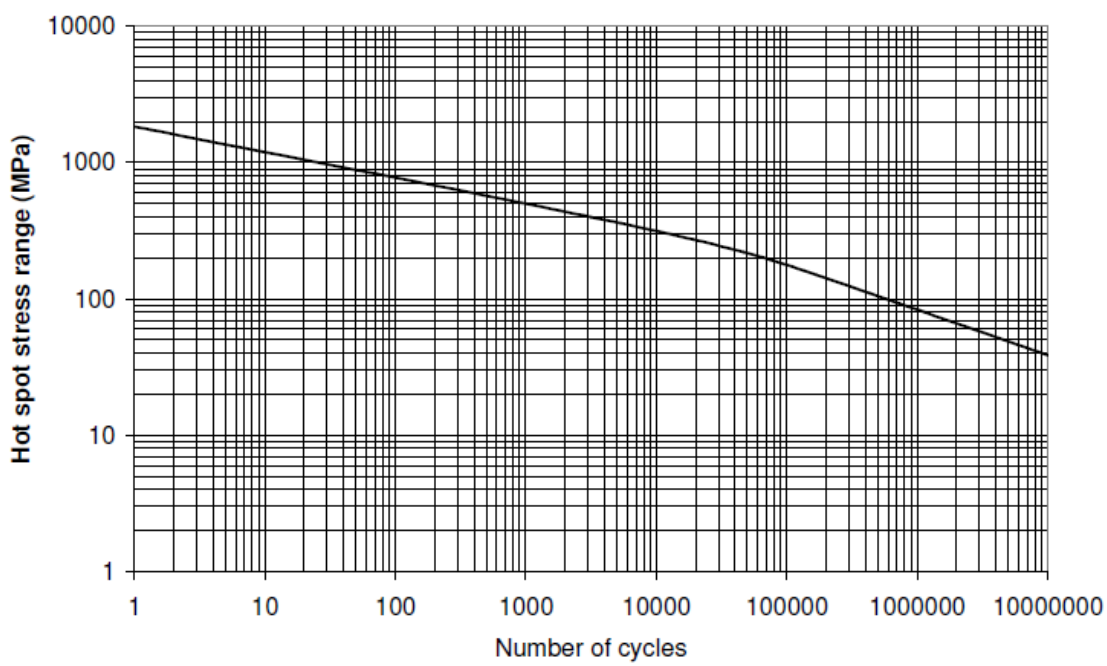

Figure 6-1 S-N Curve for LCF for Tubular Joint in Seawater with CP

The following analysis procedure for low cycle fatigue during a severe storm requires that a history of action effects corresponding to this storm profile is established (values of action effects related to number of wave cycles).

It should be noted that the stress strain curve of the steel at high stresses close to yield is normally nonlinear. A good stepwise linear approximation or the actual nonlinear curve should be used in the low cycle fatigue calculation.
The hot spot stress ranges are assumed to be derived from linear elastic analysis. The hot spot stress range during a severe storm may imply local yielding at the hot spot. Thus, a correction of the elastic stress range is needed in order to derive a stress range that is representative for the actual strain range taking the nonlinearity in material behavior into account. To account for this the fatigue capacity for low cycle fatigue can be derived by one of the following methods:

1. Prepare a finite element model of the considered detail and perform a cyclic nonlinear analysis based on a cyclic stress-strain curve. This provides the actual strain range at the hot spot.
2. Alternatively use the cyclic stress-strain relation combined with the Neuber's rule for derivation of actual strain. This procedure is illustrated in Figure 6-2.
3. If the cyclic stress-strain relation is combined with the Neuber's rule, the Neuber's formula can be written as follows:

$$\frac{\sigma_n^2 \cdot SCF^2}{E} = \sigma_{actual\,HSS}\left[\frac{\sigma_{actual\,HSS}}{E} + \left(\frac{\sigma_{actual\,HSS}}{K'}\right)^{1/n}\right] \qquad (6.4)$$

where
σ_n is the nominal stress,
SCF is the stress concentration factor from linear elastic analysis (the same as used for high cycle fatigue),
$\sigma_{actual\ HSS}$ is the actual stress at the considered hot spot from a non-linear finite analysis using a cyclic stress-strain curve,
E is the Young's modulus,
n, K' are material coefficients:
K' and n can be obtained by experiments for the actual material, weld and heat effected zone.
For assessment of magnitude of low cycle fatigue the following values may be used for a first assessment of criticality with respect to low cycle fatigue:
K' = 582 (in MPa if this value is used for stress) and n = 0,111.
Some coefficients of n and K' for base metal of different steel grades and for welded metal are given in /12/.
For the heat affected zone, it is recommended to assume welded metal, if non-linear analysis is carried out to obtain the strain range.
The equation for actual stress based on Neuber's formula can be solved by iteration. Then the strain is calculated from the Ramberg-Osgood relation as

$$\varepsilon_{nl} = \frac{\sigma_{actual\,HSS}}{E} + \left(\frac{\sigma_{actual\,HSS}}{K'}\right)^{1/n} \tag{6.5}$$

Then a pseudo elastic stress can be calculated as

$$\sigma_{pseudo} = E\,\varepsilon_{nl} \tag{6.6}$$

This hot spot stress range (pseudo elastic stress range) should be combined with the hot spot stress S-N curve T for tubular joints in DNV-RP-C203 /1/ before fatigue damage is calculated.
The procedure for low cycle fatigue presented here is used for a tubular in seawater with cathodic protection. This gives results as shown in Figure 6-2.

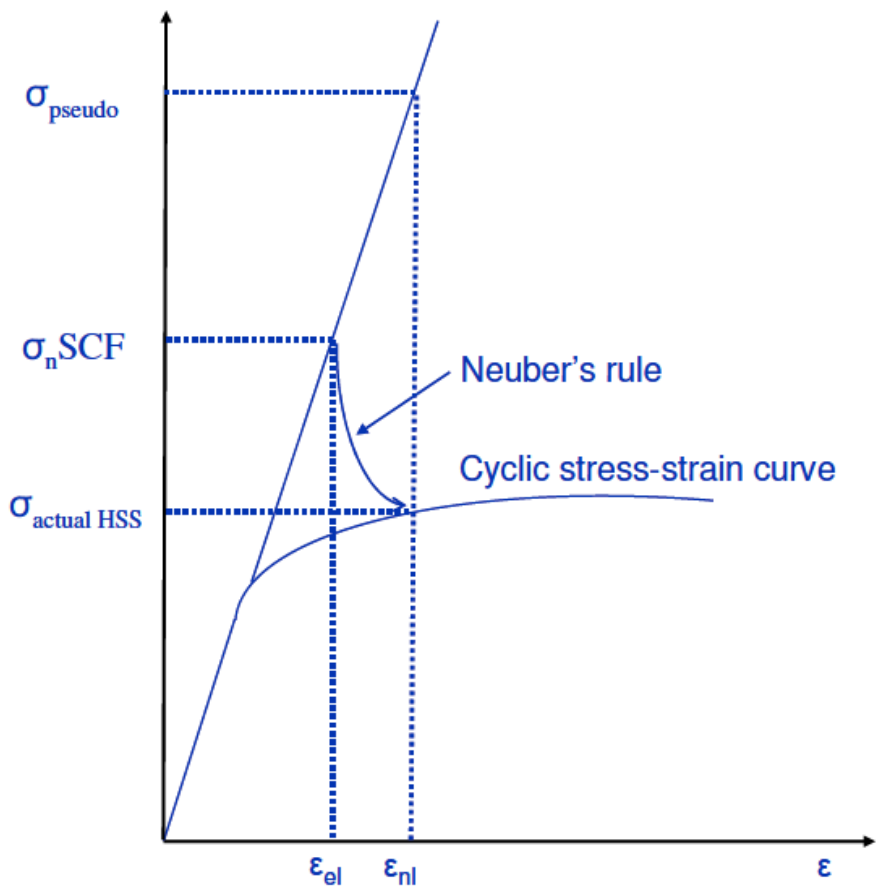

Figure 6-2 The Neuber Approach and Use of Pseudo-Elastic Stress /12/

7 FATIGUE OF FLAWED WELDS

7.1 General

The following statement is made in both API RP 2A /4/ and the proposed API 2SIM /5/:

> "All offshore structures, regardless of location, are subject to fatigue degradation. In many areas, fatigue is a major design consideration due to relatively high ratios of operational seastates to maximum design environmental events. In the U.S. Gulf of Mexico, however, this ratio is low. Still fatigue effects should be considered and engineering decisions should be consciously based on the results of any fatigue evaluations."

DNV did not as part of the scope of work for this project assess the significance of fatigue in GOM platforms. However we agree that fatigue is a significant design issue that has to be addressed for any structure subjected to cyclic stresses. Cyclic loading causes fatigue which, with time, may result in cracks at welded connections of structural components. Unless crack propagation is arrested the cracks can eventually lead to member severance at the joint. The propagation of the crack may affect other members at a joint; cracking originally in a secondary brace or appurtenance connection may eventually grow into and affect a primary member.

Deformed or corroded welds are encountered on offshore structures in the GOM as some old platforms are still performing well beyond their, in many cases, original 20 year design life. The degree of corrosion/deformation varies and may have significant effect on the remaining fatigue life at the joint.

The effect of the corrosion on increasing the nominal stress at the joint can be evaluated by stress analysis. However damage or deformation results in stress redistribution which may be harder to evaluate especially for joints predominantly loaded in compression. Typical corroded/deformed connections and methodologies for their fatigue strength quantification are discussed in this section.

7.2 Fatigue Capacity

The simplest method of measuring the remaining fatigue capacity is probably taking the difference between the calculated fatigue design life of each component and the age of the structure. However, this method will miss several important aspects of the fatigue life of a structure such as:

- Due to built-in redundancy, the structure will not fail with one through thickness crack. The member or connection experiencing the through thickness crack may have significant additional life before it fails. When the member or connection finally fails, most jacket structures are designed to survive such a single failure and will still be able to carry the original damaged condition design loading.
- Updated inspection results for an existing fatigue crack are not included in such a simple approach.
- If a component is inspected and no cracks are determined, this can be an indication of a lower crack growth rate for this component than expected from the analysis. If a fatigue crack has been found, the most realistic remaining capacity of the member, prior to repairs, may be found by fracture mechanics crack growth calculations.

- The acceptable fatigue life of the structure may be significantly increased by careful use of inspection and repair of damaged components.

7.3 Fatigue Parameters

The following parameters are usually included in fatigue calculations/assessment:

- Flaw geometry: planar or volumetric flaws, dimensions, and location in weld or base material
- Corrosion/local thinning: It is conservative to assess local thinning, due for example to pitting corrosion or erosion, as a planar flaw of the same depth and shape. However, if the thinning does not create a sharp discontinuity, the likelihood of failure will probably be controlled by plastic collapse considerations
- Stress Concentration Factor (depending on the detail geometry).
- Fluctuating Stresses
  - Primary/secondary (membrane/bending)/residual stresses
  - Stress Ratio
  - Variable amplitude loading
- Crack growth and threshold data/laws
- Uncertainty (Kukkanen/37/)
- Tubular joint complexity
- Local Joint Flexibility effect on fatigue (can be very significant, factor of 8, Buitrago/33/, /34/, /35/)
- Material properties such as strength and fracture toughness

7.4 Fatigue of Deformed/Corroded Welds

The methods for assessing the fatigue capacity for existing platforms are in principle the same as for new designs. In order to develop methods for determining the fatigue capacity that is valid for details with damages like corrosion or deformed welds it is necessary to perform testing. It is not likely that there will be a large number of situations where more precise capacity methods will make a significance difference to the conclusions. Recognizing the above, the current project scope of work was focused on fatigue life prediction of damaged/corroded joints on GOM fixed offshore platforms.

To assess the fatigue capacity of damaged structure, the following factors have to be accounted for:

- load redistribution
- increased crack growth
- fatigue analysis would have to be performed for a high number of hot spots and damage scenarios.

These factors may make fatigue assessment unrealistic if testing is to be performed for validation purposes. Simplification may be a possible solution if damage strength calculations are performed to check the collapse capacity with a component removed to simulate the damage. If the stress increase for

the surrounding members and joints are checked at the design load level, an estimate of the reduction in fatigue capacity may be calculated so that the remaining fatigue life can be obtained.

The following equations (Ersdal, /13/) can be used to estimate the reduction of fatigue capacity:

$$\log(N_{damaged}) = \log(N_{intact}) + m \log(\Delta\sigma_{intact}) - m \log(\Delta\sigma_{damaged}) \quad (7.1)$$

$$N_{damaged}/N_{intact} = 10^{[m \log(\Delta\sigma_{intact}) - m \log(\Delta\sigma_{damaged})]} = (\Delta\sigma_{intact}/\Delta\sigma_{damaged})^m \quad (7.2)$$

where:

$N_{damaged}$ = predicted number of cycles to failure for stress range $\Delta\sigma_{damaged}$ under the damaged condition

N_{intact} = predicted number of cycles to failure for stress range $\Delta\sigma_{intact}$ under the intact condition

$\Delta\sigma_{damaged}$ = stress range under damaged condition

$\Delta\sigma_{intact}$ = stress range under intact condition

m = negative inverse slope of S-N curve

7.5 Fracture Mechanics Assessment

The acceptance criteria for fatigue crack growth should be based on the actual connection considered. The assessment of crack size at fracture can be based on BS 7910:2005 /2/.

1. The fracture toughness for the base material may be used provided that it is likely that the fatigue crack tips grow into the base material. Then the fracture toughness may be derived from Charpy V values for the base material.
2. The fracture toughness should be assessed using a relevant operational temperature for the considered connection

N-006 adopted the BS-7910 crack growth methodology. For simplicity of analysis it is assumed that the defect at the hot spot is going through the plate such that crack growth can be integrated in one dimension. The fatigue life is calculated based on the following crack growth equation:

$$\int_{a_i}^{a_f} \frac{da}{\left(Y\sqrt{\pi a} - \frac{\Delta K_{th}}{\Delta\sigma}\right)^m} = C(\Delta\sigma)^m N$$

where
a_i is the initial crack size
a_f is the final crack size
m and C are material parameters
K_{th} is the threshold stress intensity factor
$\Delta\sigma$ is the nominal stress range in member outside area with defects
N is the number of stress cycles (7.3)

It should be noted that even though Eq. 7.3 is given in NORSOK N-006, it is not normally used and is replaced in BS-7910 by Equations 7.24 and 7.25 discussed in 7.5.1.5 7.5.1.5 below.

7.5.1 Fatigue Assessment

The basic components of the fatigue crack growth and fracture assessment procedure for tubular joints are given in the Figure B1 of BS7910: 2005 shown below as Figure 7-1. The elements of the procedure given in the Figure are summarized with some detail in the following subsections. This procedure is limited to the assessment of known or assumed weld toe flaws, including fatigue cracks found in service, in brace or chord members of T, Y, K, or KT joints between circular section tubes under axial and/or bending loads.

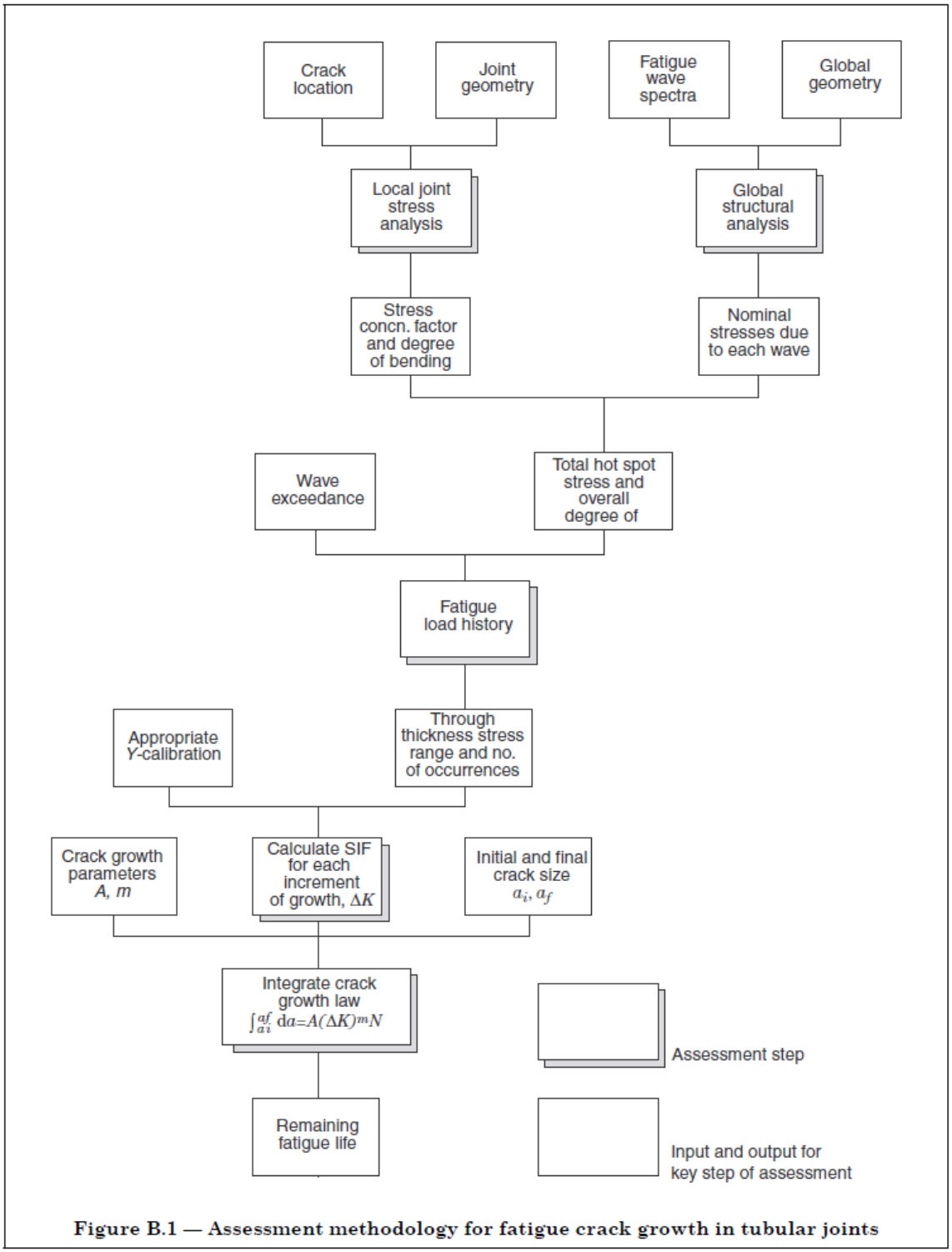

Figure 7-1 BS-7910 Annex B Assessment Methodology Flowchart

7.5.1.1 Global Structural Analysis

A global finite element analysis of the complete structure is to be performed to determine the stress spectrum corresponding to the wave loading at the flaw location. The wave statistics data are used to construct a histogram of wave height versus the number of occurrences. The stress range due to each wave height is then determined in the global structural analysis which gives the nominal brace loading due to the action of the fatigue and storm wave loading. The axial, in-plane bending and out-of-plane bending brace and chord stress ranges ($\Delta\sigma_{Ax}$, $\Delta\sigma_{IPB}$ and $\Delta\sigma_{OPB}$ respectively) are computed for each wave height in accordance with normal procedures as e.g., described in API RP 2A.

The global analysis under the chosen critical loading conditions should be available to give the forces and moments in the members in the region being assessed. These should be provided as axial force, in-plane and out-of-plane bending moments. Both maximum load and fatigue load ranges are required in order to assess the fracture and fatigue behavior of the flawed connection.

7.5.1.2 Local Joint Stress Analysis

Local Joint stress analysis is used to determine the hot-spot stress concentration factors and the degree of bending, Ω, defined as the proportion of the bending to the total stress (membrane + bending) through the wall thickness, relevant to the crack location.
The local joint stress ranges are generated by the nominal brace axial and bending loads, which are reacted by the chord internal forces. High secondary bending stresses are developed due to the local deformation of the tubular walls. These lead to high stress concentrations and through-thickness stress gradients at the brace/chord intersection. The variation of the stress range around the joint periphery needs to be determined and stress range histograms are evaluated for a minimum of eight equally spaced positions (hot spots), including the saddle and crown locations.
Each hot spot stress range component is determined from the nominal stress range, $\Delta\sigma_{nom}$, and the appropriate stress concentration factor

$$\Delta\sigma_{HS} = \Delta\sigma_{nom} k_{t,HS} \qquad (7.4)$$

The hot-spot stress range component is sub-divided into axial and bending components, thus:

$$\Delta\sigma_m = (1 - \Omega)\, \Delta\sigma_{HS} \qquad (7.5a)$$
$$\Delta\sigma_b = \Omega\, \Delta\sigma_{HS} \qquad (7.5b)$$

The local stress field can be based on published parametric equations for $k_{t,HS}$ and Ω /22/. More accurate predictions can be obtained by performing a detailed finite element analysis possibly utilizing solid elements (see e.g. DNV RP-C203).

The nominal stresses obtained from the global analysis and the stress field parameters at the crack location, $k_{t,HS}$ and Ω, obtained from the local joint stress analysis are used to calculate the total hot-spot stress and total degree of bending for each wave loading:

$$\Delta\sigma_{HS.Tot} = \Delta\sigma_{HS.Ax} + \Delta\sigma_{HS.IPB} + \Delta\sigma_{HS.OPB} = \Delta\sigma_{n.Ax}\, k_{t.Ax} + \Delta\sigma_{n.IPB}\, k_{t.IPB} + \Delta\sigma_{n.OPB}\, k_{t.OPB} \qquad (7.6)$$

where:
$\Delta\sigma_{HS.Ax}$, $\Delta\sigma_{HS.IPB}$, $\Delta\sigma_{HS.OPB}$: axial, in and out of plane hot spot stress ranges in tubular joint
$\Delta\sigma_{n.Ax}$, $\Delta\sigma_{n.IPB}$, $\Delta\sigma_{n.OPB}$, nominal axial, in and out of plane stress ranges in tubular joint
$k_{t.HS}$: hot spot stress concentration factor in tubular joint
$k_{t.IPB}$, $k_{t.OPB}$ in and out of plane stress concentration factors in tubular joints

The degree of bending for the total hot-spot stress range is determined from the following expression:

$$\Omega_{Tot} = \frac{\Omega_{Ax}\Delta\sigma_{HS.Ax} + \Omega_{IPB}\Delta\sigma_{HS.IPB} + \Omega_{OPB}\Delta\sigma_{HS.OPB}}{\Delta\sigma_{HS.Tot}} \qquad (7.7)$$

where:
Ω_{Tot}, Ω_{Ax},Ω_{IPB}, Ω_{OPB}: total, axial, in plane and out of plane degrees of bending in tubular joints
Connolly, M.P et.al. /22/ suggested a set of parametric formulae to calculate the degrees of bending as follows, which can cover the majority of tubular joints used in offshore structures:

The following Notations are employed:

- α: geometry ratio (2L/D)
- β: geometry ratio (d/D)
- γ: geometry ratio (D/2T)
- τ: geometry ratio (t/T)
- θ: brace angle (in radians)
- d: external diameter of brace
- D: external diameter of chord
- L: chord length
- t: brace wall thickness
- T: chord wall thickness

1. Degree of bending under axial loading
   a) At chord hot-spot stress site:

$$\Omega_{\mathbf{A1}} := 0.7026\alpha^{0.0236}\cdot\mathbf{exp}\left(-0.187\cdot\beta^{4} + 0.0097\cdot\gamma + \frac{0.0047}{\theta^{3}} - \frac{21.7\cdot\beta^{3}}{\gamma^{2}} + 0.3038\cdot\beta\cdot\tau - \frac{0.0867\cdot\beta^{2}}{\theta^{3}} - 0.001\gamma^{1.5}\cdot\theta\right) \qquad (7.8)$$

   b) At brace hot-spot stress site

$$\Omega_{\mathbf{A2}} := 0.6763\cdot\alpha^{0.0603}\cdot\gamma^{0.118}\cdot\tau^{0.24}\cdot\mathbf{exp}\left(-0.292\cdot\beta^{2.5} - \frac{0.0407}{\theta} - 0.142\cdot\tau\cdot\theta + 0.0833\cdot\beta^{3}\cdot\theta\right) \qquad (7.9)$$

c) At chord saddle position

$$\Omega_{\mathbf{A3}} := 0.785\cdot\alpha^{0.0122}\cdot\gamma^{0.212\beta^{2.2}}\cdot\tau^{0.0177}\cdot\mathbf{sin}(\theta)^{-0.1}\cdot\mathbf{exp}\left(-0.799\beta^{2.5}+0.165\cdot\beta\cdot\tau\right) \tag{7.10}$$

d) At brace saddle position

$$\Omega_{\mathbf{A4}} := 0.6698\cdot\alpha^{0.0431}\cdot\gamma^{0.0834}\cdot\theta^{-0.0896}\cdot\mathbf{exp}\left(-0.1846\cdot\beta^{2}-\frac{0.0672}{\tau}+0.0017\gamma\cdot\tau\right) \tag{7.11}$$

The following exceptions are noted:

- Axial brace saddle – where both $\theta < 45^{o}$ and $\tau < 0.40$, assume $\Omega_{A4} = 0$
- Validity ranges:

$6.21 \le \alpha$
$0.20 \le \beta \le 0.80$
$7.60 \le \gamma \le 32.0$
$0.20 \le \tau \le 1.00$
$35^{o} \le \theta \le 90^{o}$

2. Degree of bending under in-plane bending

a) At chord hot-spot stress site:

$$\Omega_{\mathbf{A5}} := 0.7984\cdot\alpha^{-0.0283}\cdot\tau^{-0.0017}\cdot\theta^{-0.024}\cdot\mathbf{exp}\left(\frac{0.0656}{\beta}+0.00027\cdot\gamma^{2}-\frac{0.0819\cdot\theta}{\alpha}-\frac{0.00036\cdot\theta}{\beta^{3}}-\frac{0.0001\cdot\gamma^{2}}{\beta}\right) \tag{7.12}$$

b) At brace hot-spot stress site

$$\Omega_{\mathbf{A6}} := 0.6893\cdot\alpha^{0.0158}\cdot\beta^{0.226}\cdot\gamma^{(0.272-0.0443\cdot\tau+0.0196\cdot\theta)}\cdot\tau^{0.298}\cdot\theta^{0.0869}\cdot\mathbf{exp}\left(-0.0187\cdot\beta\cdot\gamma-\frac{0.000343}{\beta^{2}}\cdot\tau-0.1\cdot\beta\cdot\theta^{2}-0.114\cdot\tau\cdot\theta\right) \tag{7.13}$$

c) At chord crown position

$$\Omega_{\mathbf{A7}} := 2.886\alpha^{-0.0464}\cdot\gamma^{-0.242}\cdot\mathbf{exp}\left(-0.617\cdot\beta^{0.5}-0.112\cdot\tau+0.738\cdot\theta+0.178\cdot\beta\cdot\tau-1.34\cdot\gamma^{-0.2}\cdot\theta\right) \tag{7.14}$$

d) At brace crown position

$$\Omega_{\mathbf{A8}} := 0.6683\cdot\alpha^{0.0143}\cdot\gamma^{\left(0.127+0.0968\cdot\tau^{2}-0.0038\cdot\theta\right)}\cdot\theta^{0.149}\cdot\mathbf{exp}\left(\frac{-0.00218}{\beta^{3}}-\frac{0.0143}{\tau^{2}}+\frac{0.000953}{\beta^{2}}\cdot\tau-0.0145\cdot\beta\cdot\gamma-0.162\cdot\tau\cdot\theta\right) \tag{7.15}$$

The following exceptions are noted:

- IPB brace hot spot – where both $\theta < 45^{o}$ and $\tau < 0.45$, assume $\Omega_{A6} = 0$
- IPB brace crown – where both $\theta < 45^{o}$ and $\tau < 0.65$, assume $\Omega_{A8} = 0$
- Validity ranges:

$6.21 \le \alpha$
$0.20 \le \beta \le 0.80$
$7.60 \le \gamma \le 32.0$
$0.20 \le \tau \le 1.00$
$35^{o} \le \theta \le 90^{o}$

3. Degree of bending under axial loading
   a) At chord hot-spot stress site:

$$\Omega_{\mathbf{A9}} := 0.768\cdot\beta^{-0.0882}\cdot\gamma^{0.0115}\cdot\tau^{0.00668}\cdot\mathbf{exp}\left(0.000122\alpha^{2}+\frac{0.04}{\theta}-0.00249\cdot\frac{\tau}{\beta^{2}}+\frac{0.0123\cdot\tau}{\theta^{2}}\right) \tag{7.16}$$

   b) At brace hot-spot stress site

$$\Omega_{\mathbf{A10}} := 0.5174\cdot\alpha^{0.0211}\cdot\gamma^{0.203}\cdot\tau^{0.159}\cdot\theta^{-0.0919}\cdot\mathbf{exp}\left(\frac{-0.000048}{\beta^{5}}-0.00963\cdot\beta\cdot\gamma\right) \tag{7.17}$$

   c) At chord saddle position

$$\Omega_{\mathbf{A11}} := 0.7964\cdot\beta^{-0.0907}\cdot\gamma^{0.0092}\cdot\theta^{-0.0793}\cdot\mathbf{exp}\left(0.000159\cdot\alpha^{2}+0.0549\cdot\tau^{2}-0.0252\cdot\frac{\tau}{\beta}+\frac{0.00223\cdot\theta^{3}}{\beta}+0.000738\cdot\gamma\cdot\tau^{3}\right) \tag{7.18}$$

   d) At brace saddle position

$$\Omega_{\mathbf{A12}} := 0.61\cdot\alpha^{-0.0045}\cdot\gamma^{0.168}\cdot\theta^{-0.103}\cdot\mathbf{exp}\left(\frac{-0.000041}{\beta^{5}}-\frac{0.0665}{\tau}-0.0095\cdot\beta^{2}\cdot\gamma\right) \tag{7.19}$$

The following exceptions are noted:

- OPB brace hot spot – where both $\theta \leq 45^{o}$ and $\beta \leq 0.25$, assume $\Omega_{A10} = 0$
- OPB brace saddle – where both $\theta < 45^{o}$ and $\beta \leq 0.20$, assume $\Omega_{A12} = 0$
- Validity ranges:

  $6.21 \leq \alpha$
  $0.20 \leq \beta \leq 0.80$
  $7.60 \leq \gamma \leq 32.0$
  $0.20 \leq \tau \leq 1.00$
  $35^{o} \leq \theta \leq 90^{o}$

7.5.1.3 Stress Ranges

After stress concentration factors and degrees of bending are obtained from the local joint stress analysis, the hot-spot stress range histogram for the joint can be generated.

Any convenient number of stress intervals can be used, but, for conservatism, each block of cycles may be assumed to experience the maximum stress range in that block first before lower stress ranges.

7.5.1.4 Stress Intensity Factor Range

If the plate stress intensity factor solution is used (see BS-7910), the stress intensity range can be expressed as follows:

$$\Delta K = \{ M_{km} Y_m (1 - \Omega_{Tot}) + M_{kb} Y_b \Omega_{Tot} \} \Delta\sigma_{HS} \sqrt{\pi a} \qquad (7.20)$$

where:

ΔK: stress intensity factor range

M_{km}, M_{kb}: stress intensity magnification factors which is a function of crack size, geometry and loading

Y_m, Y_b: stress intensity correction factors for membrane and bending stress

a: half flaw length for through-thickness flaw, flaw height for surface flaw or half height for embedded flaw

For fatigue assessments the following equation applies:

$$(Y\Delta\sigma)_p = M f_w \, [k_{tm} M_{km} M_m \Delta\sigma_m + k_{tb} M_{kb} M_b \, \{\Delta\sigma_b + (k_m - 1)\Delta\sigma_m\}] \qquad (7.21)$$

The calculation of the factors M_k, M and f_w in Eq. 7.21 is defined in BS-7910 as summarized below. The subscripts m and b correspond to membrane and bending actions, respectively. The stress concentration factors k_{tm} and k_{tb} are the same as the hot spot SCF's normally applied for fatigue calculations.

a) Calculation of M_{km} and M_{kb}

In general, the correction factor, M_k, is the product of the ratio of the *K* for a crack in material with stress concentration to the K for the same crack in material without stress concentration.

According to BS7910, M_k could be calculated by 2D finite element analysis for profiles representing sections of the welded joint geometry. For butt welds, T-butt welds, full penetration cruciform joints and members with fillet or butt-welded attachments, M_k is a function of *z*, B and L defined in Figure 7-2. Here *z* is the height, measured from the weld toe, and L is the overall length of the attachment measured from weld toe to weld toe. The resulting M_k solutions are given as follows:

$$M_k = v(z/B)^w \qquad (7.22)$$

where

v and *w* have the values given in Table 7-1 (which is Table M.9 in BS7910) for flaws at the toes of full penetration or attachment welds. The magnification factor M_k should be greater than or equal to 1.0.

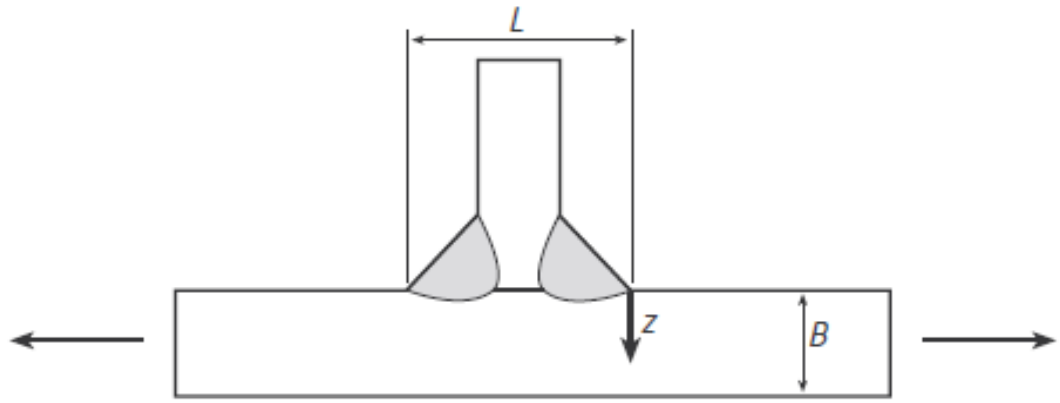

Figure 7-2 Crack and welded joint geometries

It should be stated that the application of the above formulation based on welded plate joints to tubular joints has been demonstrated through experimental research and detailed Finite Element modeling before being adopted by the code (BS-7910).

Table 7-1 Values of v and w for axial and bending loading

Table M.9 — Values of v and w for axial and bending loading

Loading mode	L/B	z/B	v	w
Axial	≤ 2	$\leq 0.05(L/B)^{0.55}$ $>0.05(L/B)^{0.55}$	$0.51(L/B)^{0.27}$ 0.83	–0.31 $-0.15(L/B)^{0.46}$
	>2	≤ 0.073 >0.073	0.615 0.83	–0.31 –0.20
Bending	≤ 1	$\leq 0.03(L/B)^{0.55}$ $>0.03(L/B)^{0.55}$	$0.45(L/B)^{0.21}$ 0.68	–0.31 $-0.19(L/B)^{0.21}$
	>1	≤ 0.03 >0.03	0.45 0.68	–0.31 –0.19

The solutions produced by this formulation are not applicable for z = 0, and near-surface M_k values should be used (z = 0.15 mm) instead for the intersection of surface flaws with the weld toe and through-thickness flaws at weld toes.
More accurate solutions based on 3D-stress analysis of semi-elliptical cracks at weld toes are discussed in BS7910.

b) Calculation of M, f_w, M_m and M_b

The expressions for M, f_w, M_m and M_b are given in BS7910 Sections **M.2** to **M.4** and **M.6** for different types of flaws in different configurations. Here, only surface flaws in plates are considered.
The estimation methods for stress intensity factor K_I do not always allow for situations where the flaw area is significant compared to the load bearing cross-section area, where misalignment or angular distortion occurs, or for long flaws in curved shells subject to internal pressure where bulging effects may occur.

Where the actual flaw area is greater than 10 % of the load bearing cross-section area (generally BW, where B is the thickness and W is the width), K_I should be multiplied by f_w.
Formulae for f_w are given in BS7910 Annex M for different geometries, but if one is not specified for the geometry under consideration, the following should be used with M=1.0:

$$f_w = \{\sec(\pi c/W)(a/B)^{0.5}\}^{0.5} \qquad (7.23)$$

which equals 1.0 if a/2c equals 0. It is also noted that this equation for f_w is safe up to 2c/W=0.8.

Expressions for M_m and M_b can be found in BS7910 **M.3** for different types of flaws in different configurations. For k_t, k_{tm}, k_{tb} and k_m, reference should be made to BS7910, **6.4.4** and Annex D.

7.5.1.5 Fatigue Crack Growth Law

The Paris Law is as follows;

$$da/dN = A(\Delta K)^m \quad \text{for } \Delta K > \Delta K_o \qquad (7.24a)$$

$$da/dN = 0 \quad \text{for } \Delta K \leq \Delta K_o \qquad (7.24b)$$

where
da/dN = crack growth per cycle
ΔK = Stress Intensity Factor Range
ΔK_o = Threshold Stress Intensity Factor Range
R-ratio = Minimum Stress / Maximum Stress

The constants "A" and "m" are defined in Table 7-2 and Table 7-3as follows:

Table 7-2 Constants for A and m in air

Table 4 — Recommended fatigue crack growth laws for steels in air[a]

R	Stage A				Stage B				Stage A/Stage B transition point ΔK N/mm$^{3/2}$	
	Mean curve		Mean + 2SD		Mean curve		Mean + 2SD			
	A^b	m	A^b	m	A^b	m	A^b	m	Mean curve	Mean + 2SD
<0.5	1.21×10^{-26}	8.16	4.37×10^{-26}	8.16	3.98×10^{-13}	2.88	6.77×10^{-13}	2.88	363	315
≥0.5	4.80×10^{-18}	5.10	2.10×10^{-17}	5.10	5.86×10^{-13}	2.88	1.29×10^{-12}	2.88	196	144

[a] Mean + 2SD for R ≥ 0.5 values recommended for assessing welded joints.
[b] For da/dN in mm/cycle and ΔK in N/mm$^{3/2}$.

Table 7-3 Constants for A and m in a marine environment

Table 5 — Recommended fatigue crack growth laws for steels in a marine environment[a]

R	Stage A				Stage B				Stage A/Stage B transition point ΔK N/mm$^{3/2}$	
	Mean curve		Mean + 2SD		Mean curve		Mean + 2SD			
	A[b]	m	A[b]	m	A[b]	m	A[b]	m	Mean curve	Mean + 2SD
Steel freely corroding in a marine environment										
<0.5	3.0×10^{-14}	3.42	8.55×10^{-14}	3.42	1.27×10^{-7}	1.30	1.93×10^{-7}	1.30	1336	993
≥0.5	5.37×10^{-14}	3.42	1.72×10^{-13}	3.42	5.67×10^{-7}	1.11	7.48×10^{-7}	1.11	1098	748
Steel in a marine environment with cathodic protection at −850 mV (Ag/AgCl)										
<0.5	1.21×10^{-26}	8.16	4.37×10^{-26}	8.16	5.16×10^{-12}	2.67	1.32×10^{-11}	2.67	462	434
≥0.5	4.80×10^{-18}	5.10	2.10×10^{-17}	5.10	6.0×10^{-12}	2.67	2.02×10^{-11}	2.67	323	290
Steel in a marine environment with cathodic protection at −1 100 mV (Ag/AgCl)										
<0.5	1.21×10^{-26}	8.16	4.37×10^{-26}	8.16	5.51×10^{-8}	1.40	9.24×10^{-8}	1.40	576	514
≥0.5	4.80×10^{-18}	5.10	2.10×10^{-17}	5.10	5.25×10^{-8}	1.40	1.02×10^{-7}	1.40	517	415

[a] Mean + 2SD values for $R \geq 0.5$ recommended for assessing welded joints.
[b] For da/dN in mm/cycle and ΔK in N/mm$^{3/2}$.

The overall life is calculated by integrating the following equation:

$$\int_{a_i}^{a_f} \frac{da}{Y^m (\pi a)^{m/2}} = A(\Delta\sigma)^m N \qquad (7.25)$$

A conservative approach is to choose small increments of crack growth and to calculate the number of cycles used extending the crack over each increment, basing the calculations on ΔK at the end of the increment. However, in the case of surface or embedded elliptical flaws, this requires knowledge of the flaw length 2c at the end of the increment, which is not known in advance. A possible approach is to assume the crack-front shape, for example on the basis of experimental observations in laboratory specimens. Any such assumption should be justified in the ECA.

Alternatively, the BS-7910 gives the following equation where the crack shape can be estimated using ΔK at the beginning of the increment:

$$\Delta c/\Delta a = (\Delta K_c/\Delta K_a)^m \qquad (7.26a)$$

$$\frac{\Delta K_c}{\Delta K_a} = \frac{M_{k,c}}{M_{k,a}} \left\{1.1 + 0.35(a/B)^2\right\}(a/c)^{0.5} \qquad (7.26b)$$

where

$M_{k,c}$ and $M_{k,a}$ are the appropriate M_k values for axial or bending loading at the ends of the major and minor axes, respectively. The BS-7910 however stated that Eq. 7.26b is only applicable for axial or bending type loading. It does not address the case of combined membrane and bending loading. Our experience indicates that the most direct approach is to calculate ΔK_c and ΔK_a independently and use Eq.(7.26a). It is then no problem to combine membrane and bending loadings without the need for Eq. 7.26b.

Therefore, the same Paris crack growth law has been assumed herein to apply at the surface and part-thickness flaw ends (see BS-7910, Sec. 8.4.1). Empirical equations for crack surface growth were proposed in /25/ and /26/ in 1981 and 1985 but were not adopted by the code. They were however used in earlier studies by DNV /31/.

Careful consideration should be given to the estimation of the initial flaw size – it is important that this is not underestimated. The size should be the estimated maximum flaw size, considering the reliability of the chosen inspection method(s) and of the welding procedure applied.
For cracking in the chord, failure is generally considered to occur when the crack penetrates the wall thickness, though the possibility of brittle fracture or plastic collapse should be taken into consideration for cracks in the weld region. This may be significant to greater depths for brace cracks than for chord cracks, due to the possibility of crack propagation in the vicinity of the weld fusion line.

7.5.2 Fracture Assessment

With the flaw present and growing to a certain size under the influence of the stress cycles, the crack could lead to fracture should the stresses due to an extreme event exceed the fracture and strength capacities. An Engineering Critical Assessment (ECA) approach is recommended in the BS-7910 Sec. 7. The ECA procedure is schematically shown in Figure 7 3. A failure assessment diagram (FAD) is defined based on the material strength and fracture properties and the flaw parameters. The vertical axis of the FAD is a ratio of the applied conditions, in fracture mechanics terms, to the conditions required to cause fracture, measured in the same terms. The horizontal axis is the ratio of the applied load to that required to cause plastic collapse.

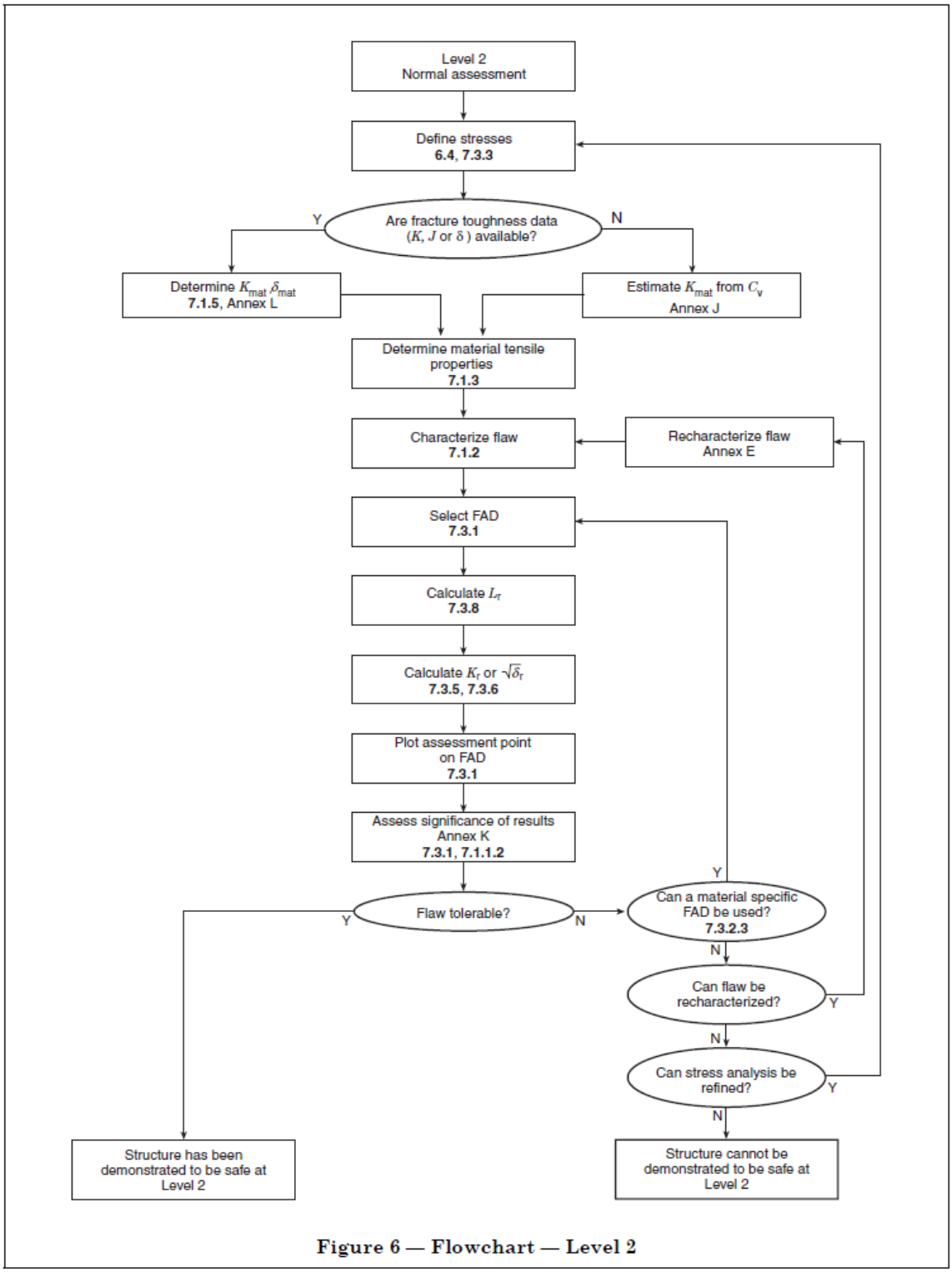

Figure 7-3 BS-7910 Fracture Assessment Methodology

Three levels of fracture assessment are presented of which Level 2 is considered appropriate for fixed offshore structure tubular joints. This is the normal assessment route for general application. It has two methods. Each method has an assessment line given by the equation of a curve and a cut-off line (see Figure 7-4). If the assessment point lies within the area bounded by the axes and the assessment line, the flaw is acceptable; if it lies on or outside the line, the flaw is unacceptable.
Figure 7-4 shows the recommended FAD for Level 2A fracture assessment which is further discussed in Sec.7.5.2.2 to 7.5.2.4 below. The figure shows different cut-offs for different materials.

For fracture assessment at Level 2 the following equation applies:

$$Y\sigma = (Y\sigma)_p + (Y\sigma)_s \qquad (7.27)$$

where

$$(Y\sigma)_p = Mf_w[k_{tm}M_{km}M_mP_m + k_{tb}M_{kb}M_b\{P_b + (k_m - 1)P_m\} \qquad (7.28a)$$

$$(Y\sigma)_s = M_mQ_m + M_bQ_b \qquad (7.28b)$$

where Q refers to residual stress.

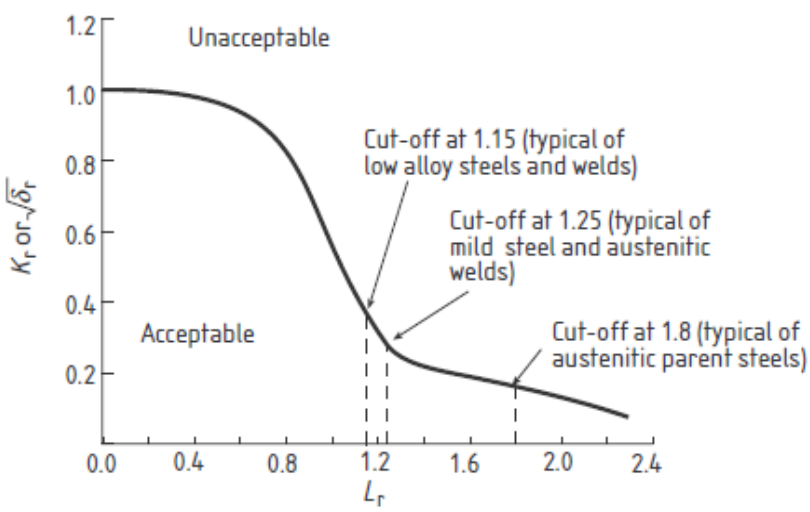

a) for $L_r \leq L_{rmax}$:

$$\sqrt{\delta_r} \text{ or } K_r = (1 - 0.14L_r^2)\{0.3 + 0.7\exp(-0.65L_r^6)\}$$

b) for $L_r > L_{rmax}$:

$$\sqrt{\delta_r} \text{ or } K_r = 0$$

Figure 7-4 Level 2A FAD

7.5.2.1 Primary and Secondary Stresses

For the selected wave, the maximum applied nominal forces and moments in the joint containing the flaw need to be determined. The maximum applied nominal forces and moments are then converted into maximum applied axial, in-plane, and out-of plane nominal stresses from which the local joint stresses are determined, as described above in Sec. 7.5.

General guidance on the treatment of residual stresses is given in BS7910 Sec. 7.3.4 and supplemented by recommendations on residual stress distribution in Annex Q.

7.5.2.2 Collapse Parameter L_r

The collapse parameter L_r for tubular joints may be calculated using either local or global collapse analyses. The local collapse approach will usually be very conservative whilst the use of the global approach tends to give more realistic predictions of plastic collapse in tubular joints. Once the reference stress σ_{ref} is determined, the load ratio L_r is calculated as σ_{ref}/σ_Y where σ_Y is the yield strength.

The cut-off is to prevent localized plastic collapse and it is set at the point at which $L_r = L_{rmax}$ where:

$$L_{rmax}=(\sigma_{Y+} \sigma_u)/(2 \sigma_Y) \qquad (7.29)$$

For the purposes of defining the cut-off, mean rather than minimum properties may be used.

a) Local collapse analysis for part-thickness flaws

For the deepest point of part-thickness flaws in circumferential butt welds, the standard solution in BS7910 Annex P should be used to calculate the reference stress, σ_{ref}, across the remaining ligament, using as the effective width the length of the joint subjected to tensile stresses. For the surface point at the ends of surface-breaking flaws in circumferential butt welds, the standard solutions in Annex P should be used to calculate the reference stress, σ_{ref}, for a through-thickness flaw having a length equal to the surface length of the part thickness flaw, $2c$. The effective width should be taken as the length of the joint subject to tensile stresses.

For surface flaw, Figure 7-5, the reference stress is calculated from either of the following equations as appropriate:

$$\sigma_{ref} = \frac{P_b + \left\{P_b^2 + 9P_m^2(1 - \alpha'')^2\right\}^{0.5}}{3(1 - \alpha'')^2} \qquad (7.30a)$$

for normal bending restraint, and

$$\sigma_{ref} = \frac{P_b + 3P_m\alpha'' + \left\{(P_b + 3P_m\alpha'')^2 + 9P_m^2(1 - \alpha'')^2\right\}^{0.5}}{3(1 - \alpha'')^2} \qquad (7.30b)$$

for negligible bending restraint, where P_m and P_b are the linearized primary membrane and bending not including stress concentration due to weld geometry (with no k_t applied), and

$\alpha'' = (a/B)/\{1 + (B/c)\}$ for $W \geq 2(c + B)$;

$\alpha'' = (2a/B)(c/W)\}$ for $W < 2(c + B)$.

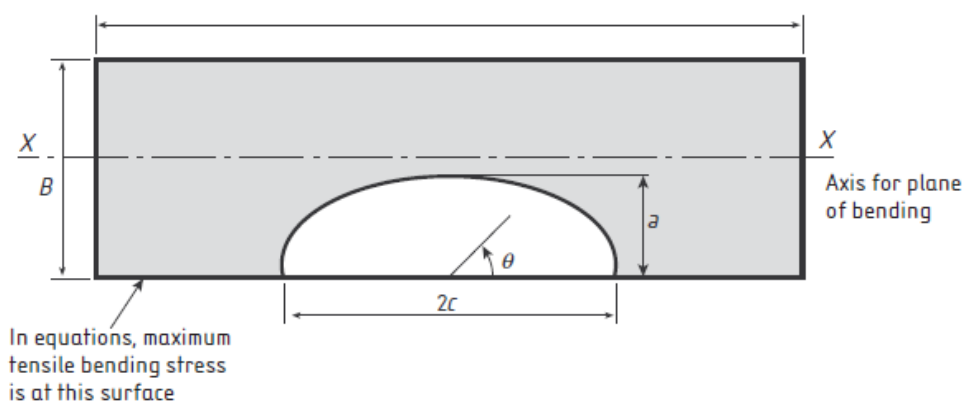

Figure 7-5 Surface Flaw Parameters

b) Global collapse analysis

For circumferential butt welds or tubular nodal joints containing a flaw in the brace, lower bound collapse loads should be calculated separately for axial loading, in-plane bending and out-of-plane bending for the overall cross-section of the member containing the flaw based on net area and yield strength. The net area for axial loading should be taken as the full area of the cross-section of the joint minus the area of rectangle containing the flaw. The collapse load P_c is the load to raise the average stress on the net area to the yield strength. The fully plastic moment of the cross-section of the joint should be calculated for in-plane or out-of-plane loads, allowing for the cross-sectional area of the rectangle containing the flaw. The net fully plastic moments, M_{ci} and M_{co}, based on the yield strength, are the collapse moments.

For tubular nodal joints containing a part-thickness or through-thickness flaw in the chord, parametric equations for the design strength of the un-cracked geometry are available; see HSE /41/ and API /4/. The lower bound characteristic ultimate strength for the geometry concerned should be calculated using the equations for the un-cracked geometry from the above references, together with the specified minimum yield strength. The ultimate strengths for axial, in-plane and out-of-plane bending loads should be calculated separately.

The plastic collapse loads for the cracked geometry are determined by reducing the plastic collapse loads for the corresponding uncracked geometry on the basis of the net load-bearing area for axial loading and the effect of the flaw area on the plastic collapse modulus for bending loads. The correction factor for axial loading is given in BS7910: 2005 by the following equation:

$$F_{AR} = \left(1 - \frac{A_c}{l_w}\right)\left(\frac{1}{Q_\beta}\right)^{m_q} \qquad (7.31)$$

where

F_{AR} is the reduction factor to allow for the loss of load-bearing cross-sectional area due to the presence of the flaw, Q_β allows for the increased strength observed at β values above 0.6;

A_c = crack area = 2aB for a through thickness flaw; or A_c = crack area = (½)πac for a surface breaking flaw; l_w = weld length = entire length of weld toe along brace/chord intersection on the chord side;

Q_β = 1 for β k 0.6;

$Q_\beta = 0.3/\{\beta(1 - 0.833\beta)\}$ for $\beta > 0.6$;

For tubular joints containing part-thickness flaws, m_q = 0. For tubular joints containing through-thickness flaws, validation of equation (7.26) is at present limited to joints with β ratios less than 0.8 and the following configurations:

— K-joint with a through-thickness crack at the crown subjected to balanced axial loading;

— tension axially loaded T and DT joint with a through-thickness crack at the saddle.

For K joints, use either of the following:

— the HSE characteristic compression design strength with m_q = 1; or

— the API RP 2A compression design strength with m_q = 0.

For T and DT joints, use either of the following:

— the HSE characteristic tension design strength with m_q = 1; or

— the API RP 2A tension design strength with m_q = 0.

For tubular nodal joints containing a part thickness or through thickness flaw in the chord, the parameter L_r is calculated from the following:

$$L_r = \left(\frac{\sigma_f}{\sigma_Y}\right)\left\{\left|\frac{P_a}{P_c}\right| + \left(\frac{M_{ai}}{M_{ci}}\right)^2 + \left|\frac{M_{ao}}{M_{co}}\right|\right\} \tag{7.32}$$

where

P_c, M_{ci} and M_{co} are plastic collapse loads in the cracked condition for axial loading, in-plane bending and out-of-plane bending respectively.

If conservative assumptions lead to a global collapse value of L_r being higher than the local collapse value of L_r, the local value may be used. For example P_c is equal to F_{AR} times the plastic collapse load in the un-cracked condition for axial loading.

It should be noted that the HSE is no longer issuing or supporting the Guidance Notes /41/ last published in 1995. The new edition of BS-7910 presently being developed should probably reference the ISO 19902 instead and the latest edition of API RP 2A /4/. The capacity formulations have changed in the newer versions of the API and ISO standards.

7.5.2.3 Determination of K_r and or $\sqrt{\delta r}$

The fracture parameter, K_r or $\sqrt{\delta r}$, is determined using the procedure in BS7910 Sec. **7.3** as:

- Level 2A: generalized FAD, not required stress/strain data $\sqrt{\delta r}$

The equations are the following:

a) for $L_r \le L_{rmax}$:

$$\sqrt{\delta_r} \text{ or } K_r = (1 - 0.14 L_r^2)\{0.3 + 0.7\exp(-0.65 L_r^6)\}$$

b) for $L_r > L_{rmax}$:

$$\sqrt{\delta_r} \text{ or } K_r = 0 \tag{7.33}$$

- Level 2B: material-specific curve:

It requires a specific stress-strain curve; it will generally give more accurate results than Level 2A.

The equations are described as follows:

a) for $L_r \le L_{r\,max}$:

$$\sqrt{\delta_r} \text{ or } K_r = \left(\frac{E\varepsilon_{ref}}{L_r\sigma_Y} + \frac{L_r^3\sigma_Y}{2E\varepsilon_{ref}}\right)^{-0.5}$$

b) for $L_r > L_r$ max:

$$\sqrt{\delta_r} \text{ or } K_r = 0 \tag{7.38}$$

7.5.2.4 Fracture Ratio K_r

The applied stress intensity factor, KI, has the following general form:

$$K_I = (Y\sigma)\sqrt{\pi a} \tag{7.39}$$

where

$$Y\sigma = M f_w M_m \sigma_{max} \tag{7.40}$$

M and f_w are bulging correction and finite width correction factors respectively, σ is the maximum tensile stress, and M_m is a stress intensity magnification factor.

Kr is the ratio of the stress intensity factor, K_I, to the fracture toughness K_{mat}, i.e.

$$K_r = \frac{K_I}{K_{mat}} \tag{7.41}$$

The BS-7910 gives an approximate relationship between the Charpy V-notch toughness and the K_{mat} ($=K_{Ic}$) which may be used if the fracture toughness for the specific material is not available:

$$K_{mat} = [(12\sqrt{C_v} - 20)(25/B)^{0.25}] + 20 \tag{7.42a}$$

A maximum value for K_{mat} is set as:

$$K_{mat} = 0.54C_v + 55 \tag{7.42b}$$

where C_v is the Charpy impact energy in Joules, B is the thickness in mm and Kmat in MPa√m.

Alternatively, applied CTOD, δ_I is determined from K_I as follows:

$$\delta_I = \frac{K_I^2}{\sigma_Y E} \qquad \text{for } \sigma_{max}/\sigma_Y \leq 0.5 \tag{7.43a}$$

$$\delta_I = \frac{K_I^2}{\sigma_Y E} / [(\frac{\sigma_Y}{\sigma_{max}})^2 \left(\frac{\sigma_{max}}{\sigma_Y} - 0.25\right)] \quad \text{for } \sigma_{max}/\sigma_Y < 0.5 \tag{7.43b}$$

And δ_r is given as:

$$\delta_r = \frac{\delta_I}{\delta_{mat}} \tag{7.44}$$

The square root of δ_r is plotted on the vertical axis of the FAD, Figure 7-4.

7.5.2.5 Flaw Assessment

As an initial assessment, the co-ordinates relating to the deepest point and surface point positions should be plotted on the Level 2A FAD for low work hardening materials. If the points lie within the locus the flaw may be acceptable. If any of the points lie on or outside the locus, the flaw is unacceptable.

7.5.3 Corrosion Assessment

It should be ensured that the condition of the considered corroded structural element is sufficiently surveyed in order that the various failure modes can be properly addressed.

Structures that are not sufficiently protected against corrosion need to be assessed with their net thicknesses at the end of the assumed total design service life. The corrosion rate should be based on relevant experience and appropriate inspection plans need to be implemented.

Structural parts that can be subjected to abrasion from normal use or by accidents need to be inspected to determine the extent of the abrasion. Structural assessments should be made on the basis of forecasted values for the net sections of the structural parts.

8 CASE STUDY

8.1 Introduction

In order to demonstrate the methodologies recommended in this report, fatigue performance from existing platform connections was employed herein as a case study. The same jacket platform used in a recent DNV study for BOEMRE under TAR 677 /**43**/ was analyzed, see Figure 8-1.

The calculations start by performing a deterministic fatigue analysis based on S-N curves as recommended in DNV RP-C203 /**1**/. The most critical connections with the lowest fatigue lives are determined. A joint was selected and a crack was assumed to start in the brace resulting in severance of the member. The fatigue analysis was repeated without the severed member and the new fatigue lives were compared for the other braces connecting to the same joint and the neighboring joints. This analysis demonstrates that existing redundancy in such a jacket structure make it unlikely that a single crack at a joint could be detrimental to the fatigue strength of the structure.

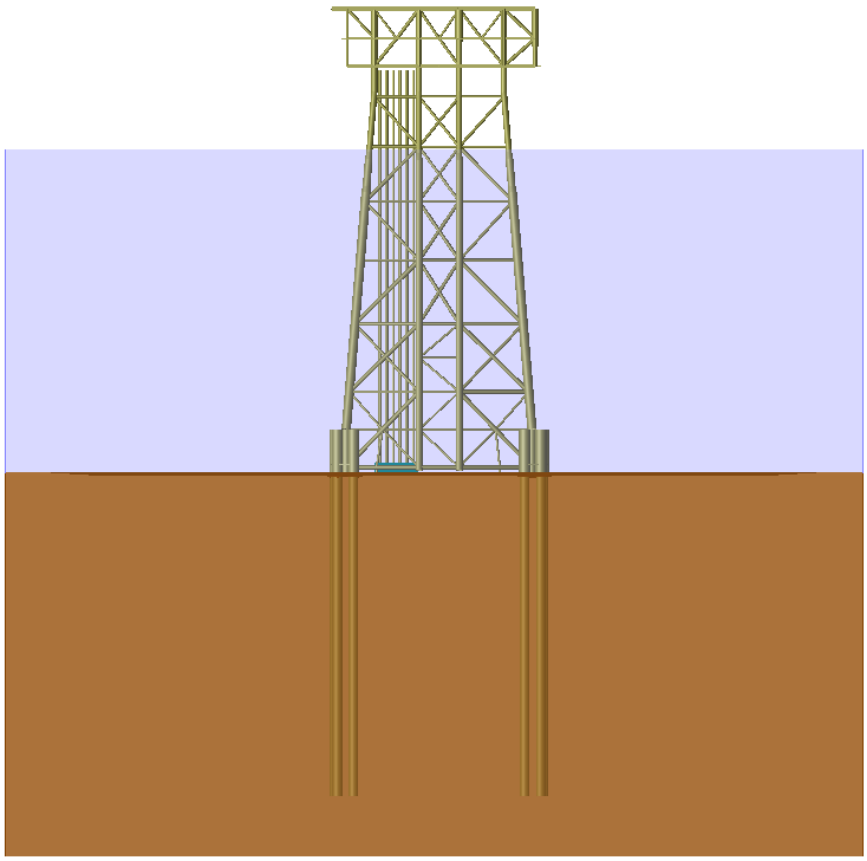

Figure 8-1 Platform Employed in Case Study

8.2 Deterministic Fatigue Analysis

8.2.1 General Information and Methodology

The analysis methodology described in Norsok N-004 /11/ and DNV-RP-C203 /1/ was followed. It was assumed that the analyzed platform is not sensitive to the dynamic effects; therefore deterministic analysis was chosen as an analysis method (the dynamic stochastic analysis method is recommended for platforms sensitive to the dynamic effects).

The wave loads based on the Stoke's 5th order theory were generated by WAJAC and applied to the model. All other loads (i.e. variable deck loads, deadweight, etc.) were not considered in the analysis. The accumulated fatigue damage was calculated based on the long term distribution of the hotspot stresses and S-N curve associated with the detail under consideration. Only the tubular members of the jacket structure were considered; the fatigue damage was calculated for 8 hotspots around the perimeter of the member (see Figure 8-2).

Figure 8-3 presents the calculation procedure for the deterministic fatigue analysis.

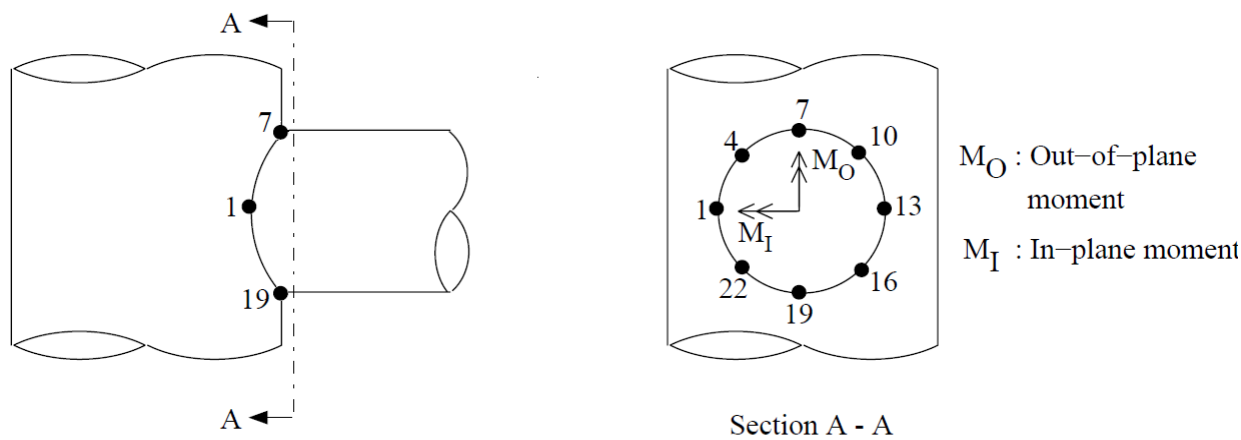

Figure 8-2 Default hotspot location for fatigue calculations (Framework)

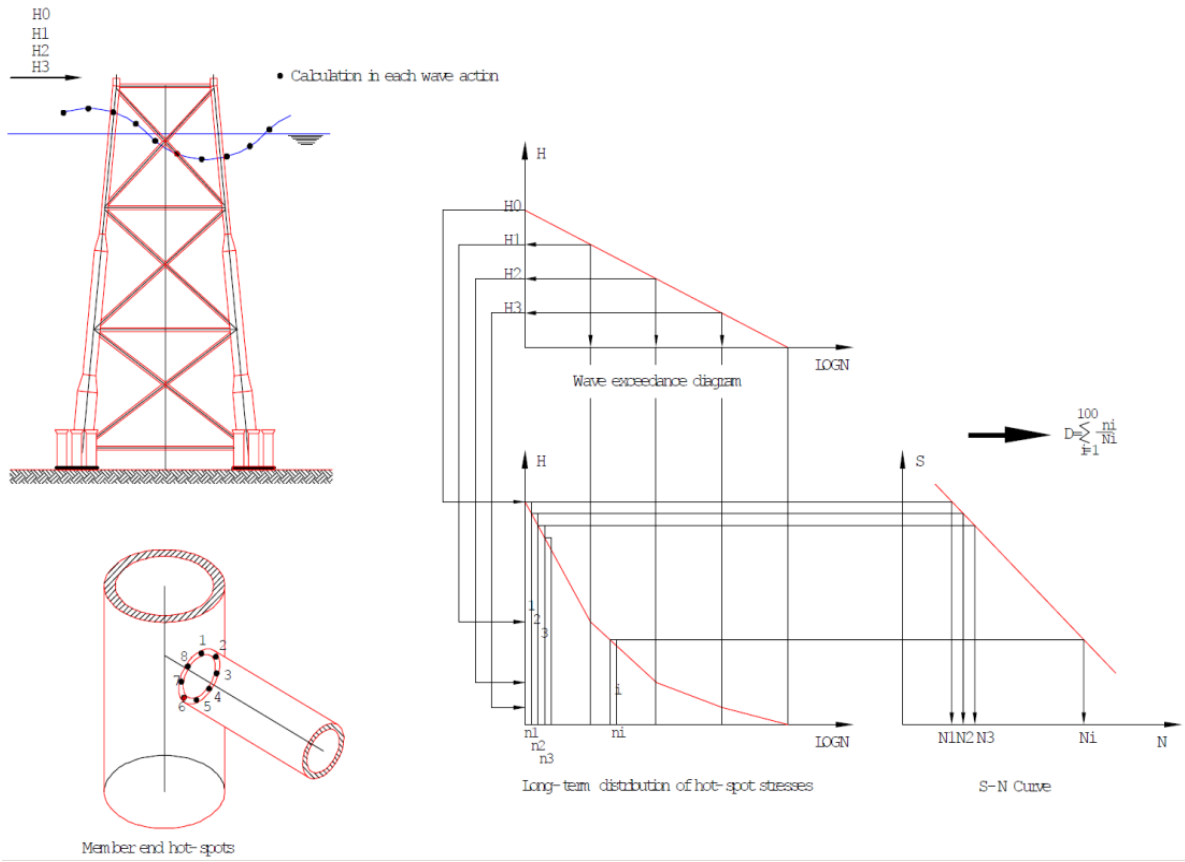

Figure 8-3 Deterministic Fatigue Analysis Procedure (Norsok N-004)

The following software packages employed widely in the industry were employed:

- GeniE
- Wajac
- Gensod/Splice
- SESTRA
- Framework
- Mathcad/Crackwise

8.2.2 Loads

The basis for the S-N fatigue calculation is the stress range due to the cyclic loads, without considering the mean stress level, therefore only the wave loads were applied to the model. Fatigue loads based on the spectral scatter diagram for the GoM presented in Annex C of ISO 19901-1 were transformed into a single wave scatter diagram to define the wave exceedance diagram (Figure 8-4). The Stoke's 5th order wave theory was used to generate the member loads used in the analysis. A long term stress distribution was derived based on the defined wave exceedance and the results of the wave/structural analysis, for 8 wave headings with even probability for all directions and 10 waves per direction. The wave forces were calculated based on 10 positions (steps) through each wave, which results in a total of 800 analysed load cases.

The hotspot stresses were calculated using the Stress Concentration Factors (SCF) based on the Efthymiou's formulae /**1**/ and the joint categorization (T, K, TK, TKT, KTK, etc.). The joint category was assigned to joints automatically by Framework using adopted methodology that accounts for load path. During the calculations, the long term hotspot stress distribution was divided into 100 blocks to calculate the accumulated fatigue damage for all joints of the structure.

Table 8-1 Spectral Scatter Diagram for the GoM (ISO 19901-1)

Wave height m	Peak period [a] s												
	0,5 to 1,5	1,5 to 2,5	2,5 to 3,5	3,5 to 4,5	4,5 to 5,5	5,5 to 6,5	6,5 to 7,5	7,5 to 8,5	8,5 to 9,5	9,5 to 10,5	10,5 to 11,5	11,5 to 12,5	Total for 0,5 to 12,5
0,2 to 0,5	0	0,16	1,99	4,26	5,67	2,74	1,05	0,67	0,05	0,01	0,02	0	16,62
0,5 to 0,8	0	0,04	1,22	3,39	7,78	6,62	1,84	0,53	0,13	0,01	0,00	0	21,56
0,8 to 1,1	0	0,01	0,35	1,41	4,80	7,84	3,14	0,61	0,08	0,03	0,00	0	18,27
1,1 to 1,4	0	0	0,07	0,27	1,97	5,89	4,78	1,50	0,08	0,01	0,01	0	14,58
1,4 to 1,7	0	0	0,01	0,05	0,49	3,02	4,28	2,32	0,14	0,03	0,01	0	10,35
1,7 to 2,0	0	0	0	0	0,13	1,16	2,87	2,37	0,23	0,03	0,01	0	6,80
2,0 to 2,3	0	0	0	0	0,03	0,36	1,54	2,05	0,39	0,08	0,02	0	4,47
2,3 to 2,6	0	0	0	0	0	0,11	0,62	1,46	0,39	0,10	0,02	0	2,70
2,6 to 2,9	0	0	0	0	0	0,02	0,20	0,88	0,37	0,11	0,02	0	1,60
2,9 to 3,2	0	0	0	0	0	0	0,06	0,46	0,42	0,08	0,02	0	1,04
3,2 to 3,5	0	0	0	0	0	0	0,02	0,20	0,25	0,10	0,03	0	0,60
3,5 to 3,8	0	0	0	0	0	0	0,01	0,12	0,17	0,13	0,03	0	0,46
3,8 to 4,1	0	0	0	0	0	0	0	0,08	0,12	0,13	0,04	0	0,37
4,1 to 4,4	0	0	0	0	0	0	0	0,02	0,05	0,08	0,03	0	0,18
4,4 to 4,7	0	0	0	0	0	0	0	0,01	0,03	0,04	0,05	0	0,13
4,7 to 5,0	0	0	0	0	0	0	0	0	0,01	0,03	0,05	0	0,09
5,0 to 5,3	0	0	0	0	0	0	0	0	0	0,01	0,05	0	0,06
5,3 to 5,6	0	0	0	0	0	0	0	0	0	0,00	0,04	0	0,04
5,6 to 5,9	0	0	0	0	0	0	0	0	0	0,01	0,04	0	0,05
5,9 to 6,3	0	0	0	0	0	0	0	0	0	0,01	0,02	0	0,03
Total for 0,2 to 6,3	0	0,21	3,64	9,38	20,87	27,76	20,41	13,28	2,91	1,03	0,51	0	100,00

[a] Data taken from NOAA buoy 42001[65].

Table 8-2 Single Wave Exceedance Used in Analysis

	H [m]	Tz [s]	N [-]
1	0.5	5.1	13000458
2	1.1	6.1	4340063
3	1.7	7.0	1539193
4	2.3	7.8	589776
5	2.9	8.4	243975
6	3.5	9.0	108080
7	4.1	9.5	50578
8	4.7	10.2	24614
9	5.3	10.9	12286
10	5.9	10.7	6084
		TOTAL (per direction)	**1.99E+07**
		TOTAL (8 directions)	**1.59E+08**

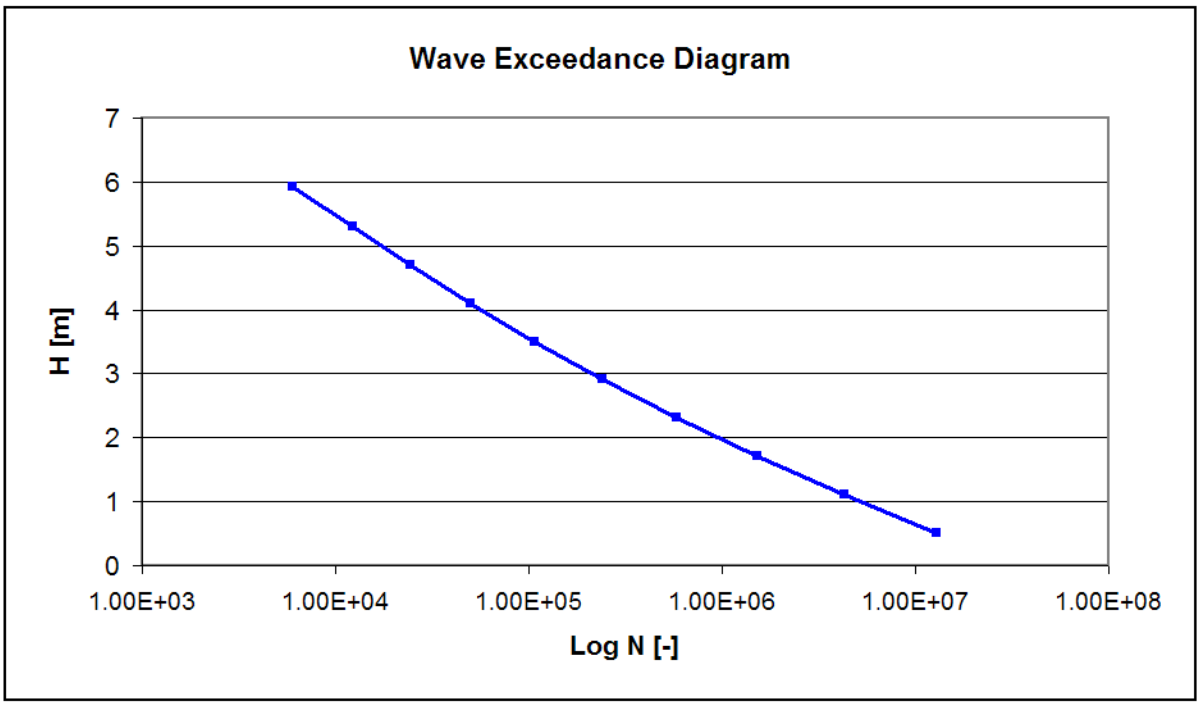

Figure 8-4 Wave Exceedance Diagram (identical for each direction)

8.2.3 Results

Two configurations of the platform were analyzed: 'As built' and 'Post failure'. One chosen member with relatively high fatigue damage calculated for 'As built' run was removed from the model and the analysis was repeated for platform 'Post failure' configuration.

The S-N curve category T was used in the fatigue life calculation for all tubular joints /**1**/. Design Fatigue Factor of 1.0 was assumed. A positive gap of 100 mm was assigned to all members, at all joint locations.

The analysis results for the platform in 'As built' configuration indicated that the accumulated 20-yr fatigue damage calculated for the brace side of the member BM73, at joint JT91 was 0.016 (at hotspot 13 – saddle location). This member was removed from the 'Post failure' analysis. Table 8-3 presents the results for these two fatigue analyses (exclusive of the fatigue damage calculated for removed member). The fatigue results are presented for 8 joints adjacent to joint JT91, connected to this joint by structural members. More detail results can be found in Appendix B.1.

It can be seen that the increase in fatigue damage calculated for the neighbouring structure is not significant, which leads to the conclusion that the jacket is a redundant structure in terms of fatigue utilization. It should however be noted that the consequence of the fatigue failure of one of the members is not limited to the change in fatigue utilization of the surrounding structure. The potential failure due to remaining failure modes (i.e. yielding or buckling) should be evaluated separately.

Table 8-3 Comparison of Calculated Fatigue Damage

Joint	Side	As built		Post failure		Damage Difference
		Fatigue Damage	Fatigue Life	Fatigue Damage	Fatigue Life	
		[-]	[years]	[-]	[years]	[%]
JT26	Chord	2.90E-04	>5000	3.42E-04	>5000	17.9
	Brace	1.97E-04	>5000	1.92E-04	>5000	-2.5
JT32	Chord	7.67E-04	>5000	7.74E-04	>5000	0.9
	Brace	1.21E-03	>5000	1.22E-03	>5000	0.8
JT47	Chord	4.52E-03	4425	4.51E-03	4435	-0.2
	Brace	8.18E-03	2445	8.32E-03	2404	1.7
JT71	Chord	4.77E-04	>5000	4.48E-04	>5000	-6.1
	Brace	1.56E-04	>5000	1.56E-04	>5000	0.0
JT91	Chord	1.73E-03	>5000	1.90E-03	>5000	9.8
	Brace	7.63E-04	>5000	8.71E-04	>5000	14.2
JT176	Chord	4.47E-03	4474	4.27E-03	4684	-4.5
	Brace	4.28E-03	4673	3.96E-03	>5000	-7.5
JT221	Chord	7.11E-02	281	7.50E-02	267	5.5
	Brace	2.63E-02	760	2.78E-02	719	5.7
JT321	Chord	3.01E-05	>5000	4.46E-05	>5000	48.2
	Brace	1.48E-05	>5000	1.71E-05	>5000	15.5
JT373	Chord	1.60E-02	1250	1.74E-02	1149	8.7
	Brace	6.09E-04	>5000	6.56E-04	>5000	7.7

8.3 Fracture Mechanics Calculations

8.3.1 Introduction and Methodology

Calculations were performed in the MathCAD worksheet Fatigue and Fracture of Flawed Tubular Joints" (FFFTJ) developed by DNV within the framework of this project to demonstrate the proposed procedure to evaluate cracked tubular joints. The worksheet is presented in Appendix A.1. A comparison with CRACKWISE, which is a commercial software developed by TWI for fracture mechanics calculations widely used by the industry, was performed and indicates good correlation of the results (see Appendix B for details).

A welded toe crack was assumed for a tubular joint connection close to the waterline. The hotspot in the analysis was located on the brace side of a KT joint, at the saddle location corresponding to hotspot No. 13 location in Figure 8-5. The analyzed joint is shown in Figure 8-6. It should be noted that shown overlap caused by the modelling simplification was eliminated during post-processing in FRAMEWORK (a positive gap of 100 mm was assigned to all joints and members of the jacket).

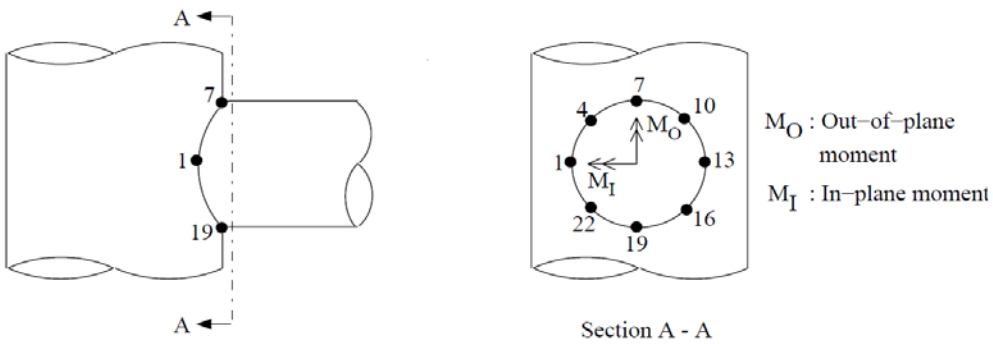

Figure 8-5 Default hotspot location for fatigue calculations (Framework)

The calculations were performed for a wide range of the initial crack size to demonstrate the impact of the crack size on the calculated fatigue life of the damaged joint. Two types of loading were used in the analysis – fatigue (obtained by the deterministic S-N fatigue analysis) and extreme loading (based on the extreme 100 year hurricane strength analysis).

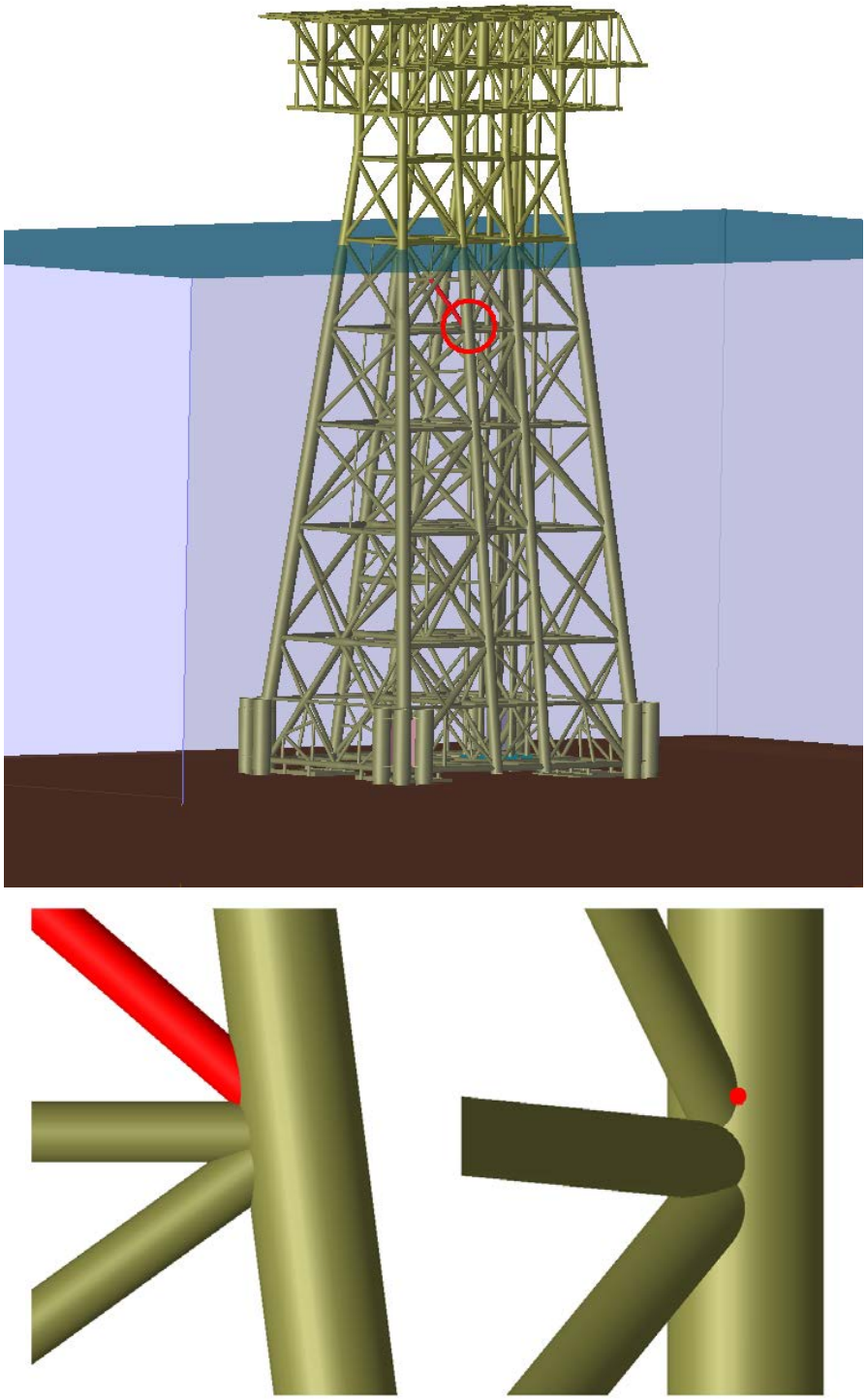

Figure 8-6 Analyzed Hotspot Location (GeniE)

8.3.2 Loads

The uncracked nominal stress range were obtained by deterministic fatigue analysis The nominal stress ranges caused by the axial force, in-plane and out-of-plane bending moment were extracted from the results of the structural analysis performed as a part of the deterministic fatigue analysis, for each of the waves separately (10 wave steps through the structure were used).

The methodology for the assessment of the cracked tubular joints is proposed in Annex B of the BS-7910 /**2**/. The case study is intended for demonstration of the procedure stated in Chapter 7. For simplicity, in the case study, one local field parameter SCF was calculated by FRAMEWORK (based on the empirical Efthymiou's formulae); another local field parameter, the degree of bending Ω was based on published parametric equations /22/ included in 7.5.1.2 and Appendix A.2. Alternatively, more accurate predictions can be obtained by performing a detailed finite element analysis.

Fluctuation of the hotspot stress for one sample wave is shown in Figure 8-7. It should be noted that the stresses due to the in-plane bending moment equal zero, as a consequence of the assumed crack location (at the neutral axis for the in-plane bending). Table 8-4 and Table 8-5 present the fatigue crack growth analysis input data, consisting of sets of membrane and bending stress ranges with associated number of the stress cycles.

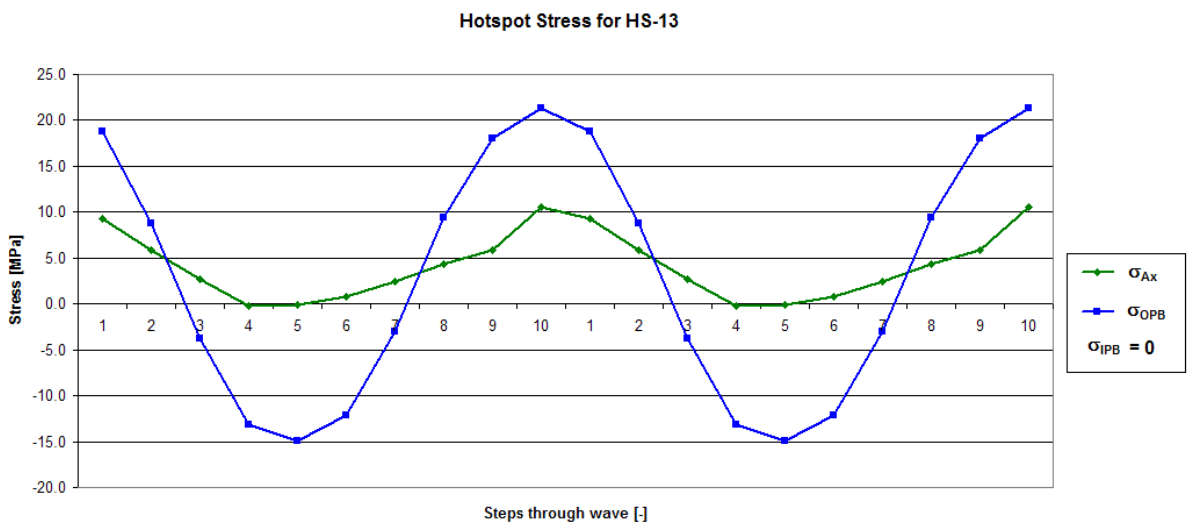

Figure 8-7 Example of Hotspot Stress Level for Analyzed Hotspot (Dir 315°, Wave 1)

The stress range input (block) in Table 8-4 and Table 8-5 represents the fatigue loading corresponding to 20-year operation in the Gulf of Mexico, exclusive of the extreme events (i.e. hurricane). In the analysis, the fatigue load input was divided into 1000 increments. After each increment the fracture assessment (Level 2A FAD) was performed based on the maximum nominal tensile stress magnitude obtained from the extreme 100-yr hurricane strength analysis at the considered location. The local primary membrane (P_m = 80.0 MPa) and primary bending stresses (P_b = 44.5 MPa) were obtained from the extreme strength analysis. If the flawed joint passed the FAD check, the crack growth parameters were re-calculated based on the new crack size and the calculation were repeated for the remaining stress cycles, or until the cracked joint failed under the extreme load.

Table 8-4Crack Growth Analysis Stress Input (for Dir 0° through 135°)

Wave Dir.	Wave	Hotspot Stress Range			Crack Growth Analysis Fatigue Loads				
		$\Delta\sigma_{Ax}$	$\Delta\sigma_{IPB}$	$\Delta\sigma_{OPB}$	$\Delta\sigma_{HS\ Tot}$	Ω_{TOT}	$\Delta\sigma_{M}$	$\Delta\sigma_{B}$	N
		[MPa]	[MPa]	[MPa]	[MPa]	[-]	[Mpa]	[Mpa]	[-]
0°	1	6.1	0.0	55.9	62.0	0.657	21.3	40.7	6.08E+03
	2	5.5	0.0	47.1	52.6	0.653	18.3	34.3	1.23E+04
	3	4.8	0.0	42.2	47.0	0.655	16.2	30.8	2.46E+04
	4	3.9	0.0	37.2	41.1	0.660	14.0	27.1	5.06E+04
	5	3.3	0.0	31.8	35.1	0.661	11.9	23.2	1.08E+05
	6	2.8	0.0	27.3	30.1	0.661	10.2	19.9	2.44E+05
	7	2.2	0.0	22.6	24.8	0.665	8.3	16.5	5.90E+05
	8	1.0	0.0	17.8	18.8	0.691	5.8	13.0	1.54E+06
	9	0.6	0.0	12.1	12.7	0.697	3.8	8.8	4.34E+06
	10	0.1	0.0	5.3	5.4	0.709	1.6	3.8	1.30E+07
45°	1	1.8	0.0	38.2	40.0	0.696	12.1	27.9	6.08E+03
	2	1.8	0.0	32.2	34.0	0.691	10.5	23.5	1.23E+04
	3	1.8	0.0	29.0	30.8	0.687	9.6	21.1	2.46E+04
	4	2.1	0.0	25.5	27.6	0.675	9.0	18.6	5.06E+04
	5	2.3	0.0	21.7	24.0	0.659	8.2	15.8	1.08E+05
	6	2.4	0.0	18.3	20.8	0.644	7.4	13.4	2.44E+05
	7	2.1	0.0	15.1	17.3	0.639	6.2	11.0	5.90E+05
	8	0.9	0.0	11.7	12.7	0.675	4.1	8.6	1.54E+06
	9	0.4	0.0	7.8	8.2	0.693	2.5	5.7	4.34E+06
	10	0.1	0.0	3.3	3.5	0.699	1.0	2.4	1.30E+07
90°	1	4.5	0.0	0.7	5.2	0.096	4.7	0.5	6.08E+03
	2	3.4	0.0	0.7	4.2	0.125	3.6	0.5	1.23E+04
	3	3.8	0.0	0.8	4.5	0.122	4.0	0.6	2.46E+04
	4	3.8	0.0	0.8	4.5	0.122	4.0	0.6	5.06E+04
	5	3.7	0.0	0.8	4.5	0.125	3.9	0.6	1.08E+05
	6	3.4	0.0	0.8	4.2	0.132	3.6	0.6	2.44E+05
	7	3.4	0.0	0.6	4.0	0.116	3.5	0.5	5.90E+05
	8	1.9	0.0	0.2	2.1	0.085	1.9	0.2	1.54E+06
	9	1.1	0.0	0.2	1.3	0.118	1.1	0.2	4.34E+06
	10	0.4	0.0	0.1	0.5	0.179	0.4	0.1	1.30E+07
135°	1	3.9	0.0	35.9	39.8	0.658	13.6	26.2	6.08E+03
	2	3.2	0.0	30.1	33.3	0.660	11.3	22.0	1.23E+04
	3	3.2	0.0	27.3	30.5	0.654	10.6	19.9	2.46E+04
	4	3.1	0.0	24.7	27.8	0.648	9.8	18.0	5.06E+04
	5	2.8	0.0	21.2	24.1	0.643	8.6	15.5	1.08E+05
	6	2.8	0.0	18.2	20.9	0.633	7.7	13.2	2.44E+05
	7	2.4	0.0	15.2	17.6	0.628	6.5	11.1	5.90E+05
	8	1.4	0.0	12.0	13.4	0.655	4.6	8.8	1.54E+06
	9	0.5	0.0	7.9	8.4	0.682	2.7	5.7	4.34E+06
	10	0.2	0.0	3.2	3.3	0.694	1.0	2.3	1.30E+07

Table 8-5 Crack Growth Analysis Stress Input (for Dir 180° through 315°)

Wave Dir.	Wave	Hotspot Stress Range			Crack Growth Analysis Fatigue Loads				
		$\Delta\sigma_{Ax}$	$\Delta\sigma_{IPB}$	$\Delta\sigma_{OPB}$	$\Delta\sigma_{HS\ Tot}$	Ω_{TOT}	$\Delta\sigma_{M}$	$\Delta\sigma_{B}$	N
		[MPa]	[MPa]	[MPa]	[MPa]	[-]	[Mpa]	[Mpa]	[-]
180°	1	2.3	0.0	53.5	55.8	0.699	16.8	39.0	6.08E+03
	2	2.2	0.0	44.6	46.8	0.694	14.3	32.5	1.23E+04
	3	2.0	0.0	40.0	42.0	0.693	12.9	29.1	2.46E+04
	4	1.9	0.0	35.9	37.7	0.693	11.6	26.1	5.06E+04
	5	2.0	0.0	30.7	32.6	0.685	10.3	22.4	1.08E+05
	6	2.2	0.0	26.7	28.9	0.674	9.4	19.5	2.44E+05
	7	2.0	0.0	22.8	24.8	0.669	8.2	16.6	5.90E+05
	8	1.0	0.0	17.9	19.0	0.690	5.9	13.1	1.54E+06
	9	0.6	0.0	11.6	12.2	0.695	3.7	8.5	4.34E+06
	10	0.2	0.0	5.3	5.5	0.709	1.6	3.9	1.30E+07
225°	1	6.7	0.0	33.2	40.0	0.606	15.8	24.2	6.08E+03
	2	5.9	0.0	27.8	33.8	0.601	13.5	20.3	1.23E+04
	3	5.5	0.0	25.8	31.3	0.601	12.5	18.8	2.46E+04
	4	5.1	0.0	23.4	28.4	0.599	11.4	17.0	5.06E+04
	5	4.5	0.0	20.4	24.9	0.597	10.0	14.9	1.08E+05
	6	4.0	0.0	17.9	21.9	0.595	8.9	13.0	2.44E+05
	7	3.0	0.0	15.3	18.3	0.611	7.1	11.2	5.90E+05
	8	0.8	0.0	12.1	13.0	0.683	4.1	8.8	1.54E+06
	9	0.4	0.0	7.9	8.3	0.693	2.5	5.8	4.34E+06
	10	0.2	0.0	3.3	3.5	0.695	1.1	2.4	1.30E+07
270°	1	11.7	0.0	1.4	13.1	0.078	12.1	1.0	6.08E+03
	2	10.2	0.0	1.3	11.5	0.083	10.5	1.0	1.23E+04
	3	9.7	0.0	1.2	10.9	0.081	10.0	0.9	2.46E+04
	4	8.2	0.0	1.0	9.3	0.082	8.5	0.8	5.06E+04
	5	7.1	0.0	0.9	8.0	0.085	7.4	0.7	1.08E+05
	6	6.4	0.0	0.8	7.2	0.085	6.6	0.6	2.44E+05
	7	4.9	0.0	0.7	5.6	0.087	5.1	0.5	5.90E+05
	8	2.2	0.0	0.2	2.4	0.067	2.2	0.2	1.54E+06
	9	1.3	0.0	0.2	1.5	0.097	1.3	0.1	4.34E+06
	10	0.4	0.0	0.1	0.6	0.164	0.5	0.1	1.30E+07
315°	1	10.8	0.0	36.2	46.9	0.562	20.6	26.4	6.08E+03
	2	9.4	0.0	30.5	39.9	0.558	17.7	22.3	1.23E+04
	3	8.5	0.0	27.5	35.9	0.557	15.9	20.0	2.46E+04
	4	7.2	0.0	24.3	31.5	0.562	13.8	17.7	5.06E+04
	5	6.3	0.0	21.2	27.4	0.562	12.0	15.4	1.08E+05
	6	5.3	0.0	18.4	23.7	0.567	10.3	13.4	2.44E+05
	7	3.8	0.0	15.3	19.0	0.585	7.9	11.1	5.90E+05
	8	1.5	0.0	11.8	13.3	0.645	4.7	8.6	1.54E+06
	9	0.6	0.0	7.6	8.2	0.673	2.7	5.5	4.34E+06
	10	0.2	0.0	3.2	3.4	0.693	1.0	2.3	1.30E+07

8.3.3 Analysis Input

Fatigue life sensitivity study was carried out on salient parameters including:

- Crack depth a
- Crack aspect ratio a/c

The material properties shown in Table 8-6 and the stress intensity magnification factor M_k presented in Table 8-7 were used in the Fatigue Crack Growth Analysis and the Fracture assessment. They can also be found in Appendix A.1.

Table 8-6 Material Properties and Input Parameters

Section Thickness	B = 17.8 mm
Section Width	W = 3456 mm
Crack Size and Aspect Ratio	See Table 8-8
Parametric Angle	Θ_1 = 0° and Θ_2 = 90°
Environment (Paris Law Constants)	Marine with Cathodic Protection (-850 mV, Ag/AgCl)
Stress Ratio	R = 1
Misalignment SCF	1.0
Fatigue Loads and Cycles	See Table 8-5 and Table 8-5
Stress Intensity Factors	See Table 8-7
Toughness	K = 2092 N/mm$^{3/2}$
Yield Strength	σ_Y = 355 MPa
Tensile Strength	σ_U = 490 MPa
Young's Modulus	E = 200000 MPa
Poisson's Ratio	ν = 0.3 [-]
Primary Membrane Stress	80.0 MPa
Primary Bending Stress	44.5 MPa
Secondary Membrane Stress	0 MPa
Secondary Bending Stress	0 MPa

Table 8-7 Stress Intensity Magnification Factors M_k(for L/B = 2)

z/B	Axial			Bending		
	v	w	Mkm	v	w	Mkb
0	0.61	-0.31	4.222	0.45	-0.31	3.090
0.002	0.61	-0.31	4.222	0.45	-0.31	3.090
0.004	0.61	-0.31	3.406	0.45	-0.31	2.492
0.006	0.61	-0.31	3.003	0.45	-0.31	2.198
0.008	0.61	-0.31	2.747	0.45	-0.31	2.010
0.01	0.61	-0.31	2.564	0.45	-0.31	1.876
0.02	0.61	-0.31	2.068	0.45	-0.31	1.513
0.03	0.61	-0.31	1.824	0.68	-0.19	1.324
0.04	0.61	-0.31	1.668	0.68	-0.19	1.253
0.05	0.61	-0.31	1.557	0.68	-0.19	1.201
0.06	0.61	-0.31	1.471	0.68	-0.19	1.161
0.07	0.61	-0.31	1.402	0.68	-0.19	1.127
0.08	0.83	-0.21	1.398	0.68	-0.19	1.099
0.09	0.83	-0.21	1.364	0.68	-0.19	1.074
0.1	0.83	-0.21	1.335	0.68	-0.19	1.053
0.175	0.83	-0.21	1.189	0.68	-0.19	1.000
0.2	0.83	-0.21	1.157	0.68	-0.19	1.000
0.3	0.83	-0.21	1.064	0.68	-0.19	1.000
0.4	0.83	-0.21	1.003	0.68	-0.19	1.000
0.5	0.83	-0.21	1.000	0.68	-0.19	1.000
0.6	0.83	-0.21	1.000	0.68	-0.19	1.000
0.7	0.83	-0.21	1.000	0.68	-0.19	1.000
0.8	0.83	-0.21	1.000	0.68	-0.19	1.000
0.9	0.83	-0.21	1.000	0.68	-0.19	1.000
1	0.83	-0.21	1.000	0.68	-0.19	1.000

8.3.4 Results

The results are presented for two separate runs – for pure fatigue (Table 8-8) and combined fatigue and fracture calculations (Table 8-9). The fatigue crack propagation was calculated for 1000 steps (increments) or until the crack size reached the validity limit (see /**2**/, **M.3.2.2.1**). For the combined failure run after each increment of the fatigue calculations the fracture assessment (FAD) was performed for the new calculated crack size.

The results for the assumed crack sizes with initial crack height a≤5 mm and various aspect ratios a/2c indicate that the crack propagation at the calculated crack growth rate does not cause fatigue failure. For fatigue with fracture assessment, the combined failure (i.e. failure due to hurricane after the fatigue crack reaches the critical size) is limiting the life of the joint or connection under consideration.

It should be highlighted that the study presented herein is intended for demonstration of fracture mechanics analysis procedure only. For actual cracked tubular joints assessment, very careful consideration of the problem with close attention to the analysis input and quality of the performed calculations is advisable.

Table 8-8 Analysis Results – Fatigue

a/2c	a [mm]	2c [mm]	a_{final} [mm]	$2c_{final}$ [mm]	Increments	Fatigue Life [year]
0.50	**3**	**6**	3.48	22.30	1000	>20
	4	**8**	5.18	41.32	1000	>20
	5	**10**	7.53	75.03	1000	>20
	6	**12**	16.18	254.11	996	19.92
	7	**14**	16.20	253.43	725	14.5
0.33	**3**	**9**	3.59	24.24	1000	>20
	4	**12**	5.39	44.53	1000	>20
	5	**15**	7.96	82.32	1000	>20
	6	**18**	16.20	253.55	947	18.94
	7	**21**	16.20	253.38	685	13.7
0.25	**3**	**12**	3.71	26.09	1000	>20
	4	**16**	5.59	47.59	1000	>20
	5	**20**	8.41	90.01	1000	>20
	6	**24**	16.19	253.87	904	18.08
	7	**28**	16.20	253.50	651	13.02
0.20	**3**	**15**	3.81	27.96	1000	>20
	4	**20**	5.79	50.80	1000	>20
	5	**25**	8.94	99.25	1000	>20
	6	**30**	16.20	253.50	863	17.26
	7	**35**	16.20	253.50	618	12.36
0.17	**3**	**18**	3.92	29.93	1000	>20
	4	**24**	6.01	54.26	1000	>20
	5	**30**	9.61	111.18	1000	>20
	6	**36**	16.20	253.57	824	16.48
	7	**42**	16.19	253.74	587	11.74
0.14	**3**	**21**	4.03	32.02	1000	>20
	4	**28**	6.25	58.11	1000	>20
	5	**35**	10.43	126.51	1000	>20
	6	**42**	16.19	253.88	787	15.74
	7	**49**	16.19	253.87	558	11.16

Table 8-9 Analysis Results – Fatigue and Fracture

a/2c	a [mm]	2c [mm]	a_{final} [mm]	$2c_{final}$ [mm]	Increments	Fatigue Life [yrs]	Lr [-]	Kr [-]	FAD
0.50	3	6	3.48	22.30	1000	>20	0.297	0.209	Acceptable
	4	8	5.18	41.32	1000	>20	0.332	0.253	Acceptable
	5	10	7.53	75.03	1000	>20	0.409	0.319	Acceptable
	6	12	12.45	166.35	947	18.9	0.812	0.536	Unacceptable
	7	14	12.45	165.45	675	13.5	0.812	0.535	Unacceptable
0.33	3	9	3.59	24.24	1000	>20	0.300	0.213	Acceptable
	4	12	5.39	44.53	1000	>20	0.338	0.259	Acceptable
	5	15	7.96	82.32	1000	>20	0.428	0.335	Acceptable
	6	18	12.45	166.47	897	17.9	0.812	0.536	Unacceptable
	7	21	12.45	165.47	635	12.7	0.812	0.535	Unacceptable
0.25	3	12	3.71	26.09	1000	>20	0.302	0.218	Acceptable
	4	16	5.59	47.59	1000	>20	0.344	0.265	Acceptable
	5	20	8.41	90.01	1000	>20	0.449	0.352	Acceptable
	6	24	12.45	166.45	855	17.1	0.813	0.536	Unacceptable
	7	28	12.45	165.49	601	12.0	0.812	0.535	Unacceptable
0.20	3	15	4.30	37.32	1000	>20	0.317	0.239	Acceptable
	4	20	5.79	50.80	1000	>20	0.350	0.271	Acceptable
	5	25	8.94	99.25	1000	>20	0.478	0.372	Acceptable
	6	30	12.45	166.56	814	16.3	0.813	0.536	Unacceptable
	7	35	12.45	165.61	568	11.4	0.812	0.535	Unacceptable
0.17	3	18	3.92	29.93	1000	>20	0.307	0.225	Acceptable
	4	24	6.01	54.26	1000	>20	0.357	0.277	Acceptable
	5	30	9.61	111.18	1000	>20	0.519	0.400	Acceptable
	6	36	12.44	166.61	774	15.5	0.813	0.536	Unacceptable
	7	42	12.45	165.81	537	10.7	0.812	0.535	Unacceptable
0.14	3	21	4.03	32.02	1000	>20	0.310	0.229	Acceptable
	4	28	6.25	58.11	1000	>20	0.364	0.284	Acceptable
	5	35	10.43	126.51	1000	>20	0.581	0.436	Acceptable
	6	42	12.45	166.64	737	14.7	0.813	0.536	Unacceptable
	7	49	12.45	165.92	508	10.2	0.812	0.535	Unacceptable

9 CONCLUSIONS AND RECOMMENDATIONS

The following conclusions are drawn from the work carried out in this project:

1. Experience indicates that fatigue of welded tubular joints in fixed offshore platforms in the Gulf of Mexico may not be a significant issue. However extensive corrosion or damage due to collisions or dropped objects can be of greater significance. Redundancy, when present, can be effective in reducing the consequence of fatigue failure or redistributing the stresses in neighbouring joints and members.
2. The estimation of reduced strength due to damage caused by reduced scantlings resulting from corrosion or deformation due to impact or collision is possible by applying a methodology that accounts for these effects on increased stress range. Estimating the remaining number of stress cycles (fatigue life) may then be calculated from relevant S-N curves.
3. The use of risk based inspection (RBI) techniques may be considered to be more appropriate than deterministic fatigue or fracture assessment since RBI also addresses the failure consequences issue and quantifies the uncertainties involved.
4. The calculation of fatigue life of a welded joint in the presence of a flaw is possible through application of Fracture Mechanics procedure that is derived based on the BS-7910:2005 standard. A viable preliminary tool has been proposed herein for specific application.
5. The proposed fracture mechanics and Engineering Criticality Assessment (ECA) procedure was applied to an example jacket platform under GOM environment. Results indicate that the presence of a crack in a connection can significantly reduce the connection strength in a storm condition. However the ultimate strength of the structure may not be greatly affected if redundancy is present.
6. A method for calculating fatigue damage due to low cycle high stress environmental conditions due to tropical storms or hurricanes is proposed based on NORSOK N-006.

The following recommendations are made:

1. Research work is needed for further verification of the parameters employed in fracture and fatigue calculation. The effect of combined membrane and bending stresses in calculating the surface and part-thickness crack growth requires further investigation. This includes also the effect of load shedding during crack growth which implies reduced crack growth.
2. Further case studies for actual scenarios of damaged or cracked welds covering both surface and through thickness flaws and complex tubular joint geometries would be valuable to further the understanding of the fracture behaviour of cracked welded joints with cracks present in the brace or the chord.
3. Further development of the MathCAD sheets to include more scenarios and scope and to perform verification work to turn it into a tool that can be applied by specialist engineers.
4. Perform additional parametric and sensitivity studies to rank the many variables involved according to their significance.

5. In order to verify the calculation procedures employed herein, further modelling or full scale testing may be needed. Development of S-N curves for cracked welds in tubular connections can also be considered to simplify the calculation procedures. This may be performed by detailed finite element and fracture mechanics analyses.
6. It is recommended to create a new database that includes reported damages to offshore platforms due to environmental or mechanical damage. A procedure for consistency of reporting would be valuable as evident by the current vast differences in format of inspection reports.
7. As noted in this study, thousands of platforms have been removed over the 65 years age of the offshore industry. It is possible to gain significant knowledge by inspecting and reporting the condition of the structure at time of removal.
8. Develop an API or ISO standard similar to BS-7910 but dedicated to tubular joints and focused on significant effects in order to produce more simplified assessment procedures entailing the above recommendations.

10 REFERENCES

/1/ DNV-RP-C203 Fatigue Design of Offshore Structures, Oct 2011.

/2/ BS 7910:2005, "Guide on Methods for Assessing the Acceptability of Flaws in Structures", British Standard Institution.

/3/ DNV RP-C206, "Fatigue Methodology of Offshore Ships Structures", October 2010.

/4/ API RP 2A (WSD) - Recommended Practice for Planning, Designing and Constructing Fixed Offshore Platforms – Working Stress Design, 21st Edition, December, 2000, with Supplements in December, 2002, September, 2005, and October 2007.

/5/ API RP 2SIM (Ballot Draft 1) – Structural Integrity Management of Fixed Offshore Structures, 1st Edition.

/6/ API 579-1/ASME FFS-1 - Fitness-For-Service, 2nd Edition, June 5, 2007.

/7/ API 579-2/ASME FFS-2 – Fitness-For-Service Example Problem Manual, August 11,2009.

/8/ ISO 19900 – Petroleum and natural gas industries - General Requirements for Offshore Structures, 1st edition, December 2002.

/9/ ISO 19902 - Petroleum and natural gas industries - Fixed Steel Offshore Structures, 1st edition, December 2007.

/10/ NORSOK Standard N-001 - Integrity of Offshore Structures, 7th edition, June 2010.

/11/ NORSOK Standard N-004 - Design of Steel Structures, 2nd edition, October 2004.

/12/ NORSOK Standard N-006 - Assessment of Structure Integrity for Existing Offshore Load-bearing Structures, 1st edition, March 2009.

/13/ Ersdal, G. (2005). "Assessment of Existing Offshore Structures for Life Extension". Doctorial Thesis, University of Stavanger.

/14/ Kruse III, B.J. and Patterson, K.S., MMS, WISTA, Oct. 2008.

/15/ Puskar, F. J., Ku, A. and Sheppard, R. E.. (2004) "Hurricane Lili's Impact on Fixed Platforms and Calibration of Platform Performance to API RP 2A ", OTC 16802, Offshore Technology Conference, 2006.

/16/ Puskar, F.J., Spong, R.E. and Ku, A. etc. (2006) "Assessment of Fixed Offshore Platform Performance in Hurricane Ivan", OTC 18325, Offshore Technology Conference, 2006.

/17/ Puskar, F.J., and Sean M. Verret (2007) "Performance of Steel Jacket Platforms in Recent Gulf of Mexico Hurricanes", OMAE 2007-29633, Proceedings of the 26th International Conference on Offshore Mechanics and Arctic Engineering, OMAE 2007.

/18/ Puskar, F.J., Verret, S. M. and Roberts, C. (2007) "Fixed Platform Performance During Recent Hurricanes: Comparison to Design Standards", OTC 18989, Offshore Technology Conference, 2007.

/19/ Energo Engineering Report (2006) – Assessment of Fixed Offshore Platform Performance in Hurricanes Andrew, Lili and Ivan, MMS Project No. 549, January 2006.

/20/ Energo Engineering Report (2007) – Assessment of Fixed Offshore Platform Performance in Hurricanes Katrina and Rita, MMS Project No. 578, May 2007.

/21/ Energo Engineering Report (2010) –" Assessment of Damage and Failure Mechanisms for Offshore Structures and Pipelines in Hurricanes Gustav and Ike", MMS Project No. 642, February 2010.

/22/ Connolly, M. P., Hellier, A. K., Dover, W. D., and Sutomo, J., "A parametric study of the ratio of bending to membrane stress in tubular Y and T joints". International Journal of Fatigue. 12 (1) 3-11. ISSN 0142-1123,1990.

/23/ Raju, I.S. and Newman, J.C., (1981), "An empirical stress-intensity factor equation for surface crack," Engineering Fracture Mechanics, Vol. 15, pp.185-192.

/24/ Shang-Xian, W., (1985), "Shape change of surface crack during fatigue growth," Engineering Fracture Mechanics, Vol. 22, pp.897-913.

/25/ Health and Safety Executive (2000) - Static Strength of Cracked Joints in tubular members. Offshore Technology Report 2000/080.

/26/ Health and Safety Executive (2000) - Static Strength of Cracked High Strength Steel Tubular Joints. Offshore Technology Report 2000/078.

/27/ Sigurdsson, G. and Mathisen, J. (1999). "Inspection Interval for Tendon Joints of Jolliet TLP," OMAE99/S&R-6010, 18th International Conference on Offshore Mechanics and Arctic Engineering OMAE 1999.

/28/ Lotsberg, I. (2005). "Background for revision of DNV-RP-C203 fatigue analysis of offshore steel structure," OMAE2005-67549, 24th International Conference on Offshore Mechanics and Arctic Engineering OMAE 2005.

/29/ Lotsberg, I. and Ronold, K. O. (2011). "On the derivation of design S-N curves based on limited fatigue test data," OMAE2011-49175, 30th International Conference on Offshore Mechanics and Arctic Engineering OMAE 2011.

/30/ Lotsberg, I. (2011). "On stress concentration factors for tubular Y- and T-joints in frame structures," Marine Structures 24 (2011), pp.60-69.

/31/ Vormwald, M. (1991). "A fracture mechanics based fatigue life prediction for offshore tubular joints," Proceedings of the First International Offshore and Polar Engineering Conference, ISBN 0-9626104-9-6, Vol IV, pp.451-457.

/32/ Stacey, A., Birkinshaw M., andSharp, J.V. (2008). "Life extension issues for aging offshore installations," OMAE2008-57411, 27th International Conference on Offshore Mechanics and Arctic Engineering OMAE 2008.

/33/ Buitrago J., and Healy, B.E. (1993). "Local joint flexibility of tubular joints," OMAE1993, Offshore Technology Vol. I, pp. 405-416.

/34/ Health and Safety Executive (2001) – The effects of local joint flexibility on the reliability of fatigue life estimates and inspection planning. Offshore Technology Report 2000/056.

/35/ Health and Safety Executive (1997) – The ultimate strength of cracked tubular K-joints. Offshore Technology Report 497

/36/ DNV (2005) – Framework – User Manual

/37/ Kukkanen, T. (1996). "Spectral fatigue analysis for ship structures – uncertainties in fatigue actions," Licentiate's thesis, Helsinki University of Technology.

/38/ Xu, T., and Bea, R. (1998) - Reassessment of the Tubular Joint Capacity: Uncertainty and Reliability, Screening Methodologies Project Phase IV, Report to Joint Industry Project – Dynamic Non-linear Loading Effects on Offshore Platforms, TAR 224 AS, 1998.

/39/ DNV (2012) – Comparison of API, ISO and NORSOK Offshore Structural Standards, BOEMRE TA&R N0. 677, Final Report, January 12, 2012.

/40/ Bowness, D. and Lee, M.M.K. 2000. Fracture Mechanics Assessment of Fatigue Cracks in Offshore Tubular Structures, HSE Offshore Technology Report 2000/077.

/41/ Health and Safety Executive (1995) – Offshore installations: Guidance on Design, Construction and Certification. 4th ed. 3rd amendment. London: Her Majesty's Station Office. ISBN 0114129614.

/42/ Ghoneim, G.A. and Sigurdsson, G., "Fundamentals of Risk Based Inspection – A Practical Approach", Oceans, Biloxi, MS, 2009.

/43/ DNV-RP-C205 Environmental Conditions and Environmental Loads, Oct 2010.

/44/ ISO 19901-1 - Petroleum and natural gas industries – Metocean Design and Operating Considerations, 1st edition, November 2005.

APPENDIX A MATHCAD WORKSHEETS

APPENDIX A.1 CRACK GROWTH OF SURFACE FLAW IN TUBULAR JOINT

"FFFTJ" SHEET:
FATIGUE AND FRACTURE OF FLAWED TUBULAR JOINTS

"FFFTJ"

To Calculate Crack Growth of Surface Flaw in Tubular Joint
BS7910:2005, Level 2A
(Units must be N and mm)

Disclaimer: This Mathcad file is intented only for demonstration of the procedure and is not guaranteed to produce results that can be applied directly to actual situations without further expert verification. The user of this sheet will have to assume the responsibility for any associated risks for any application.

INPUT DATA

Outside Radius	$r_o := 550$
Wall Thickness	$B := 17.8$
Weldment length	$L := 35.6$
Post Weld Heat Treatment:	$PWHT :=$ "Yes" (with PWHT: "Yes", without PWHT: "No")
Primary membrane stress (uncracked):	$P_m := 80$
Primary bending stress (uncracked):	$P_b := 44.5$
Stress concentration due to misalignment	$k_m := 1.0$
Membrane Stress concentration factor	$k_{tm} := 1.0$
Bending Stress concentration factor	$k_{tb} := 1.0$
Crack tip opening displacement	$\delta_{mat} :=$ "unknown"
The lower bound Charpy V-notch impact energy at the service temperature (in joules)	$C_v := 27$
Specified minimum yield strength	$\sigma_y := 355$
Ultimate tensile strength	$\sigma_u := 490$
Elastic modulus	$E := 200000$
Loading Cycles	$cycles := READPRN(\text{"cycles.txt"})$
Axial hot spot stress range:	$\Delta\sigma_m := READPRN(\text{"srangesigmam.txt"})$
Bending hot spot stress range:	$\Delta\sigma_b := READPRN(\text{"srangesigmab.txt"})$

"FFFTJ"

BASIC PARAMETERS

1) Stress intensity magnification factors (M.5.1.2 - Table M9 Values of v and w for axial and bending loading)

$deep \equiv 0 \qquad surface \equiv 1 \qquad z_{tip} \equiv 0.15$

$$M_{km}(a,c,loc) := \left| \begin{array}{l} z \leftarrow \max(a, z_{tip}) \ \text{ if } loc = deep \\ z \leftarrow z_{tip} \ \text{ if } loc = surface \\ \text{if } \frac{L}{B} \le 2 \\ \quad \left| \begin{array}{l} \text{if } \frac{z}{B} \le 0.05 \cdot \left(\frac{L}{B}\right)^{0.55} \\ \quad \left| \begin{array}{l} v \leftarrow 0.51 \cdot \left(\frac{L}{B}\right)^{0.27} \\ w \leftarrow -0.31 \end{array} \right. \\ \text{otherwise} \\ \quad \left| \begin{array}{l} v \leftarrow 0.83 \\ w \leftarrow -0.15 \cdot \left(\frac{L}{B}\right)^{0.46} \end{array} \right. \end{array} \right. \\ \text{if } \frac{L}{B} > 2 \\ \quad \left| \begin{array}{l} \text{if } \frac{z}{B} \le 0.073 \\ \quad \left| \begin{array}{l} v \leftarrow 0.615 \\ w \leftarrow -0.31 \end{array} \right. \\ \text{otherwise} \\ \quad \left| \begin{array}{l} v \leftarrow 0.83 \\ w \leftarrow -0.20 \end{array} \right. \end{array} \right. \\ \max\left[1, v \cdot \left(\frac{z}{B}\right)^{w}\right] \end{array} \right.$$

$$M_{kb}(a,c,loc) := \left| \begin{array}{l} z \leftarrow \max(a, z_{tip}) \ \text{ if } loc = deep \\ z \leftarrow z_{tip} \ \text{ if } loc = surface \\ \text{if } \frac{L}{B} \le 1 \\ \quad \left| \begin{array}{l} \text{if } \frac{z}{B} \le 0.03 \cdot \left(\frac{L}{B}\right)^{0.55} \\ \quad \left| \begin{array}{l} v \leftarrow 0.45 \cdot \left(\frac{L}{B}\right)^{0.21} \\ w \leftarrow -0.31 \end{array} \right. \\ \text{otherwise} \\ \quad \left| \begin{array}{l} v \leftarrow 0.68 \\ w \leftarrow -0.19 \cdot \left(\frac{L}{B}\right)^{0.21} \end{array} \right. \end{array} \right. \\ \text{if } \frac{L}{B} > 1 \\ \quad \left| \begin{array}{l} \text{if } \frac{z}{B} \le 0.03 \\ \quad \left| \begin{array}{l} v \leftarrow 0.45 \\ w \leftarrow -0.31 \end{array} \right. \\ \text{otherwise} \\ \quad \left| \begin{array}{l} v \leftarrow 0.68 \\ w \leftarrow -0.19 \end{array} \right. \end{array} \right. \\ \max\left[1, v \cdot \left(\frac{z}{B}\right)^{w}\right] \end{array} \right.$$

2) Caculation of fw, Mm and Mb (Annex M.3.2.2 and M.3.2.3)

The following conditions apply:

$0 \le \frac{a}{2c} \le 1.0,\ 0 \le \theta \le \pi$

and a/B < 1.25(a/c+0.6) for $0 \le \frac{a}{2c} \le 1.0$; a/B < 1.0 for $0.1 \le \frac{a}{2c} \le 1.0$

"FFFTJ"

$$M1(a,c) := \begin{cases} 1.13 - 0.09\cdot\left(\frac{a}{c}\right) & \text{if } 0 \le \frac{a}{2\cdot c} \le 0.5 \\ \left(\frac{c}{a}\right)^{0.5}\cdot\left[1 + 0.04\cdot\left(\frac{c}{a}\right)\right] & \text{otherwise} \end{cases}$$

$$M2(a,c) := \begin{cases} \frac{0.89}{0.2 + \frac{a}{c}} - 0.54 & \text{if } 0 \le \frac{a}{2\cdot c} \le 0.5 \\ 0.2\cdot\left(\frac{c}{a}\right)^{4} & \text{otherwise} \end{cases}$$

$$M3(a,c) := \begin{cases} 0.5 - \frac{1}{0.65 + \frac{a}{c}} + 14\cdot\left(1 - \frac{a}{c}\right)^{24} & \text{if } 0 \le \frac{a}{2\cdot c} \le 0.5 \\ -0.11\cdot\left(\frac{c}{a}\right)^{4} & \text{otherwise} \end{cases}$$

$$\Phi(a,c) := \begin{cases} \left[1 + 1.464\cdot\left(\frac{a}{c}\right)^{1.65}\right]^{0.5} & \text{if } 0 \le \frac{a}{2\cdot c} \le 0.5 \\ \left[1 + 1.464\cdot\left(\frac{c}{a}\right)^{1.65}\right]^{0.5} & \text{otherwise} \end{cases}$$

$$f\theta(a,c,loc) := \begin{cases} \text{if } loc = deep \\ \quad \begin{cases} 1 & \text{if } 0 \le \frac{a}{2\cdot c} \le 0.5 \\ \left(\frac{c}{a}\right)^{0.5} & \text{otherwise} \end{cases} \\ \text{if } loc = surface \\ \quad \begin{cases} \left(\frac{a}{c}\right)^{0.5} & \text{if } 0 \le \frac{a}{2\cdot c} \le 0.5 \\ 1 & \text{otherwise} \end{cases} \end{cases}$$

$$fg(a,c,loc) := \begin{cases} 1 & \text{if } loc = deep \\ \text{if } loc = surface \\ \quad \begin{cases} 1.1 + 0.35\cdot\left(\frac{a}{B}\right)^{2} & \text{if } 0 \le \frac{a}{2\cdot c} \le 0.5 \\ 1.1 + 0.35\cdot\left(\frac{c}{a}\right)\cdot\left(\frac{a}{B}\right)^{2} & \text{otherwise} \end{cases} \end{cases}$$

$$M_m(a,c,loc) := \begin{array}{l} M_1 \leftarrow M1(a,c) \\ M_2 \leftarrow M2(a,c) \\ M_3 \leftarrow M3(a,c) \\ \Phi \leftarrow \Phi(a,c) \\ f_\theta \leftarrow f\theta(a,c,loc) \\ gg \leftarrow fg(a,c,loc) \\ \left[M_1 + M_2\cdot\left(\frac{a}{B}\right)^{2} + M_3\cdot\left(\frac{a}{B}\right)^{4}\right]\cdot\frac{gg\cdot f_\theta}{\Phi} \end{array}$$

$$f_w(a,c) := 1$$

$$G1(a,c) := \begin{cases} -1.22 - 0.12\cdot\frac{a}{c} & \text{if } 0 \le \frac{a}{2\cdot c} \le 0.5 \\ -2.11 + 0.77\cdot\frac{c}{a} & \text{otherwise} \end{cases}$$

$$G2(a,c) := \begin{cases} 0.55 - 1.05\cdot\left(\frac{a}{c}\right)^{0.75} + 0.47\cdot\left(\frac{a}{c}\right)^{1.5} & \text{if } 0 \le \frac{a}{2\cdot c} \le 0.5 \\ 0.55 - 0.72\cdot\left(\frac{c}{a}\right)^{0.75} + 0.14\cdot\left(\frac{c}{a}\right)^{1.5} & \text{otherwise} \end{cases}$$

$$H1(a,c) := \begin{cases} 1 - 0.34\cdot\left(\frac{a}{B}\right) - 0.11\cdot\left(\frac{a}{c}\right)\cdot\left(\frac{a}{B}\right) & \text{if } 0 \le \frac{a}{2\cdot c} \le 0.5 \\ 1 - \left(0.04 + 0.41\cdot\frac{c}{a}\right)\cdot\frac{a}{B} + \left[0.55 - 1.93\cdot\left(\frac{c}{a}\right)^{0.75} + 1.38\cdot\left(\frac{c}{a}\right)^{1.5}\right]\cdot\left(\frac{a}{B}\right)^{2} & \text{otherwise} \end{cases}$$

$$H2(a,c) := \begin{cases} G_1 \leftarrow G1(a,c) \\ G_2 \leftarrow G2(a,c) \\ 1 + G_1\cdot\left(\frac{a}{B}\right) + G_2\cdot\left(\frac{a}{B}\right)^{2} \end{cases}$$

$$H(a,c,loc) := \begin{cases} H2(a,c) & \text{if } loc = deep \\ H1(a,c) & \text{if } loc = surface \end{cases}$$

$$M_b(a,c,loc) := \begin{cases} H \leftarrow H(a,c,loc) \\ M_m \leftarrow M_m(a,c,loc) \\ H\cdot M_m \end{cases}$$

3) Reference Stress

$$a''(a,c) := \begin{cases} \dfrac{\frac{a}{B}}{1 + \frac{B}{c}} & \text{if } 2\pi\cdot r_o \ge 2(c+B) \\ \left(\frac{2a}{B}\right)\cdot\left(\frac{c}{2\pi\cdot r_o}\right) & \text{otherwise} \end{cases}$$

$$\sigma_{ref}(a,c) := \begin{cases} a'' \leftarrow a''(a,c) \\ \dfrac{P_b + \left[P_b^{\,2} + 9\cdot P_m^{\,2}\cdot(1-a'')^2\right]^{0.5}}{3(1-a'')^2} \end{cases}$$

(Annex P, Eqn. P.2)

4) Collapse parameter Lr

the cut-off to prevent localized plastic collapse:

$$L_{rmax} := \frac{\sigma_y + \sigma_u}{2\cdot\sigma_y}$$

(Equation 9)

$$\sigma_f := \frac{\sigma_y + \sigma_u}{2}$$

"FFFTJ"

$$Lr(a,c) := \left| \begin{array}{l} \sigma_{ref} \leftarrow \sigma_{ref}(a,c) \\ \dfrac{\sigma_{ref}}{\sigma_y} \end{array} \right.$$

If tubular nodal joints containing a part thickness or through thickness flaw in the chord, Lr to be replaced by $\dfrac{\sigma_f}{\sigma_y}\cdot\left[\left|\dfrac{P_a}{P_c}\right| + \left(\dfrac{M_{ai}}{M_{ci}}\right)^2 + \left|\dfrac{M_{ao}}{M_{co}}\right|\right]$

5) Residual Stress

$$Q_m(a,c) := \left| \begin{array}{l} 0 \ \text{ if } \ PWHT = \text{"Yes"} \\ \text{otherwise} \\ \quad \left| \begin{array}{l} \sigma_{ref} \leftarrow \sigma_{ref}(a,c) \\ \sigma_y \ \text{ if } \ \sigma_y < \left(1.4 - \dfrac{\sigma_{ref}}{\sigma_f}\right)\cdot\sigma_y \\ \left[\left(1.4 - \dfrac{\sigma_{ref}}{\sigma_f}\right)\cdot\sigma_y\right] \ \text{ otherwise} \end{array} \right. \end{array} \right.$$

$$Q_b := 0$$

(Equation 14a and 14b)

FATIGUE ASSESSMENT

$$Y\sigma pf(a,c,\Delta\sigma_m,\Delta\sigma_b,loc) := \left| \begin{array}{l} f_w \leftarrow f_w(a,c) \\ M \leftarrow 1 \\ M_m \leftarrow M_m(a,c,loc) \\ M_b \leftarrow M_b(a,c,loc) \\ M_{km} \leftarrow M_{km}(a,c,loc) \\ M_{kb} \leftarrow M_{kb}(a,c,loc) \\ Y\sigma p \leftarrow M\cdot f_w\cdot\left[k_{tm}\cdot M_{km}\cdot M_m\cdot\Delta\sigma_m + k_{tb}\cdot M_{kb}\cdot M_b\cdot\left[\Delta\sigma_b + (k_m - 1)\cdot\Delta\sigma_m\right]\right] \end{array} \right.$$

1) Stress Intensity Factor Range (Plate Solutions, Equation B8)

$$\Delta K(a,c,\Delta\sigma_m,\Delta\sigma_b,loc) := \left| \begin{array}{l} Y\sigma p \leftarrow Y\sigma pf(a,c,\Delta\sigma_m,\Delta\sigma_b,loc) \\ Y\sigma p\cdot\sqrt{\pi\cdot a} \end{array} \right.$$

2) Crack growth paramaters (Table 5 - Steel in a marine environ. with CP at -850 mV(Ag/AgCl)

Threshold Intensity	Transition Intensity	Slope	Constant	
$\Delta K_0 := 63$	$\Delta K_t := 290$	$m_A := 5.10$	$A_A := 2.10\cdot10^{-17}$	**(Stage A)**
		$m_B := 2.67$	$A_B := 2.02\cdot10^{-11}$	**(Stage B)**

3) Paris'Law (Equation 25)

"FFFTJ"

$$\mathrm{dabydN}(a, c, \Delta\sigma_m, \Delta\sigma_b) := \left| \begin{array}{l} \Delta K \leftarrow \Delta K(a, c, \Delta\sigma_m, \Delta\sigma_b, \mathrm{deep}) \\ \mathrm{dabydN} \leftarrow 0 \cdot a \quad \text{if } \Delta K < \Delta K_0 \\ \mathrm{dabydN} \leftarrow A_A \cdot \Delta K^{m_A} \quad \text{if } \Delta K_0 \le \Delta K < \Delta K_t \\ \mathrm{dabydN} \leftarrow A_B \cdot \Delta K^{m_B} \quad \text{if } \Delta K \ge \Delta K_t \\ \mathrm{dabydN} \end{array} \right.$$

$$\mathrm{dcbydN}(a, c, \Delta\sigma_m, \Delta\sigma_b) := \left| \begin{array}{l} \Delta K \leftarrow \Delta K(a, c, \Delta\sigma_m, \Delta\sigma_b, \mathrm{surface}) \\ \mathrm{dcbydN} \leftarrow 0 \cdot a \quad \text{if } \Delta K < \Delta K_0 \\ \mathrm{dcbydN} \leftarrow A_A \cdot \Delta K^{m_A} \quad \text{if } \Delta K_0 \le \Delta K < \Delta K_t \\ \mathrm{dcbydN} \leftarrow A_B \cdot \Delta K^{m_B} \quad \text{if } \Delta K \ge \Delta K_t \\ \mathrm{dcbydN} \end{array} \right.$$

FRACTURE RESISTANCE

$$Y\sigma p(a, c, \mathrm{loc}) := \left| \begin{array}{l} f_w \leftarrow f_w(a, c) \\ M \leftarrow 1 \\ M_m \leftarrow M_m(a, c, \mathrm{loc}) \\ M_b \leftarrow M_b(a, c, \mathrm{loc}) \\ M_{km} \leftarrow M_{km}(a, c, \mathrm{loc}) \\ M_{kb} \leftarrow M_{kb}(a, c, \mathrm{loc}) \\ Y\sigma p \leftarrow M \cdot f_w \cdot \left[k_{tm} \cdot M_{km} \cdot M_m \cdot P_m + k_{tb} \cdot M_{kb} \cdot M_b \cdot \left[P_b + (k_m - 1) \cdot P_m \right] \right] \end{array} \right. \qquad \text{(Equation 16)}$$

$$Y\sigma s(a, c, \mathrm{loc}) := \left| \begin{array}{l} M_m \leftarrow M_m(a, c, \mathrm{loc}) \\ M_b \leftarrow M_b(a, c, \mathrm{loc}) \\ Q_m \leftarrow Q_m(a, c) \\ Y\sigma s \leftarrow M_m \cdot Q_m + M_b \cdot Q_b \end{array} \right. \qquad \text{(Equation 17)}$$

"FFFTJ"

$$\mathbf{K}(a,c,loc) := \left| \begin{array}{l} Y\sigma s \leftarrow Y\sigma s(a,c,loc) \\ K_{Is} \leftarrow Y\sigma s \cdot \sqrt{\pi \cdot a} \\ Y\sigma p \leftarrow Y\sigma p(a,c,loc) \\ K_{Ip} \leftarrow Y\sigma p \cdot \sqrt{\pi \cdot a} \\ L_r \leftarrow Lr(a,c) \\ K \leftarrow K_{Is} \cdot \left(\frac{L_r}{K_{Ip}}\right) \end{array} \right.$$

$$\rho(a,c,loc) := \left| \begin{array}{l} K \leftarrow K(a,c,loc) \\ L_r \leftarrow Lr(a,c) \\ \rho 1 \leftarrow 0.1 \cdot K^{0.714} - 0.007 \cdot K^2 + 3 \cdot 10^{-5} \cdot K^5 \\ \text{if } K \le 4 \\ \quad \left| \begin{array}{l} \rho \leftarrow \rho 1 \ \text{ if } L_r \le 0.8 \\ \rho \leftarrow 4 \cdot \rho 1 \cdot (1.05 - L_r) \ \text{ if } 0.8 < L_r < 1.05 \\ \rho \leftarrow 0 \ \text{ if } 1.05 \le L_r \end{array} \right. \\ \rho \end{array} \right. \qquad \text{(AnnexR2)}$$

$$KI(a,c,loc) := \left| \begin{array}{l} Y\sigma p \leftarrow Y\sigma p(a,c,loc) \\ Y\sigma s \leftarrow Y\sigma s(a,c,loc) \\ Y\sigma \leftarrow Y\sigma p + Y\sigma s \\ K_I \leftarrow Y\sigma \cdot \sqrt{\pi \cdot a} \end{array} \right. \qquad \text{(Equation 2)}$$

$$\delta I(a,c,loc) := \left| \begin{array}{l} K_I \leftarrow KI(a,c,loc) \\ \delta_I \leftarrow \frac{K_I^2}{\sigma_y \cdot E} \end{array} \right. \qquad \text{(Equation 5)}$$

$$K_{mat} := \left| \begin{array}{l} Kmat \leftarrow \text{"unknown"} \ \text{ if } C_v = \text{"unknown"} \\ \text{otherwise} \\ \quad \left| \begin{array}{l} K_{matJ1} \leftarrow \left(12 \cdot \sqrt{C_v} - 20\right)\left(\frac{25}{B}\right)^{0.25} + 20 \\ K_{matJ5} \leftarrow 0.54 C_v + 55 \\ 31.63 \min\left(K_{matJ1}, K_{matJ5}\right) \end{array} \right. \end{array} \right. \qquad \text{(Annex J)}$$

$$K_r(a,c,loc) := \left| \begin{array}{l} K_r \leftarrow \text{"unknown"} \ \text{ if } K_{mat} = \text{"unknown"} \\ \frac{KI(a,c,loc)}{K_{mat}} + \rho(a,c,loc) \ \text{ otherwise} \end{array} \right. \qquad \text{(Equation 19)}$$

$$root\delta r(a,c,loc) := \left| \begin{array}{l} root\delta_r \leftarrow \text{"unknown"} \ \text{ if } \delta_{mat} = \text{"unknown"} \\ \sqrt{\frac{\delta I(a,c,loc)}{\delta_{mat}}} + \rho(a,c,loc) \ \text{ otherwise} \end{array} \right. \qquad \text{(Equation 22b)}$$

$$FractureRatio(a,c,loc) := \left| \begin{array}{l} root\delta r(a,c,loc) \ \text{ if } K_{mat} = \text{"unknown"} \\ K_r(a,c,loc) \ \text{ otherwise} \end{array} \right.$$

$$FAD(Lr) := \left| \begin{array}{l} \left(1 - 0.14 \cdot Lr^2\right) \cdot \left[0.3 + 0.7 \cdot e^{\left(-0.65 \cdot Lr^6\right)}\right] \ \text{ if } Lr < L_{rmax} \\ 0 \ \text{ otherwise} \end{array} \right. \qquad \text{(Equation 10)}$$

"FFFTJ"

EVALUATION of CRACK SIZE AND FATIGUE LIFE

```
end := | a ← a_start
       | c ← c_start
       | for i ∈ 1 .. increment
       |   | for j ∈ 1 .. last(cycles)
       |   |   | da_by_dN ← dabydN(a, c, Δσm_j, Δσb_j)
       |   |   | Δa ← da_by_dN · cycles_j / increment
       |   |   | dc_by_dN ← dcbydN(a, c, Δσm_j, Δσb_j)
       |   |   | Δc ← dc_by_dN · cycles_j / increment
       |   |   | a ← a + Δa
       |   |   | c ← c + Δc
       |   |   | L_r ← Lr(a, c)                                          (Annex S1)
       |   |   | FR_deep ← FractureRatio(a, c, deep)
       |   |   | FR_surface ← FractureRatio(a, c, surface)
       |   |   | M_3221 ← a/B − 1.25(a/c + 0.6)  if  0 ≤ a/(2c) ≤ 0.1
       |   |   | M_3221 ← a/B − 1  otherwise
       |   |   | if M_3221 > 0
       |   |   |   | fail ← 1
       |   |   |   | checkA ← 0
       |   |   | if CHECK(FR_deep, L_r) = "FAIL"
       |   |   |   | fail ← 1
       |   |   |   | checkB ← 0
       |   |   | if CHECK(FR_surface, L_r) = "FAIL"
       |   |   |   | fail ← 1
       |   |   |   | checkC ← 0
       |   |   | break if fail = 1
       |   | break if fail = 1
       | End_increment ← i
       | checkT ← checkA + checkB + checkC
       | a_end ← a
       | c_end ← c
       | Lr_end ← L_r
       | FractureRatio_d_end ← FR_deep
       | FractureRatio_s_end ← FR_surface
       | ("End_increment" "a_end" "c_end" "Lr_end" "FractureRatiod_end" "FractureRatios_end" "checkT")
       |  (End_increment  a_end  c_end  Lr_end  FractureRatio_d_end  FractureRatio_s_end  checkT)
```

"FFFTJ"

RESULTS SUMMARY

$a_{start} \equiv 3$ $c_{start} \equiv 3$ $increment \equiv 1000$

$$end = \begin{pmatrix} \text{"End_increment"} & \text{"a_end"} & \text{"c_end"} & \text{"Lr_end"} & \text{"FractureRatiod_end"} & \text{"FractureRatios_end"} & \text{"checkT"} \\ 1 \times 10^3 & 3.475 & 11.148 & 0.297 & 0.209 & 0.305 & 0 \end{pmatrix}$$

APPENDIX A.2 PARAMETRIC FORMULAE OF THE DEGREE OF BENDING

Parametric Formulae of the ratio of bending to membrane stress in Tubular Y and T joints

Validity Range

$0.2 \le \beta \le 0.80$

$0.2 \le \tau \le 1.0$

$7.6 \le \gamma \le 32$

$6.21 \le \alpha$

$35^{o} \le \theta \le 90^{o}$

INPUT: Basic Geometric Parameters for Simple Tubular Joints

$\theta := 42°$	Brace included angle
$t := 17.8$	Brace wall thickness at intersection
$T := 75.6$	Chord wall thickness at intersection
$d := 1070$	Brace outside diameter
$D := 2560$	Chord outside diameter
$Length := 39000$	Length of chord, length of thickness transition

$\beta := \frac{d}{D}$ $\qquad \beta = 0.418$

$\alpha := \frac{2Length}{D}$ $\qquad \alpha = 30.469$

$\gamma := \frac{D}{2 \cdot T}$ $\qquad \gamma = 16.931$

$\tau := \frac{t}{T}$ $\qquad \tau = 0.235$

Parametric Equation for the degree of bending under axial loading

At chord hot-spot stress site:

$$\Omega_{A1} := 0.7026\alpha^{0.0236}\cdot\exp\left(-0.187\cdot\beta^{4}+0.0097\cdot\gamma+\frac{0.0047}{\theta^{3}}-\frac{21.7\cdot\beta^{3}}{\gamma^{2}}+0.3038\cdot\beta\cdot\tau-\frac{0.0867\cdot\beta^{2}}{\theta^{3}}-0.001\gamma^{1.5}\cdot\theta\right)$$

At brace hot-spot stress site:

$$\Omega_{A2} := 0.6763\cdot\alpha^{0.0603}\cdot\gamma^{0.118}\cdot\tau^{0.24}\cdot\exp\left(-0.292\cdot\beta^{2.5}-\frac{0.0407}{\theta}-0.142\cdot\tau\cdot\theta+0.0833\cdot\beta^{3}\cdot\theta\right)$$

At chord saddle position:

$$\Omega_{A3} := 0.785\cdot\alpha^{0.0122}\cdot\gamma^{0.212\beta^{2.2}}\cdot\tau^{0.0177}\cdot\sin(\theta)^{-0.1}\cdot\exp\left(-0.799\beta^{2.5}+0.165\cdot\beta\cdot\tau\right)$$

At brace saddle position:

$$\Omega_{A4} := \begin{cases} 0.6698\cdot\alpha^{0.0431}\cdot\gamma^{0.0834}\cdot\theta^{-0.0896}\cdot\exp\left(-0.1846\cdot\beta^{2}-\frac{0.0672}{\tau}+0.0017\gamma\cdot\tau\right) \\ 0 \quad \text{if} \quad \begin{cases} \theta < 45 \\ \tau < 0.4 \end{cases} \end{cases}$$

Parametric Equation for the degree of bending under in-plane bending

At chord hot-spot stress site:

$$\Omega_{A5} := 0.7984\cdot\alpha^{-0.0283}\cdot\tau^{-0.0017}\cdot\theta^{-0.024}\cdot\exp\left(\frac{0.0656}{\beta}+0.00027\cdot\gamma^{2}-\frac{0.0819\cdot\theta}{\alpha}-\frac{0.00036\cdot\theta}{\beta^{3}}-\frac{0.0001\cdot\gamma^{2}}{\beta}\right)$$

At brace hot-spot stress site:

$$\Omega_{A6} := \begin{cases} 0.6893\cdot\alpha^{0.0158}\cdot\beta^{0.226}\cdot\gamma^{(0.272-0.0443\cdot\tau+0.0196\cdot\theta)}\cdot\tau^{0.298}\cdot\theta^{0.0869}\cdot\exp\left(-0.0187\cdot\beta\cdot\gamma-\frac{0.000343}{\beta^{2}}\cdot\tau-0.1\cdot\beta\cdot\theta^{2}-0.114\cdot\tau\cdot\theta\right) \\ 0 \quad \text{if} \quad \begin{cases} \theta < 45 \\ \tau < 0.45 \end{cases} \end{cases}$$

At chord crown position:

$$\Omega_{A7} := 2.886\alpha^{-0.0464}\cdot\gamma^{-0.242}\cdot\exp\left(-0.617\cdot\beta^{0.5}-0.112\cdot\tau+0.738\cdot\theta+0.178\cdot\beta\cdot\tau-1.34\cdot\gamma^{-0.2}\cdot\theta\right)$$

At brace crown position:

$$\Omega_{A8} := \begin{cases} 0.6683\cdot\alpha^{0.0143}\cdot\gamma^{\left(0.127+0.0968\cdot\tau^{2}-0.0038\cdot\theta\right)}\cdot\theta^{0.149}\cdot\exp\left(\frac{-0.00218}{\beta^{3}}-\frac{0.0143}{\tau^{2}}+\frac{0.000953}{\beta^{2}}\cdot\tau-0.0145\cdot\beta\cdot\gamma-0.162\cdot\tau\cdot\theta\right) \\ 0 \quad \text{if} \quad \begin{cases} \theta < 45 \\ \tau < 0.65 \end{cases} \end{cases}$$

Parametric Equation for the degree of bending under out-of-plane bending

At chord hot-spot stress site:

$$\Omega_{A9} := 0.768\cdot\beta^{-0.0882}\cdot\gamma^{0.0115}\cdot\tau^{0.00668}\cdot\exp\left(0.000122\alpha^{2}+\frac{0.04}{\theta}-0.00249\cdot\frac{\tau}{\beta^{2}}+\frac{0.0123\cdot\tau}{\theta^{2}}\right)$$

At brace hot-spot stress site:

$$\Omega_{A10} := \begin{cases} 0.5174\cdot\alpha^{0.0211}\cdot\gamma^{0.203}\cdot\tau^{0.159}\cdot\theta^{-0.0919}\cdot\exp\left(\frac{-0.000048}{\beta^{5}}-0.00963\cdot\beta\cdot\gamma\right) \\ 0 \quad \text{if} \quad \begin{cases} \theta \le 45 \\ \beta \le 0.25 \end{cases} \end{cases}$$

At chord saddle position:

$$\Omega_{A11} := 0.7964\cdot\beta^{-0.0907}\cdot\gamma^{0.0092}\cdot\theta^{-0.0793}\cdot\exp\left(0.000159\cdot\alpha^{2}+0.0549\cdot\tau^{2}-0.0252\cdot\frac{\tau}{\beta}+\frac{0.00223\cdot\theta^{3}}{\beta}+0.000738\cdot\gamma\cdot\tau^{3}\right)$$

At brace saddle position:

$$\Omega_{A12} := \begin{cases} 0.61\cdot\alpha^{-0.0045}\cdot\gamma^{0.168}\cdot\theta^{-0.103}\cdot\exp\left(\frac{-0.000041}{\beta^{5}}-\frac{0.0665}{\tau}-0.0095\cdot\beta^{2}\cdot\gamma\right) \\ 0 \quad \text{if} \quad \begin{cases} \theta < 45 \\ \beta \le 0.20 \end{cases} \end{cases}$$

Summary of Degree of Bending

1) Under Axial Loading

At chord hot-spot stress site: $\Omega_{A1} = 0.846$

At brace hot-spot stress site: $\Omega_{A2} = 0.736$

At chord saddle position: $\Omega_{A3} = 0.842$

At brace saddle position: $\Omega_{A4} = 0$

2) Under In-plane Bending

At chord hot-spot stress site: $\Omega_{A5} = 0.859$

At brace hot-spot stress site: $\Omega_{A6} = 0$

At chord crown position: $\Omega_{A7} = 0.812$

At brace crown position: $\Omega_{A8} = 0$

3) Under Out-of-plane Bending

At chord hot-spot stress site: $\Omega_{A9} = 1.006$

At brace hot-spot stress site: $\Omega_{A10} = 0.751$

At chord saddle position: $\Omega_{A11} = 1.042$

At brace saddle position: $\Omega_{A12} = 0.729$

APPENDIX B CASE SUDY DETAILS

APPENDIX B.1 DETERMINISTIC Fatigue (S-N)

Table B.1-1 presents the comparison of fatigue damages calculated for the structural brace joints to leg members at elevations shown in Figure B.1-1. The joint selection for this comparison was based on the anticipated extent of the effect of the removed (severed) member of the structure on the fatigue utilization of the remaining members would be the greatest.

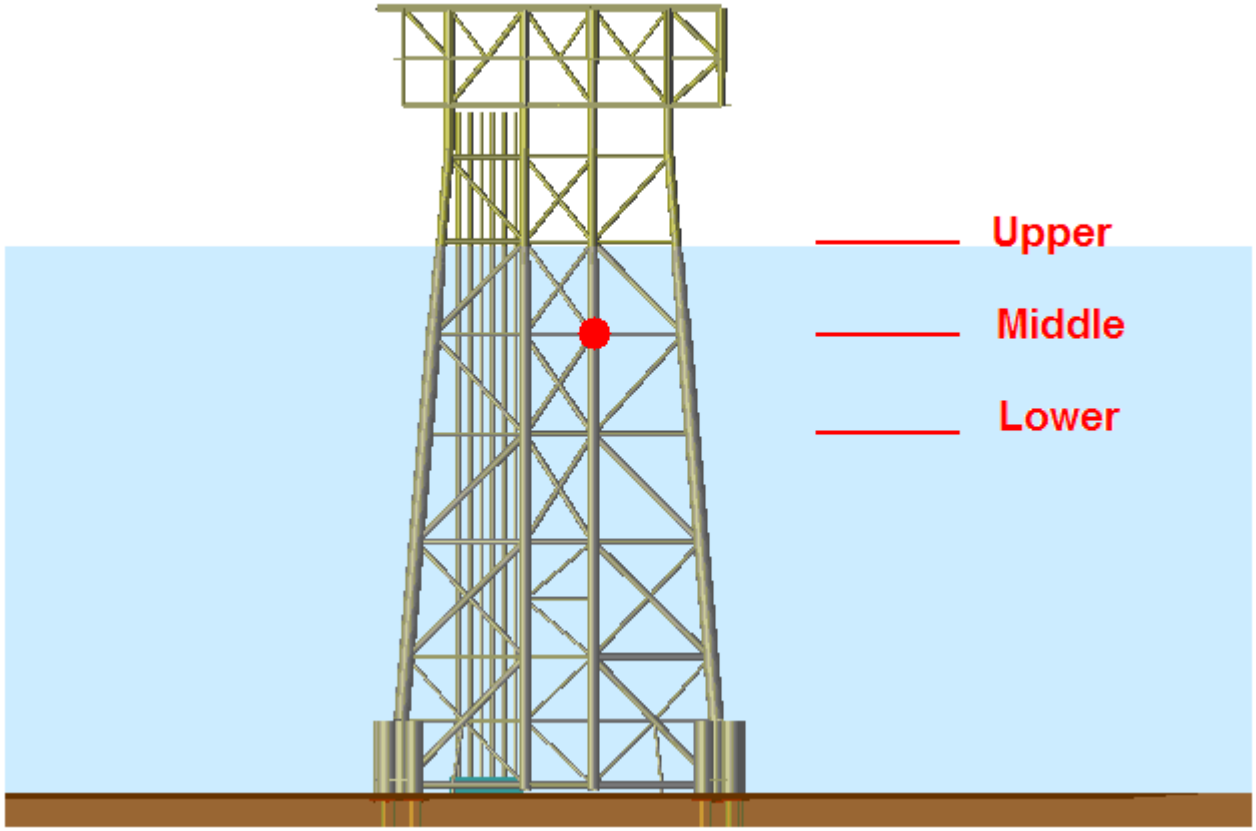

Figure B.1-1 Elevation of the Jacket Chosen for the Comparison

Table B.1-1 Comparison of Fatigue Damage (Extended)

Elevation	Joint	Side	As built		Post failure		Damage Difference
			Fatigue Damage	Fatigue Life	Fatigue Damage	Fatigue Life	
			[-]	[years]	[-]	[years]	[%]
LOWER	JT95	Chord	3.62E-04	>5000	3.62E-04	>5000	0.0
		Brace	8.32E-05	>5000	8.32E-05	>5000	0.0
	JT71	Chord	4.77E-04	>5000	4.48E-04	>5000	-6.1
		Brace	1.56E-04	>5000	1.56E-04	>5000	0.0
	JT72	Chord	7.31E-04	>5000	7.15E-04	>5000	-2.2
		Brace	2.53E-04	>5000	2.48E-04	>5000	-2.0
	JT48	Chord	1.67E-03	>5000	1.67E-03	>5000	0.0
		Brace	1.53E-03	>5000	1.52E-03	>5000	-0.7
	JT193	Chord	4.99E-04	>5000	5.12E-04	>5000	2.6
		Brace	4.19E-04	>5000	4.27E-04	>5000	1.9
	JT70	Chord	1.10E-03	>5000	1.10E-03	>5000	0.0
		Brace	3.28E-04	>5000	3.26E-04	>5000	-0.6
	JT69	Chord	8.59E-04	>5000	8.32E-04	>5000	-3.1
		Brace	2.40E-04	>5000	2.32E-04	>5000	-3.3
	JT51	Chord	1.69E-03	>5000	1.69E-03	>5000	0.0
		Brace	1.15E-03	>5000	1.15E-03	>5000	0.0
MIDDLE	JT176	Chord	4.47E-03	4474	4.27E-03	4684	-4.5
		Brace	4.28E-03	4673	3.96E-03	>5000	-7.5
	JT91	Chord	1.73E-03	>5000	1.90E-03	>5000	9.8
		Brace	7.63E-04	>5000	8.71E-04	>5000	14.2
	JT47	Chord	4.52E-03	4425	4.51E-03	4435	-0.2
		Brace	8.18E-03	2445	8.32E-03	2404	1.7
	JT43	Chord	8.18E-03	2445	7.28E-03	2747	-11.0
		Brace	1.33E-02	1504	1.33E-02	1504	0.0
	JT175	Chord	1.33E-02	1504	4.23E-03	4728	-68.2
		Brace	1.33E-02	1504	3.06E-03	>5000	-77.0
	JT68	Chord	1.44E-03	>5000	1.50E-03	>5000	4.2
		Brace	4.03E-04	>5000	9.04E-04	>5000	124.3
	JT67	Chord	1.29E-03	>5000	1.33E-03	>5000	3.1
		Brace	5.28E-04	>5000	5.21E-04	>5000	-1.3
	JT166	Chord	7.10E-03	2817	6.94E-03	2882	-2.3
		Brace	6.59E-03	3035	6.57E-03	3044	-0.3
UPPER	JT220	Chord	8.95E-02	223	8.97E-02	223	0.2
		Brace	3.36E-02	595	3.37E-02	593	0.3
	JT221	Chord	7.11E-02	281	7.50E-02	267	5.5
		Brace	2.63E-02	760	2.78E-02	719	5.7
	JT74	Chord	1.84E-01	109	1.86E-01	108	1.1
		Brace	3.32E-01	60	3.32E-01	60	0.0
	JT73	Chord	9.56E-01	21	9.56E-01	21	0.0
		Brace	3.62E-01	55	3.63E-01	55	0.3
	JT197	Chord	9.38E-02	213	9.46E-02	211	0.9
		Brace	3.52E-02	568	3.54E-02	565	0.6
	JT198	Chord	6.61E-02	303	7.11E-02	281	7.6
		Brace	4.05E-02	494	4.33E-02	462	6.9
	JT76	Chord	7.54E-01	27	7.53E-01	27	-0.1
		Brace	2.74E-01	73	2.74E-01	73	0.0
	JT75	Chord	8.52E-02	235	8.51E-02	235	-0.1
		Brace	3.16E-02	633	4.60E-02	435	45.6

APPENDIX B.2 Fracture mechanics Results Comparison

Table B.2-1 Comparison of Results (Fatigue)

a/2c	a	2c	Crackwise				DNV Worksheet				Difference		
			a_{final}	$2c_{final}$	Increments	Life	a_{final}	c_{final}	Increments	Life	a_{final}	$2c_{final}$	Life
	[mm]	[mm]	[mm]	[mm]	[-]	[year]	[mm]	[mm]	[-]	[year]	[%]	[%]	[%]
0.50	3	6	3.51	23.12	1000	>20	3.48	22.30	1000	>20	1.0	3.6	0.0
	4	8	5.25	43.07	1000	>20	5.18	41.32	1000	>20	1.5	4.1	0.0
	5	10	7.70	79.09	1000	>20	7.53	75.03	1000	>20	2.2	5.1	0.0
	6	12	16.05	253.59	966	19.3	16.18	254.11	996	19.9	-0.8	-0.2	-3.1
	7	14	16.13	255.15	702	14.0	16.20	253.43	725	14.5	-0.5	0.7	-3.3
0.33	3	9	3.62	25.03	1000	>20	3.59	24.24	1000	>20	0.8	3.2	0.0
	4	12	5.46	46.32	1000	>20	5.39	44.53	1000	>20	1.4	3.9	0.0
	5	15	8.15	86.86	1000	>20	7.96	82.32	1000	>20	2.4	5.2	0.0
	6	18	16.00	252.27	919	18.4	16.20	253.55	947	18.9	-1.2	-0.5	-3.0
	7	21	16.08	253.90	664	13.3	16.20	253.38	685	13.7	-0.8	0.2	-3.2
0.25	3	12	3.73	26.85	1000	>20	3.71	26.09	1000	>20	0.8	2.8	0.0
	4	16	5.66	49.39	1000	>20	5.59	47.59	1000	>20	1.3	3.7	0.0
	5	20	8.63	95.19	1000	>20	8.41	90.01	1000	>20	2.6	5.4	0.0
	6	24	16.08	254.31	879	17.6	16.19	253.87	904	18.1	-0.7	0.2	-2.8
	7	28	16.14	255.36	632	12.6	16.20	253.50	651	13.0	-0.4	0.7	-3.0
0.20	3	15	3.84	28.68	1000	>20	3.81	27.96	1000	>20	0.7	2.5	0.0
	4	20	5.87	52.64	1000	>20	5.79	50.80	1000	>20	1.3	3.5	0.0
	5	25	9.20	105.40	1000	>20	8.94	99.25	1000	>20	2.9	5.8	0.0
	6	30	16.09	254.58	840	16.8	16.20	253.50	863	17.3	-0.6	0.4	-2.7
	7	35	16.12	254.94	601	12.0	16.20	253.50	618	12.4	-0.5	0.6	-2.8
0.17	3	18	3.94	30.63	1000	>20	3.92	29.93	1000	>20	0.7	2.3	0.0
	4	24	6.09	56.16	1000	>20	6.01	54.26	1000	>20	1.3	3.4	0.0
	5	30	9.94	118.90	1000	>20	9.61	111.18	1000	>20	3.4	6.5	0.0
	6	36	16.11	255.10	803	16.1	16.20	253.57	824	16.5	-0.5	0.6	-2.6
	7	42	16.03	252.71	571	11.4	16.19	253.74	587	11.7	-1.0	-0.4	-2.8
0.14	3	21	4.05	32.69	1000	>20	4.03	32.02	1000	>20	0.7	2.1	0.0
	4	28	6.33	60.07	1000	>20	6.25	58.11	1000	>20	1.2	3.3	0.0
	5	35	10.88	137.01	1000	>20	10.43	126.51	1000	>20	4.1	7.7	0.0
	6	42	16.05	253.65	767	15.3	16.19	253.88	787	15.7	-0.9	-0.1	-2.6
	7	49	16.12	254.97	543	10.9	16.19	253.87	558	11.2	-0.5	0.4	-2.8
										AVG.	0.7	2.6	-1.2

Table B.2-1 Comparison of Results (Fatigue and Fracture)

			Crackwise							DNV Worksheet						
a/2c	a [mm]	2c [mm]	a_{final} [mm]	$2c_{final}$ [mm]	Increments	Fatigue Life [yrs]	Lr [-]	Kr [-]	FAD	a_{final} [mm]	$2c_{final}$ [mm]	Increments	Fatigue Life [yrs]	Lr [-]	Kr [-]	FAD
0.50	3	6	3.51	23.12	1000	>20	0.298	0.307	Acceptable	3.48	22.30	1000	>20	0.297	0.209	Acceptable
	4	8	5.25	43.07	1000	>20	0.335	0.256	Acceptable	5.18	41.32	1000	>20	0.332	0.253	Acceptable
	5	10	7.70	79.09	1000	>20	0.417	0.327	Acceptable	7.53	75.03	1000	>20	0.409	0.319	Acceptable
	6	12	13.27	187.29	936	18.7	0.973	0.589	Unacceptable	12.45	166.35	947	18.9	0.812	0.536	Unacceptable
	7	14	13.31	187.50	672	13.4	0.981	0.591	Unacceptable	12.45	165.45	675	13.5	0.812	0.535	Unacceptable
0.33	3	9	3.62	25.03	1000	>20	0.301	0.309	Acceptable	3.59	24.24	1000	>20	0.300	0.213	Acceptable
	4	12	5.46	46.32	1000	>20	0.341	0.262	Acceptable	5.39	44.53	1000	>20	0.338	0.259	Acceptable
	5	15	8.15	86.86	1000	>20	0.438	0.343	Acceptable	7.96	82.32	1000	>20	0.428	0.335	Acceptable
	6	18	13.31	188.17	890	17.8	0.982	0.592	Unacceptable	12.45	166.47	897	17.9	0.812	0.536	Unacceptable
	7	21	13.30	187.08	634	12.7	0.977	0.590	Unacceptable	12.45	165.47	635	12.7	0.812	0.535	Unacceptable
0.25	3	12	3.73	26.85	1000	>20	0.303	0.311	Acceptable	3.71	26.09	1000	>20	0.302	0.218	Acceptable
	4	16	5.66	49.39	1000	>20	0.346	0.268	Acceptable	5.59	47.59	1000	>20	0.344	0.265	Acceptable
	5	20	8.63	95.19	1000	>20	0.462	0.362	Acceptable	8.41	90.01	1000	>20	0.449	0.352	Acceptable
	6	24	13.28	187.55	849	17.0	0.976	0.590	Unacceptable	12.45	166.45	855	17.1	0.813	0.536	Unacceptable
	7	28	13.32	187.59	602	12.0	0.982	0.591	Unacceptable	12.45	165.49	601	12.0	0.812	0.535	Unacceptable
0.20	3	15	3.84	28.68	1000	>20	0.306	0.312	Acceptable	4.30	37.32	1000	>20	0.317	0.239	Acceptable
	4	20	5.87	52.64	1000	>20	0.353	0.274	Acceptable	5.79	50.80	1000	>20	0.350	0.271	Acceptable
	5	25	9.20	105.40	1000	>20	0.495	0.385	Acceptable	8.94	99.25	1000	>20	0.478	0.372	Acceptable
	6	30	13.28	187.64	810	16.2	0.976	0.590	Unacceptable	12.45	166.56	814	16.3	0.813	0.536	Unacceptable
	7	35	13.31	187.47	571	11.4	0.980	0.591	Unacceptable	12.45	165.61	568	11.4	0.812	0.535	Unacceptable
0.17	3	18	3.94	30.63	1000	>20	0.308	0.313	Acceptable	3.92	29.93	1000	>20	0.307	0.225	Acceptable
	4	24	6.09	56.15	1000	>20	0.360	0.280	Acceptable	6.01	54.26	1000	>20	0.357	0.277	Acceptable
	5	30	9.94	118.89	1000	>20	0.544	0.416	Acceptable	9.61	111.18	1000	>20	0.519	0.400	Acceptable
	6	36	13.29	187.85	773	15.5	0.978	0.591	Unacceptable	12.44	166.61	774	15.5	0.813	0.536	Unacceptable
	7	42	13.33	188.10	542	10.8	0.986	0.592	Unacceptable	12.45	165.81	537	10.7	0.812	0.535	Unacceptable
0.14	3	21	4.05	32.69	1000	>20	0.311	0.231	Acceptable	4.03	32.02	1000	>20	0.310	0.229	Acceptable
	4	28	6.33	60.07	1000	>20	0.368	0.287	Acceptable	6.25	58.11	1000	>20	0.364	0.284	Acceptable
	5	35	10.88	136.99	1000	>20	0.623	0.459	Acceptable	10.43	126.51	1000	>20	0.581	0.436	Acceptable
	6	42	13.27	187.40	737	14.7	0.973	0.589	Unacceptable	12.45	166.64	737	14.7	0.813	0.536	Unacceptable
	7	49	13.30	187.59	513	10.3	0.979	0.591	Unacceptable	12.45	165.92	508	10.2	0.812	0.535	Unacceptable

Det Norske Veritas:

DNV is a global provider of knowledge for managing risk. Today, safe and responsible business conduct is both a license to operate and a competitive advantage. Our core competence is to identify, assess, and advise on risk management, and so turn risks into rewards for our customers. From our leading position in certification, classification, verification, and training, we develop and apply standards and best practices. This helps our customers to safely and responsibly improve their business performance.

Our technology expertise, industry knowledge, and risk management approach, has been used to successfully manage numerous high-profile projects around the world.

DNV is an independent organisation with dedicated risk professionals in more than 100 countries. Our purpose is to safeguard life, property and the environment. DNV serves a range of industries, with a special focus on the maritime and energy sectors. Since 1864, DNV has balanced the needs of business and society based on our independence and integrity. Today, we have a global presence with a network of 300 offices in 100 countries, with headquarters in Oslo, Norway.

Global impact for a safe and sustainable future:

Learn more on www.dnv.com